

Distribution Agreement

In presenting this thesis or dissertation as a partial fulfillment of the requirements for an advanced degree from Emory University, I hereby grant to Emory University and its agents the non-exclusive license to archive, make accessible, and display my thesis or dissertation in whole or in part in all forms of media, now or hereafter known, including display on the world wide web. I understand that I may select some access restrictions as part of the online submission of this thesis or dissertation. I retain all ownership rights to the copyright of the thesis or dissertation. I also retain the right to use in future works (such as articles or books) all or part of this thesis or dissertation.

Signature:

Benjamin Siciliano

Date

Identification of psychoneuroimmune drug targets in hiPSC-derived astrocytes

By

Benjamin Siciliano
BS, Biology, Bucknell University, 2020

Graduate Division of Biological and Biomedical Sciences
Molecular & Systems Pharmacology

Zhexing Wen, PhD
Advisor

Randy Hall, PhD
Committee Member

Thomas Kukar, PhD
Committee Member

Michael Owens, PhD
Committee Member

Accepted:

Kimberly Jacob Arriola, PhD, MPH
Dean of the James T. Laney School of Graduate Studies

Date

Identification of psychoneuroimmune drug targets in hiPSC-derived astrocytes

By

Benjamin Siciliano
BS, Biology, Bucknell University, 2020

Advisor: Zhexing Wen, PhD

An abstract of
A dissertation submitted to the Faculty of the
James T. Laney School of Graduate Studies of Emory University
in partial fulfillment of the requirements for the degree of
Doctor of Philosophy
in the Graduate Division of Biological and Biomedical Sciences
Molecular & Systems Pharmacology
2025

Abstract

Identification of psychoneuroimmune drug targets in hiPSC-derived astrocytes

By Benjamin Siciliano

Major Depressive Disorder (MDD) and Alzheimer's Disease (AD) represent two highly prevalent and debilitating brain disorders, yet their shared pathophysiological mechanisms remain poorly understood. Recent epidemiological studies suggest a bidirectional link between MDD and AD, highlighting the need for novel therapeutic strategies. This research focuses on astrocytes, key glial cells implicated in neuroinflammation, synaptic maintenance, and the blood-brain barrier (BBB), to investigate how astrocyte-specific dysfunction may drive disease processes in MDD and AD. Using human induced pluripotent stem cell (hiPSC) technology, astrocytes were derived from MDD patients, categorized as responders (R) or nonresponders (NR) to selective serotonin reuptake inhibitors (SSRIs), and from individuals with familial AD (fAD) and healthy controls. Comprehensive transcriptomic and kinomic analyses revealed distinct and overlapping molecular signatures across these astrocyte groups. Notably, NR astrocytes exhibited pronounced dysregulation in chemotaxis-related genes and upregulated stress-responsive pathways, whereas fAD astrocytes displayed impairment in extracellular matrix (ECM) organization, neuroinflammation, and lipid metabolism. Further transcription factor (TF) activity inference identified differential modulation of factors such as HIF3A, KLF17 and kinase pathways such as DDR2, PI3K associated with SSRI responsiveness and AD pathogenesis. Functional network analyses underscored astrocytes' active roles in synaptic modulation and inflammatory cascades, supporting the hypothesis that astrocyte dysfunction contributes to both treatment resistance in MDD and neurodegenerative processes in AD. By querying the Library of Integrated Network-based Cellular Signatures (LINCS), this work uncovered several FDA-approved drugs, including certain antidepressants and anti-inflammatory agents, capable of reversing pathological astrocyte phenotypes *in vitro*. These findings highlight promising avenues for drug repurposing and astrocyte-targeted intervention. Overall, this dissertation advances the emerging concept of astrocytes as central players in neuropsychiatric and neurodegenerative disorders. It identifies novel molecular candidates and pathways for therapeutic development, emphasizing the need for a precision medicine approach tailored to astrocyte-specific dysfunction. Collectively, these results contribute to our understanding of how glial dysregulation underpins MDD and AD, providing a foundation for future translational efforts aimed at improving clinical outcomes.

Identification of psychoneuroimmune drug targets in hiPSC-derived astrocytes

By

Benjamin Siciliano
BS, Biology, Bucknell University, 2020

Advisor: Zhexing Wen, PhD

A dissertation submitted to the Faculty of the
James T. Laney School of Graduate Studies of Emory University
in partial fulfillment of the requirements for the degree of
Doctor of Philosophy
in the Graduate Division of Biological and Biomedical Sciences
Molecular & Systems Pharmacology
2025

Table of Contents

<i>Table of Contents</i>	6
<i>List of Abbreviations</i>	12
Chapter 1: Introduction	1
Major depressive disorder and treatment-resistant depression	1
Sporadic and familial Alzheimer’s disease	3
Epidemiological link between major depressive disorder and Alzheimer’s disease	4
Precision medicine approaches to major depressive disorder and Alzheimer’s disease.....	6
Modeling major depressive disorder and Alzheimer’s disease using hiPSC-derived neurons	7
hiPSC-derived astrocytes models of major depressive disorder and Alzheimer’s disease.....	9
Chapter 2: Astrocyte-mediated neuroimmune dysfunction and extracellular matrix remodeling define a cellular biomarker of SSRI-resistant depression	15
Abstract	15
Introduction	16
Materials and methods	18
Subjects	18
hiPSC culture and astrocyte differentiation	19
Immunocytochemistry	20
RNA extraction and sequencing.....	21
Differential gene expression analysis	21
Pathway enrichment analysis	22
Weighted gene coexpression network analysis	22
Protein-protein interaction network analysis of divergent modules	23

Transcription factor activity inference	24
Transcription factor activity overlap analysis	24
Correlation analysis of transcription factor activity across conditions	25
Protein-protein interaction network analysis of differentially active transcription factors ..	25
Real-time PCR quantification of spliced X-box binding protein 1	26
Analysis of transcription factor target expression	27
LINCS-based identification of discordant perturbagens	27
Statistical analysis and data visualization	28
Results	29
Astrocytic molecular signatures linked to SSRI responsiveness in MDD	29
Gene co-expression networks associated with the SSRI response in MDD astrocytes	36
Key genes driving the distinct transcriptional signatures between SSRI responders and non-responders in astrocytes	40
Altered XBP1 signaling in SSRI-nonresponder astrocytes	45
Identification of discordant perturbagens in SSRI-responder and nonresponder astrocytes	48
Discussion	52
Conclusions	57
<i>Chapter 3: Proinflammatory transcriptomic and kinomic alterations in astrocytes derived from patients with familial Alzheimer's disease</i>	<i>59</i>
Abstract	59
Introduction	60
Materials and methods	62
Culture of human iPSCs and differentiation into astrocytes	62

Sample preparation and processing for transcriptomics	64
Sample preparation and processing for kinomics	65
Transcriptomic analysis	66
Transcriptomic pathway analysis.....	66
Protein-protein interaction network analysis	66
Transcription factor activity inference.....	67
Kinomic analysis.....	67
Multiomic integration	68
Sample size and statistical analyses.....	69
Results	69
Characterization of hiPSC-derived astrocytes	69
Transcriptomic profiling reveals key dysregulated pathways in fAD astrocytes	70
Identification of astrocyte-specific molecular targets in fAD.....	74
Kinomic profiling reveals dysregulated kinase activity in fAD astrocytes	77
Multiomics integration highlights dysregulated pathways in fAD astrocytes	80
Discussion.....	83
Conclusions.....	87
 <i>Chapter 4: Shared and distinct psychoneuroimmune dysregulation in hiPSC astrocyte transcriptomes across depressive and neurodegenerative disorders.....</i>	
Abstract.....	89
Introduction.....	90
Materials and methods	93
Data acquisition and processing.....	93

Differential gene expression analysis	93
Correlation analysis of differential gene expression.....	94
Functional enrichment analysis.....	94
Clustering of differentially expressed genes in overlapping biological processes	94
Transcription factor activity inference	95
Kinase enrichment analysis.....	95
Results	96
Differential gene expression and functional enrichment in hiPSC-derived astrocytes.....	96
Integrated transcription factor and kinase activity analysis in hiPSC-derived astrocytes ..	100
LINCS-derived mechanisms of action and perturbagens in R, NR, and fAD hiPSC-derived astrocytes.....	105
Discussion.....	109
Conclusions.....	116
<i>Chapter 5: Conclusions</i>	<i>118</i>
Summary of key findings.....	118
Mechanistic insights into astrocyte dysfunction in MDD and AD	125
Therapeutic implications and drug repurposing opportunities	127
Comparative analysis with existing literature.....	129
Limitations of the current research	131
Future directions for astrocyte-centric research.....	133
Concluding remarks	134
<i>References</i>	<i>136</i>
Table of Figures	

Figure 2.1. Transcription factor-based differentiation of astrocytes from human induced pluripotent stem cells.	31
Figure 2.2. Astrocytic gene expression signatures associated with depression with differential antidepressant responses.	34
Figure 2.3. Differentially expressed gene clustering in healthy control, responder, and non-responder hiPSC-derived astrocytes.	35
Figure 2.4. Hierarchical clustering of genes and module detection in hiPSC-derived astrocytes.	36
Figure 2.5. Identification of significant modules in hiPSC-derived astrocytes from SSRI-responders and nonresponders.	39
Figure 2.6. Key transcription factors driving the astrocytic signatures of SSRI-responders and non-responders.	43
Figure 2.7. Alterations in XBP1 signaling and XBP1 target genes in hiPSC-derived astrocytes.	46
Figure 2.8. Identification of potential therapeutics using LINCS analysis.	50
Figure 3.1. Study design and characterization of hiPSC-derived astrocytes.	70
Figure 3.2. Transcriptomic analysis of fAD versus HC hiPSC-derived astrocytes.	73
Figure 3.3. Identification of astrocyte-specific molecular targets in fAD.	76
Figure 3.4. Differential kinase activity in fAD astrocytes versus healthy control astrocytes.	80
Figure 3.5. Identification of molecular pathways altered in fAD astrocytes via multiomic integration.	82
Figure 4.1. Comparative analysis of differential gene expression and functional enrichment in NR, R, and fAD hiPSC-derived astrocytes.	97
Figure 4.2. Integrated analysis of transcription factor and kinase activities in R, NR, and fAD hiPSC-derived astrocytes.	102

Figure 4.3. LINCS-derived MOAs and perturbagens in R, NR, and fAD hiPSC-derived astrocytes.....	106
Figure 5.1 Distinct astrocyte states in SSRI-responders and non-responders.	119
Figure 5.2 Transcriptomic and kinomic dysregulation in fAD astrocytes.....	122
Figure 5.3 Shared Molecular Dysregulation in NR and fAD Astrocytes.	123

List of Abbreviations

A β	Amyloid Beta
AD	Alzheimer's Disease
APOE	Apolipoprotein E
APP	Amyloid Precursor Protein
BBB	Blood-Brain Barrier
BDNF	Brain-Derived Neurotrophic Factor
BSA	Bovine Serum Albumin
BP	Biological Processes
CC	Cellular Components
CNS	Central Nervous System
DBS	Deep Brain Stimulation
DEG	Differentially Expressed Gene
DDR1	Discoidin Domain Receptor 1
DDR2	Discoidin Domain Receptor 2
DGE	Differential Gene Expression
ECM	Extracellular Matrix
eQTL	Expression Quantitative Trait Loci
ER	Endoplasmic Reticulum
fAD	Familial Alzheimer's Disease
GABA	Gamma-Aminobutyric Acid
GFAP	Glial Fibrillary Acidic Protein
GO	Gene Ontology

GSEA	Gene Set Enrichment Analysis
GSK	Glycogen Synthase Kinase
GWAS	Genome-Wide Association Study
HC	Healthy Control
hiPSC	Human Induced Pluripotent Stem Cell
HPA	Hypothalamic-Pituitary-Adrenal
IL	Interleukin
iPSC	Induced Pluripotent Stem Cell
JAK	Janus Kinase
KEA3	Kinase Enrichment Analysis version 3
KRSA	Kinome Random Sampling Analyzer
LINCS	Library of Integrated Network-based Cellular Signatures
MAPK	Mitogen-Activated Protein Kinase
MCI	Mild Cognitive Impairment
MDD	Major Depressive Disorder
MF	Molecular Functions
MMP	Matrix Metalloproteinase
MOA	Mechanisms of Action
mTOR	Mechanistic Target of Rapamycin
NF- κ B	Nuclear factor kappa B
NIH	National Institutes of Health
NR	SSRI Non-Responder
ORA	Overrepresentation Analysis

padj	Adjusted p value
PDGFR	Platelet-Derived Growth Factor Receptor
PI3K	Phosphoinositide 3-Kinase
PNI	Psychoneuroimmunology
PPI	Protein-Protein Interaction
PSEN	Presenilin
PTM-SEA	Posttranslational Modification Signature Enrichment Analysis
R	SSRI Responder
RIN	RNA Integrity Number
RNA	Ribonucleic acid
RNase	Ribonuclease
RT-qPCR	Real-Time quantitative PCR
SEM	Standard Error of the Mean
siRNA	Small Interfering Ribonucleic Acid
SSRI	Selective Serotonin Reuptake Inhibitor
STAT3	Signal Transducer and Activator of Transcription 3
STK	Serine/Threonine Kinase
STRING	Search Tool for the Retrieval of Interacting Genes/Proteins
sXBP1	Spliced XBP1
TF	Transcription Factor
TIMP-1	Tissue Inhibitor of Metalloproteinase-1
TMS	Transcranial Magnetic Stimulation
TNF	Tumor Necrosis Factor

TOM	Topological Overlap Matrix
TRD	Treatment-Resistant Depression
uXBP1	unspliced XBP1
UKA	Upstream Kinase Analysis
ULM	Univariate Linear Model
UMAP	Uniform Manifold Approximation and Projection
UPR	Unfolded Protein Response
VEGFR	Vascular Endothelial Growth Factor Receptor
VIM	Vimentin
VST	Variance-Stabilizing Transformation
WGCNA	Weighted Gene Co-Expression Network Analysis
XBP1	X-Box Binding Protein 1
ZNF	Zinc Finger Protein

Chapter 1: Introduction

Major depressive disorder and treatment-resistant depression

Major Depressive Disorder (MDD) is one of the most common psychiatric illnesses and leading causes of global disability, with over 300 million individuals estimated to experience depression worldwide [1-3]. MDD can manifest with both cognitive and somatic symptoms, including weight change, sleep disturbance, psychomotor agitation or slowing, and persistent fatigue, alongside cognitive symptoms such as loss of interest or pleasure, persistent feelings of sadness or worthlessness, difficulty concentrating, and low mood recurring thoughts of death [4]. It is thought to be caused by the interaction of environmental, genetic, and neurobiological forces [5-9]. Genetic studies estimate that heritability of MDD ranges from 40% to 50%, suggesting that genetic factors, such as polymorphisms affecting serotonin transporter, neurotrophic pathways, and stress response, may influence the development of MDD [10]. Environmental factors, such as chronic psychosocial stress, early life adversity, socioeconomic disadvantage, social isolation, interpersonal trauma, occupational burnout, and lack of social support networks, have also been shown to contribute to the onset of MDD [1, 11]. Neurobiological factors involve alterations in neurotransmitter systems, including serotonin, norepinephrine, and dopamine imbalances, disrupted GABA and glutamate signaling pathways, dysregulated neurotrophin expression, impaired synaptic plasticity, altered hypothalamic-pituitary-adrenal (HPA) axis function, which are targeted by many antidepressant medications through mechanisms that enhance monoaminergic transmission, modulate receptor sensitivity [11]. Despite the widespread availability of antidepressant medications, many patients with MDD fail to achieve full remission of depressive symptoms with standard interventions. This is termed treatment-resistant

depression (TRD) and is defined as not having responded to two or more distinct antidepressant medications at appropriate doses and durations [12-16].

Patients with TRD are at higher risk of chronic depression, hospitalization, functional impairment, and comorbid medical conditions, including cardiovascular diseases, chronic kidney diseases, and cancers [17]. Moreover, TRD is associated with substantially higher healthcare costs and an overall lower quality of life when compared to non-treatment-resistant depression patients and the general population [18-21]. Studies indicate that TRD patients incur healthcare costs roughly double those of non-TRD patients, with annual costs potentially exceeding \$17,000 per patient [22]. Additionally, TRD is linked to a lower overall quality of life, characterized by reduced productivity, increased absenteeism, and employment challenges, with TRD patients experiencing an average of 35.8 work-loss days per year [22]. Attempts to address TRD involve a range of strategies, including augmentation or combination pharmacological approaches, such as the addition of lithium or second-generation antipsychotics to existing antidepressant regimens, as well as neuromodulatory interventions, including Deep Brain Stimulation (DBS) and Transcranial Magnetic Stimulation (TMS) [23-27]. Additionally, precision medicine strategies are being explored for their ability to improve outcomes in both MDD and TRD by personalizing treatments based on individual patient profiles. These precise approaches aim to estimate the likelihood of individual treatment response by integrating genetic, genomic, and clinical data, thereby allowing for earlier identification of treatment-resistant patients and preemptive personalization of treatment strategies [28-30]. However, the success of precision medicine has thus far been limited by our incomplete understanding of biological determinants of antidepressant response, underscoring the need for continued research into more effective and personalized interventions for depression.

Sporadic and familial Alzheimer's disease

Alzheimer's Disease (AD) is a progressive neurodegenerative disorder that has been implicated in approximately 60-70% of all dementia cases [31, 32]. Patients with AD typically present with progressive memory loss, cognitive decline, and behavioral symptoms such as anxiety, agitation, and aggression. These clinical manifestations have been largely attributed to the accumulation of amyloid- β ($A\beta$) plaques and hyperphosphorylated tau protein tangles. It has been hypothesized that the presence of these $A\beta$ plaques and tau tangles leads to CNS-wide synaptic dysfunction, chronic neuroinflammation, and neuronal death, which cumulatively produce the cognitive and functional deficits observed in AD patients [33-37]. AD can be broadly categorized into sporadic and familial subtypes. Approximately 95% of patients present with the sporadic form of AD, which is thought to arise from a confluence of genetic and environmental forces. In contrast, familial AD follows a more predictable pattern of autosomal dominant inheritance but only accounts for a small minority of AD cases. This autosomal dominant form of AD is primarily linked to genetic mutations in the amyloid precursor protein (APP) and presenilin 1/2 (PSEN1/2) genes, which can lead to early-onset AD that often manifests before the age of 65 [38]. Additionally, recent studies have attempted to delineate biological subtypes of AD based on the regional distribution of brain atrophy and tau-related pathology. Of these biological subtypes, typical AD is the most common subtype, accounting for approximately 55% of cases, while limbic-predominant, hippocampal-sparing, and minimal atrophy AD occur with frequencies of 21%, 17% and 15%, respectively [39].

The global public health impact of AD is substantial and continues to grow as life expectancies increase, and more people live to older ages, intensifying the socioeconomic burden

of the disease. In the United States, approximately 6.9 million people aged 65 and older are walking around with AD, and this estimate is expected to increase to 13.8 million by 2060, barring significant medical breakthroughs [31, 32]. This increase will strain healthcare systems and exacerbate the economic and social challenges associated with AD, including increased healthcare costs and the need for extensive caregiving. Although considerable progress has been made in our understanding of the molecular underpinnings of AD, effective disease-modifying therapies remain challenging to develop. Most pharmacotherapies explored thus far have shown limited success in clinical trials [35, 40]. For example, numerous drugs targeting amyloid- β , such as monoclonal antibodies, have failed to demonstrate significant benefits in slowing cognitive decline [41-43]. These disappointing results have led researchers to explore alternative mechanisms, such as neuroinflammation, dysregulated neurotransmission, and disruptions in extracellular matrix (ECM) remodeling, for potential therapeutic targets [44-47]. Moreover, multiple lines of evidence have indicated that AD does not manifest in isolation, with depression appearing as both an early symptom of AD and a risk factor for its development [48-50]. As such, elucidation of the pathophysiological pathways underlying both MDD and AD may provide critical insights into the development of more effective treatments for both neuropsychiatric and neurodegenerative disorders.

Epidemiological link between major depressive disorder and Alzheimer's disease

MDD and AD are among the most prevalent and debilitating brain disorders, with a growing body of evidence suggesting an epidemiological connection between them [50-54]. Depression has been identified both as a risk factor for developing AD and a common comorbidity in individuals with neurodegenerative disease, raising questions about whether it

serves as a prodromal phase of AD or an independent contributor to neurodegeneration [52, 55, 56]. Clinical studies have indicated that depression can precede cognitive decline by decades, suggesting that depression may contribute to or be an early indicator for progressive neurodegenerative diseases like AD [53, 57, 58]. This association appears to be particularly strong when depressive episodes occur in mid-to-late life, with several studies indicating that individuals with late-life depression may have up to a twofold higher risk of AD compared to those without depression [59-65]. Beyond its role as a risk factor, depression is also a common symptom in AD patients [66]. A substantial percentage of individuals with AD also experience depressive symptoms, though they can be difficult to diagnose and treat due to their overlap with the symptoms of dementia [67]. This bidirectional relationship between depression and AD highlights the need for further research into their shared underlying mechanisms and underscores the potential for this line of investigation to unlock never-before-realized treatments.

The significant epidemiological overlap between MDD and AD is complimented by the potential therapeutic crossover between pharmacological treatments for these conditions. The use of antidepressants, particularly selective serotonin reuptake inhibitors (SSRIs), in AD has shown promising preliminary results across multiple clinical trials. For instance, one previous study found that sertraline, an SSRI, was effective in treating major depression in AD patients [68]. Another found that mirtazapine, a tetracyclic antidepressant, was effective at managing anxiety, agitation, and depressive symptoms in AD patients, likely due to its antagonism of adrenergic α_2 and serotonergic 5-HT₂ and 5-HT₃ receptors [69]. Beyond mood improvement, studies have also shown that long-term SSRI treatment cannot only improve mild cognitive impairment (MCI) and cognitive function in patients with AD but may also delay the progression from MCI to AD [57]. Anti-Alzheimer's medications have similarly been explored for their potential antidepressant

effects. For instance, cholinesterase inhibitors (ChEIs), though originally prescribed to treat cognitive symptoms, have been found to also improve behavioral symptoms in patients with AD [70]. However, research specifically examining the therapeutic impact of ChEIs on depression in AD remains limited. Furthermore, recent clinical trials for anti-amyloid therapies like lecanemab and donanemab have focused primarily on cognitive outcomes in clinical trials at the expense of assessing their impact on depression or other behavioral symptoms of dementia [71]. Moreover, the specific exclusion of patients with significant psychiatric symptoms from these trials limits their applicability to the nontrivial subset of AD patients with depression and perpetuates the gaps in our knowledge of the interaction between two of the most pervasive brain disorders.

Precision medicine approaches to major depressive disorder and Alzheimer's disease

Traditional one-size-fits-all treatment strategies have shown limited efficacy in both MDD and AD due to the complex and heterogeneous nature of these disorders, highlighting the need for personalized treatment strategies. Precision medicine approaches aim to improve the diagnosis, treatment, and prevention of disorders by accounting for patient-specific genetic, molecular, and environmental factors [6, 7, 30, 72-74]. Advances in omics and multi-omics technologies, including genomics, transcriptomics, proteomics, metabolomics, and kinomics, have enabled the identification of distinct molecular subtypes of MDD and AD, which may respond differentially to targeted interventions [75-79]. For instance, prior studies using human-induced pluripotent stem cells (hiPSC) combined MDD-relevant hiPSC-derived cells with environmental perturbations to explore the gene-environment interactions underlying predisposition to MDD [77]. Additionally, precision medicine approaches in AD aim to address multiple contributors to cognitive decline, such as insulin resistance, hyperlipidemia, and

inflammation, by using comprehensive biomarker testing, genetic screening, imaging, and lifestyle assessments to tailor interventions based on individual patient profiles [74]. As research progresses, machine learning (ML) models leveraging patient-specific biomarker profiles and clinical histories show promise for optimizing treatment selection for AD as well as MDD [80-83]. In theory, ML-assisted precision medicine approaches could facilitate the stratification of MDD and AD patients to enable more personalized and effective treatment strategies. For example, these strategies could facilitate the identification of MDD and AD patient subgroups with heightened inflammatory responses as having a higher-than-average chance of responding positively to the administration of anti-inflammatory or immunomodulatory agents [84-86]. Similarly, such approaches could identify individuals with dysregulated neurotrophic signaling, particularly those with altered BDNF levels, who may benefit from therapies like ketamine that have been shown to enhance neuroplasticity through BDNF-related pathways [57, 87, 88]. This integration of precision medicine into clinical practices has the potential to enable the earlier administration of more effective interventions but has thus far been limited by our inadequate understanding of the biological determinants of treatment response, highlighting the need for continued research into the shared pathophysiology of MDD and AD.

Modeling major depressive disorder and Alzheimer's disease using hiPSC-derived neurons

iPSC technology has gained recognition as a powerful tool for probing the molecular and cellular mechanisms underlying brain disorders. These cells can be differentiated into astrocytes, neurons, or microglia to provide a physiologically relevant platform for exploring disease mechanisms, discovering novel drug targets, and screening potentially therapeutic compounds [89-93]. By capturing patient-specific symptom histories and genetic profiles, iPSC models

allow researchers to study patient-specific differences in gene expression and cellular function, enabling personalized disease modeling that mirrors the unique biological characteristics of each individual and providing insights that are not fully captured in traditional animal models [89, 94-97]. This is particularly advantageous because traditional animal models often fail to replicate the complex genetic factors that contribute to human brain disorders and may not accurately reflect the genetic diversity seen in human populations [98]. Postmortem brain studies also provide a translational element that is difficult to replicate in animal models, making them valuable for understanding disease pathophysiology, but they come with their own significant limitations, including the effect of the postmortem interval on tissue quality, the reliance of postmortem studies on limited clinical information, and the demographic bias in the availability of postmortem brain tissue [99-102]. Unlike these traditional animal and postmortem brain models, iPSC technology offers controlled and experimentally manipulable disease models that capture the patient-specific genetic factors underlying human brain disorders.

iPSC-derived neuron models have provided key insights into the molecular and cellular dysfunctions underlying both MDD and AD [89, 90, 95, 103]. iPSC-derived neurons from MDD patients display significantly impaired synaptic plasticity, as evidenced by diminished dendritic complexity, altered spine morphology, and decreased synaptic transmission [89, 90, 104-106]. Neurons from MDD patients also presented with dysregulated BDNF signaling, supporting the role of this neuronal survival and synaptic plasticity in the pathogenesis of depression [107, 108]. In AD, iPSC-derived neurons from patients with familial and sporadic forms of the disease have demonstrated alterations in A β production, tau phosphorylation, and mitochondrial dysfunction [109-111]. These neurons also exhibited impaired bioenergetics and heightened susceptibility to oxidative stress, which are thought to produce neurodegeneration over time [109, 112]. Studies

have also shown that inflammatory signaling pathways involving NF- κ B are upregulated in neurons and brain tissue from AD patients, as well as *in vivo* models of AD [113, 114]. Despite the nascency of this field, iPSC-derived neurons have already begun unraveling the intricate neuron-specific molecular and cellular mechanisms of these disorders.

Recent studies have also begun to explore common molecular signatures between MDD and AD using iPSC-derived neurons. These studies have observed shared features between these disorders, including dysregulated stress response pathways, impaired neurotrophic signaling, increased oxidative stress, and epigenetic alterations in both MDD and AD models [89, 115-121]. However, no investigations thus far have directly compared these two conditions in a head-to-head study of MDD and AD patient-derived hiPSC models. As iPSC technology continues to evolve, its integration into neuropsychiatric and neurodegenerative disease research will be instrumental in uncovering novel mechanistic insights and advancing personalized treatment strategies within these overlapping populations.

hiPSC-derived astrocytes models of major depressive disorder and Alzheimer's disease

Astrocytes are the most abundant cell type in the central nervous system (CNS), outnumbering neurons, oligodendrocytes, and microglia [122]. These cells not only provide structural and metabolic support for neurons but also play an active role in maintaining brain homeostasis [123]. They directly modulate synaptic function by regulating neurotransmitter uptake, synaptic plasticity, and neuronal excitability through mechanisms such as glutamate and GABA transport, calcium signaling, and gliotransmitter release [124-127]. Astrocytes are highly enriched for excitatory amino acid transporters (EAATs), namely EAAT1 (GLAST) and EAAT2 (GLT-1), which enable them to act as high-efficiency filtration systems for clearing excess glutamate to

prevent excitotoxicity while maintaining sufficient availability for proper synaptic function [128-131]. In addition to glutamate filtration, astrocytes also release signaling molecules such as ATP, D-serine, and GABA, which modulate synaptic strength, plasticity, and neuronal excitability in a dynamic, activity-dependent manner. For instance, ATP can influence neuronal activity via P2X and P2Y receptors, GABA can modulate inhibitory synaptic transmission, and D-serine can act as a co-agonist at NMDA receptors, facilitating synaptic plasticity and learning processes [126, 132, 133]. Rather than merely supporting neurons, astrocytes dynamically fine-tune the synaptic environment to ensure the optimal function of neural circuits by precisely regulating levels of neurotransmitters and gliotransmitters.

Beyond glutamate clearance and gliotransmitter release, the diverse synaptic functions of astrocytes are further enhanced by their ability to regulate the extracellular space in which neurons operate. The ECM is a complicated network of proteins and polysaccharides surrounding neurons and glia in the CNS. It occupies approximately 20% of total adult brain volume and provides critical structural and biochemical support to the CNS [134-137]. Astrocytes dynamically regulate ECM turnover by producing and degrading key matrix components, such as hyaluronic acid (HA), chondroitin sulfate proteoglycans, and tenascin C, through interactions with matrix metalloproteinases (MMPs) and tissue inhibitors of metalloproteinases (TIMPs) like TIMP-1. This regulation influences various aspects of both healthy and diseased brain physiology, including synaptic organization, plasticity, and neuronal migration [138-145]. This interplay between astrocytes and the ECM represents yet another dimension of astrocytic function in the broader context of brain homeostasis and protection.

Beyond their roles in synaptic maintenance and ECM regulation, astrocytes are also key regulators of neuroimmune signaling, responding to and producing cytokines, chemokines, and

other inflammatory mediators [146, 147]. Under homeostatic conditions, astrocytes help maintain an anti-inflammatory environment in the CNS by secreting neuroprotective factors, modulating microglial activity, and regulating neurotransmitter levels. This function is critical not only for maintaining brain homeostasis and protecting neurons from potential damage but also for the pathophysiology of neuropsychiatric and neurodegenerative disorders [148-151]. Astrocytes can modulate microglial activity by influencing their phenotypic switch between pro-inflammatory (M1) and anti-inflammatory (M2) states. For instance, astrocytes can secrete factors that promote the M2 phenotype, which is associated with tissue repair and anti-inflammatory responses [152]. This bidirectional communication between astrocytes and microglia represents a crucial regulatory axis in the brain's immune response, with significant implications for both neuropsychiatric and neurodegenerative conditions.

For much of the 20th century, research on these disorders was overwhelmingly neuron-focused, with pathological changes in neuronal activity, connectivity, and degeneration viewed as the primary drivers of disease [153, 154]. This neuron-centric paradigm shaped the development of therapeutics, leading to interventions aimed at restoring neurotransmitter balance, enhancing synaptic plasticity, or preventing neuronal loss [155-157]. However, the limited efficacy of these approaches in treating complex brain disorders, such as MDD and AD, has highlighted the need for a broader perspective [15, 158]. In recent decades, growing evidence has implicated glial cells, particularly astrocytes, which were historically regarded as passive support cells, as active regulators of synaptic plasticity, neuroimmune interactions, BBB integrity, and ECM remodeling, and central players in both neuropsychiatric and neurodegenerative pathophysiology [127, 159-170]. Their role in modulating synaptic function, regulating neuroimmune signaling, and

maintaining the structural environment of the brain highlights the importance of considering glial contributions in disease mechanisms.

In the context of MDD and AD, astrocyte dysfunction is being increasingly recognized as a key factor contributing to synaptic deficits, chronic neuroinflammation, and altered ECM dynamics, making astrocytes a compelling target for therapeutic development [160, 171-173]. In MDD, postmortem studies and neuroimaging data have revealed astrocyte atrophy, reduced astrocytic markers, and impaired glutamate clearance [171, 174, 175]. These findings suggest that astrocytic dysfunction contributes to synaptic and network dysregulation observed in depression, particularly in corticolimbic circuits involved in mood regulation [176]. In AD, astrocytes associated with amyloid plaques have been found to exhibit similar morphological, molecular, and functional alterations. Prior studies of these astrocytes have revealed alterations in ECM production and remodeling, including increased activity of MMP-2 and MMP-9, which contribute to abnormal matrix composition, blood-brain barrier (BBB) breakdown, and neuroinflammatory responses that may exacerbate neurodegeneration and impair synaptic function [177-183]. These astrocytes also display increased secretion of inflammatory factors and dysregulation of immunoinflammatory kinase signaling pathways, including JAK/STAT3 and NF- κ B, which are linked to synaptic deficits and cognitive decline in neurodegenerative disorders such as AD can contribute to neuroinflammation and neurodegeneration [171, 179, 184-197]. Collectively, these core functions position astrocytes as critical mediators of neural health and disease, and their dysregulation in MDD and AD suggests a shared pathological axis involving synaptic failure, chronic inflammation, and ECM disruption.

This shift toward a more comprehensive neuron-glia model has expanded our conception of brain function and disease, revealing astrocytes as key contributors to brain pathology and

opening new avenues for therapeutic development targeting glial dysfunction. Understanding astrocyte-specific contributions to these diseases could inform novel therapeutic strategies aimed at restoring glial function to improve neuropsychiatric and neurodegenerative outcomes. The recognition of astrocytes as active contributors to brain disorders has profound implications for therapeutic development. Traditional pharmacological treatments for MDD, such as SSRIs, primarily target neuronal monoaminergic systems. However, growing evidence suggests that astrocyte dysfunction plays a significant role in MDD pathophysiology, potentially contributing to treatment resistance in some cases [176, 198]. Likewise, recent failures of amyloid-targeting drugs in AD clinical trials suggest that targeting amyloid accumulation alone may be insufficient to halt disease progression, indicating a more complex pathophysiology [199, 200]. Targeting astrocytes presents a promising avenue for therapeutic exploration in neurodegenerative and neuroinflammatory disorders. This approach can involve modulating astrocyte inflammatory responses, enhancing their neuroprotective functions, or targeting specific pathways within astrocytes [191, 201-204]. As the field continues to move beyond a neuron-centric framework, understanding the molecular and functional contributions of astrocytes to brain disorders will be critical in developing more effective pharmacotherapies.

Despite this growing recognition of astrocytes' involvement in MDD and AD, existing research models have limitations in capturing patient-specific astrocyte dysfunction. Postmortem tissue analyses provide valuable but static snapshots of disease states, while animal and *in vitro* models struggle to fully replicate human astrocyte biology and disease pathology [171, 176, 205-209]. These limitations underscore the need for advanced research techniques to better understand the dynamic role of astrocytes in these disorders. hiPSC-derived astrocytes address many limitations of traditional research models, allowing for investigation of patient-specific

astrocyte phenotypes, disease-relevant molecular mechanisms, and potential therapeutic targets. These models provide a valuable platform for studying astrocyte contributions to disease pathology in a controlled, patient-relevant context, enabling the identification of novel pathways that may not be captured in traditional systems [90, 210-216]. hiPSC-derived astrocytes can reveal molecular targets and disease phenotypes that may remain elusive in conventional models by capturing patient-specific genomic backgrounds. This approach supports the development of personalized therapeutic strategies. By leveraging patient-derived hiPSC astrocytes, researchers can investigate disease-specific astrocyte dysfunction, explore potential astrocyte-targeted therapies, and develop precision medicine approaches for neurodegenerative disorders, including those associated with MDD.

The studies to follow aim to (1) determine the molecular mechanisms mediating antidepressant effects in astrocytes by delineating astrocyte-specific signatures of antidepressant response and identifying novel targets for astrocyte-based antidepressant development, (2) identify novel therapeutic targets for AD by investigating astrocyte-specific pathways underlying familial AD and assessing the impact of manipulating newly identified AD risk genes in astrocytes, and (3) determine common astrocyte features in relation to depression and AD by examining shared molecular and functional alterations and assessing how astrocyte dysfunction in MDD may contribute to AD pathogenesis. Through these investigations, hiPSC-derived astrocyte models will serve as a foundation for advancing precision medicine approaches, providing new insights into astrocyte-driven mechanisms that may inform the development of targeted therapies for both disorders.

Chapter 2: Astrocyte-mediated neuroimmune dysfunction and extracellular matrix remodeling define a cellular biomarker of SSRI-resistant depression

Abstract

MDD is a debilitating psychiatric condition that significantly strains healthcare systems across the globe. This strain is further exacerbated by the cases of TRD, wherein patients inadequately respond to multiple courses of antidepressants. Precision medicine aims to address this challenge by personalizing treatments based on individual molecular and clinical characteristics. In line with this approach, the present study sought to delineate the molecular signatures of patients who had clinically responded to SSRIs and those who had not, with a specific emphasis on astrocytes. As key regulators of neurotransmitter metabolism, synaptic activity, and neuroimmune responses, astrocytes have increasingly been implicated in the underlying pathophysiology of depression. To explore patient-specific genetic variations in these pathways, we used hiPSC technology to generate astrocytes from SSRI responders, nonresponders, and healthy controls. Our comprehensive transcriptomic profiling, differential gene expression assessment, and coexpression network analysis revealed significant differences in immune signaling, extracellular matrix remodeling, and cell cycle regulation between SSRI responders and nonresponders, while transcription factor analysis further indicated altered unfolded protein response signaling in nonresponders. Additionally, LINCS-based computational screening of established transcriptomic signatures identified novel repurposing candidates and preclinical compounds with the potential to counteract the differential gene expression observed in patient-derived astrocytes. Collectively, these results provide a foundation for levying patient-specific astrocyte

models to advance predictive biomarkers of SSRI efficacy while improving treatment outcomes through innovative astrocyte-targeted pharmacotherapies.

Introduction

Major depressive disorder (MDD) is one of the most pervasive mental illnesses, contributing substantially to disability and healthcare costs around the world [1, 217-219]. MDD is characterized by persistent depressed mood and anhedonia, often accompanied by psychomotor dysregulation, sleep disturbances, persistent fatigue, and impaired concentration. These symptoms significantly impair occupational functioning, social relationships, and overall quality of life, with substantial reductions in psychosocial functioning persisting even during periods of symptomatic remission [5, 8, 220-222]. While a range of pharmacological and psychotherapeutic treatments is available, some patients experience only partial improvement or fail to respond at all [158, 223-225]. Patients who fail to respond to adequate courses of at least two different classes of antidepressants are deemed to have treatment-resistant depression (TRD) [13, 226, 227]. These patients incur significantly higher healthcare costs, experience more hospitalizations, and suffer nearly twice as much work loss as non-TRD patients do [228], highlighting the urgent need for more effective interventions.

Precision medicine offers a promising route for improving therapeutic interventions by personalizing prescriptions based on the genetic makeup, treatment history, and biomarker profiles of individual patients [229]. The observed variability in response to different classes of antidepressants, along with advances in understanding individual biological and environmental factors, supports the potential of precision medicine approaches to improve treatment outcomes in major depressive disorder [28, 79, 230, 231]. For example, while SSRIs are commonly

prescribed for MDD, research indicates that a significant proportion of patients experience partial response or fail to achieve remission. Meta-analyses suggest that absolute efficacy rates for antidepressants are around 50%, with remission rates for SSRI therapy specifically ranging from 23% to 45% [232-235]. Variations in antidepressant efficacy can be attributed to multiple factors, including common genetic variants, alterations in neurotransmitter systems, and changes in cellular signaling pathways, with genetic factors alone potentially explaining up to 42% of individual differences in treatment response [236-239]. Recent advances in genomics, transcriptomics, and proteomics have identified potential biomarkers for predicting antidepressant response, offering hope for a future with refined patient stratification and improved antidepressant selection [240-243]. Personalized medicine approaches and pharmacogenetics-guided interventions for MDD show promise for improving treatment efficacy and reducing adverse effects. However, the application of this precision approach to MDD is constrained by the gaps in our understanding of the neurobiological, molecular, and pathophysiological underpinnings of TRD [16, 28].

Human induced pluripotent stem cell (hiPSC) technology has established itself as a powerful platform for studying the molecular underpinnings of depression and antidepressant response [244-246]. These studies have primarily focused on neurons, resulting in significant insights into neuron-specific disease mechanisms. Profiling of hiPSC-derived neurons from MDD patients has revealed distinct gene expression patterns, electrophysiological profiles, and cellular phenotypes in MDD [89, 247-249]. hiPSC-derived neurons have also enabled researchers to investigate the transcriptional and functional consequences of antidepressant treatment in patient-specific models [247, 250, 251]. Collectively, these studies provide valuable insights into the neuronal mechanisms associated with depression and antidepressant response.

However, emerging evidence warrants a closer examination of the role that astrocytes play in MDD pathophysiology [[214](#), [247](#), [252](#)].

In addition to being the most abundant cells in the central nervous system (CNS), astrocytes are also instrumental in regulating neurotransmitter metabolism, providing metabolic support, and modulating immune activity via cytokine and chemokine release [[146](#), [198](#), [253-255](#)]. However, systematic exploration of astrocyte-specific contributions to antidepressant response, particularly in treatment-resistant cases, remains limited. In the present study, we address this gap by investigating hiPSC-derived astrocytes from SSRI responders, nonresponders, and healthy controls. We extensively analyze gene expression in these patient-specific astrocyte models to identify differentially expressed genes and dysregulated signaling pathways that may be associated with SSRI resistance. We further employ network-based gene correlation analyses and drug-gene signature screening to identify coordinated gene modules and to predict potential therapeutic compounds. Through this multifaceted approach, we aim to facilitate the development of more effective treatments for patients who are currently underserved by current standard-of-care antidepressants.

Materials and methods

Subjects

Healthy control (HC), SSRI-responder (R), and SSRI-nonresponder (NR) subjects were participants in the Pharmacogenomics Research Network Antidepressant Medication Pharmacogenomic Study (PGRN-AMPS), as previously described [[256](#)]. Patients were adult females between the ages of 33 and 53. Treatment outcomes were determined via the HAMD-17 and QIDS-C16 [[257](#)] depression rating scales before the start of SSRI (20 mg of citalopram or 10

mg of escitalopram) treatment and 8 weeks after SSRI treatment. Patient blood samples were collected, and drug levels were measured as previously described [256]. SSRI-Rs and -NRs were selected on the basis of treatment outcomes after 8 weeks in PGRN-AMPS, and skin punch biopsies from subjects were obtained under sterile conditions for further studies. Risks and benefits were discussed with the study participants, and all the subjects provided written informed consent at the start of the study. All procedures were monitored and approved by the Institutional Review Board of the Mayo Clinic or the Salk Institute. Fibroblasts from punch biopsies of patients and healthy controls were cultured and reprogrammed into iPSCs as previously described [258]. Three healthy control (HC-001, HC-002, HC-003), three SSRI-responder (R-001, R-002, R-003), and three SSRI-nonresponder (NR-001, NR-002, NR-003) human iPSC lines were generated and fully characterized as previously described [258]. The healthy control, SSRI-responder, and SSRI-nonresponder subjects from which our iPSCs were derived were matched for age and sex. For our analyses, SSRI-responder and SSRI-nonresponder cells were compared with nonisogenic healthy controls. All experiments were performed in compliance with the relevant laws and institutional guidelines.

hiPSC culture and astrocyte differentiation

Human iPSCs were cultured in mTeSR1 medium (Stemcell Technologies, 85850) in cell culture dishes coated with Geltrex LDEV-Free Reduced Growth Factor Basement Membrane Matrix (Gibco, A1413201) diluted 1:100 in DMEM/F-12 (Gibco, 11320033). Briefly, mTeSR1 was replaced every other day or every day once the cells reached 50% confluence. When 80–90% confluent, the cells were passaged as follows: aspirating media, washing with DPBS, incubating with ReLeSR (Stemcell Technologies, 100–0484) at RT for 3 minutes, aspirating with

ReLeSR, incubating at 37°C for 10 minutes, resuspending in mTeSR1 supplemented with 10 nM Y-27632 dihydrochloride ROCK inhibitor (Tocris, 125410), counting, and plating onto Geltrex-coated plates at the desired number.

Human iPSC-derived astrocytes were generated as previously described [259]. Briefly, iPSCs were plated on Geltrex-coated 6-well plates and infected with rtTA, SOX9, or NFIB lentivirus. On Day 0, the medium was replaced with fresh mTeSR-1 media containing 2.5 µg/mL doxycycline. From Days 1-7, the cells were cultured in expansion medium (DMEM/F12, 10% FBS, 1% N2, 1.25 µg/mL puromycin, and 200 µg/mL hygromycin) and gradually transitioned to FGF medium (Neurobasal, 2% B27, 1% NEAA, 1% GlutaMax, 1% FBS, 8 ng/mL FGF, 5 ng/mL CNTF, 10 ng/mL BMP4, and 200 µg/mL hygromycin) by Day 7. On Day 7, the cells were dissociated via StemPro Accutase Cell Dissociation Reagent (Gibco, A1110501) for 10 minutes and then replated on Geltrex-coated 6-well plates in FGF medium. From Day 9, the FGF medium was changed to maturation medium (1:1 DMEM/F12 and neurobasal medium, 1% N2, 1% sodium pyruvate, 10 µg/µL NAC, 10 µg/µL hbEGF, 10 ng/mL CNTF, 10 ng/mL BMP4, and 500 µg/mL cAMP), and half of the medium was changed every 2–3 days.

Immunocytochemistry

For immunocytochemistry, astrocytes were fixed with 4% paraformaldehyde for 15 min at room temperature. The samples were permeabilized and blocked with 0.25% Triton X-100 and 10% donkey serum in PBS for 20 min, as previously described [260]. The samples were then incubated with anti-GFAP (rat, 1:500; Invitrogen, 13-0300) and anti-VIM (mouse, 1:500; Abcam, ab8978) primary antibodies at 4°C overnight, followed by incubation with secondary antibodies (donkey anti-rat Alexa Fluor 488, 1:1000; Invitrogen A-21208; donkey anti-mouse

Alexa Fluor 568, 1:1000; Invitrogen A10037) for 2 hours at room temperature. Coverslips were mounted with Fluoromount-G (Southern Biotech, 0100-01) and imaged via a Nikon Eclipse Ti-E microscope.

RNA extraction and sequencing

Total RNA was extracted from each of the nine hiPSC-derived astrocyte cell lines via TRIzol reagent (Invitrogen, 15596026) per the manufacturer's instructions. Total RNA from each line was treated with DNase I (Zymo Research, E1010) and then cleaned and concentrated via the Clean & Concentrator Kit (Zymo Research, D4033). A NanoDrop One/OneC Microvolume UV-Vis Spectrophotometer (Thermo Scientific, ND-ONE-W) was then used to determine the RNA yield from each of the nine RNA extractions. For RNA sequencing (RNA-seq), 150-cycle PE sequencing via the Illumina HiSeq2500 platform was performed by Admera Health (South Plainfield, New Jersey, United States) with 1 μ g of RNase-free RNA (>10 ng/ μ L, RIN > 7) per technical triplicate for each of the nine lines.

Differential gene expression analysis

For transcriptomic analysis, RNA-seq reads were trimmed via Trimmomatic Version 0.40 [261] and aligned against the human reference transcriptome (GRCh38.p14) [262] via Salmon v1.9.0 [263]. Transcriptome-wide gene counts were obtained through gene-level transcript summarization with the tximeta R package [264]. Differential gene expression analysis was performed after filtering out genes with low expression, followed by variance-stabilizing transformation (VST) for downstream analysis via the DESeq2 R package [265]. The ggplot2 R package was used for volcano plots to depict differential expression profiles [266]. The volcano

plots display the difference in gene expression ($\log_2\text{FoldChange}$) between experimental comparisons and significance values ($\log_{10}(\text{adjusted } p \text{ value})$), with thresholds of adjusted p values < 0.05 and absolute $\log_2\text{FoldChange}$ values > 1.2 .

Pathway enrichment analysis

Gene Ontology (GO) enrichment analyses for biological processes (BP), molecular functions (MF), and cellular components (CC) were performed via the clusterProfiler R package in conjunction with the org.Hs.eg.db annotation package [267-270]. The DEGs were first divided into upregulated (adjusted p value < 0.05 and $\log_2\text{FoldChange} > 1.2$) and downregulated (adjusted p value < 0.05 and $\log_2\text{FoldChange} < -1.2$) groups. The gene symbols were then converted to Entrez IDs via the bitr function [267-270]. For each GO, enrichment analysis was conducted separately for the upregulated and downregulated gene sets via the enrichGO function [267-270], with the p value and q value cutoff set at 0.05. The results across the three ontologies were combined, and for visualization, the top five GO terms per regulation direction (based on $-\log_{10}(\text{adjusted } p \text{ value})$) [266].

Weighted gene coexpression network analysis

Weighted gene coexpression network analysis

To identify gene co-expression modules associated with NR and R status relative to HC, we performed a Weighted Gene Co-Expression Network Analysis (WGCNA). For WGCNA, gene expression variance was calculated via the R package matrixStats [271], and the top 50% of the most variable genes were retained. Network analysis was performed via the R package WGCNA to identify gene modules with coordinated expression patterns [272, 273]. A soft-

thresholding power was selected on the basis of scale-free topology criteria to construct an adjacency matrix, which was transformed into a topological overlap matrix (TOM) to account for gene connectivity. Genes were hierarchically clustered via average linkages on the basis of TOM-derived dissimilarity, and dynamic tree cutting was applied to define modules. Module eigenvalues were compared between NR and HC groups, and p values were calculated using Welch's t -tests. The same approach was applied to identify significant modules in R vs. HC. Modules with significant correlations were further analyzed via enrichment analysis to identify biological functions and pathways associated with module genes. Gene set enrichment analysis was conducted to identify biological pathways associated with significant modules, leveraging annotations from GO.db [274, 275]. The modules were annotated based on known biological processes, excluding those lacking functional annotation (i.e., those with no significant pathway enrichment).

Protein-protein interaction network analysis of divergent modules

To investigate the protein-protein interaction (PPI) networks of divergent modules across responders and non-responders versus healthy controls, STRINGdb (v11.0, species 9606, score threshold = 400) was used to map gene symbols from each module to their STRING protein identifiers. PPI interactions were retrieved, and networks were constructed using the igraph package. Each module-specific network was visualized using the Graphopt layout algorithm, with nodes representing genes and edges representing known PPIs. Nodes were colored based on \log_2 fold-change values from the NR vs. R contrast, using a gradient from blue (downregulated in NR) to red (upregulated in NR). Node sizes were scaled according to the absolute \log_2 fold-change value.

Transcription factor activity inference

Transcription factor (TF) activity was inferred from bulk RNA-seq data using the decoupleR package. Differential expression analysis was performed with DESeq2 and differentially expressed genes (DEGs) with an adjusted p value below 0.05 were retained for TF activity estimation. The univariate linear model (ULM) method from decoupleR was applied to infer TF activity scores using the CollecTRI network as a prior knowledge source of TF-target interactions. For each TF, ULM fits a linear model where the t -values of differentially expressed genes serve as input, and the inferred activity score represents the estimated regulatory influence of the TF. Positive scores indicate TF activation, while negative scores suggest inhibition. The results were visualized by selecting the top 10 activated and deactivated TFs for each contrast and plotting their activity scores as bar plots.

Transcription factor activity overlap analysis

To visualize the overlap between TF activity changes across conditions, we generated a four-set Venn diagram using the VennDiagram package. The four TF sets were defined as Activated in R vs. HC, Activated in NR vs. HC, Deactivated in R vs. HC, and Deactivated in NR vs. HC. For each set, we computed the number of TFs and their pairwise, triple, and quadruple intersections. To complement the Venn diagram, we used the UpSetR package to create an UpSet plot, which provides a quantitative representation of TF set intersections. A binary matrix was constructed to indicate TF membership across the four conditions, and intersections were ranked by frequency.

Correlation analysis of transcription factor activity across conditions

To evaluate the concordance of TF activity between R and NR conditions relative to HC, we computed the Pearson correlation between TF activity scores inferred using the ULM method from decoupleR. TF activity scores from the R vs. HC and NR vs. HC contrasts were merged based on TF identity, and a Pearson correlation coefficient (r) was calculated along with the associated p value to assess statistical significance. A scatter plot was generated using ggplot2 to visualize the correlation between TF activity scores in the two contrasts. Each point represents a TF, with its activity score in R vs. HC, plotted on the x-axis and NR vs. HC on the y-axis. A dashed linear regression line with a confidence interval was overlaid to illustrate the trend.

Protein-protein interaction network analysis of differentially active transcription factors

To investigate TFs with differential activity between NR vs. R relative to HC, we computed the difference in TF activity scores (NR vs. HC minus R vs. HC). A distribution-based filtering approach was used to identify TFs with the most substantial activity differences by selecting those in the top 25th percentile of absolute differential scores. To assess PPIs among these differentially active TFs, we utilized the STRING database (v11.0, species: Homo sapiens, minimum confidence score = 700). TFs that met the filtering threshold were mapped to their corresponding STRING protein identifiers, and known PPI interactions were retrieved. An undirected graph representation of the network was constructed using igraph, where nodes represent TFs, and edges represent PPIs. For network visualization, we applied a Graphopt force-directed layout. To identify the most influential TFs within this network, we calculated multiple centrality measures including degree, betweenness, closeness, eigenvector centrality, and PageRank. These metrics were normalized to a 0-1 scale to ensure comparability across different

measures. For each TF, we computed a composite score by averaging the normalized centrality values, and a composite rank based on the average ranking across all metrics.

Real-time PCR quantification of spliced X-box binding protein 1

X-box binding protein 1 (XBP1) splicing activity in total RNA extracts from each of the nine hiPSC-derived astrocyte cell lines was detected was quantitatively determined via real-time PCR using specific primer sets for unspliced XBP1 (forward: 5'-CAGACTACGTGCACCTCTGC-3', reverse: 5'-CTGGGTCCAAGTTGTCCAGAAT-3') and spliced XBP1 (forward: 5'-GCTGAGTCCGCAGCAGCAGGT-3', reverse: 5'-CTGGGTCCAAGTTGTCCAGAAT-3') [276], with GAPDH used as the housekeeping gene (forward: 5'-CCATGAGAAGTATGACAACAGCC-3', reverse: 5'-GGGTGCTAAGCAGTTGGTG-3'). Total RNA was reverse transcribed and amplified using the Luna Universal One-Step RT-qPCR Kit (New England Biolabs, E3005E) following the manufacturer's protocol in a QuantStudio 6 Real-Time PCR System (Applied Biosystems, 4485692) under standard cycling conditions. Relative expression levels were calculated via the $\Delta\Delta\text{Ct}$ method [277], with GAPDH used as the housekeeping gene for normalization. Fold changes in gene expression were determined as $2^{(-\Delta\Delta\text{Ct})}$, and the ratio of spliced XBP1 (sXBP1) to unspliced XBP1 (uXBP1) was computed. Additionally, statistical analysis and visualization of uXBP1, sXBP1, and the sXBP1:uXBP1 ratio were performed via the R packages ggplot2 [266] and ggpubr [278].

Analysis of transcription factor target expression

To generate a heatmap of XBP1 target genes, XBP1 target genes were identified from a curated list obtained from the TFLink database, which provides experimentally validated transcription factor–target gene interactions [279]. These targets were cross-referenced with significant DEGs ($\log_2\text{FoldChange} > 1.2$, $\text{padj} < 0.05$). Z scores were calculated via the scale function in R, ensuring normalized values for comparison across samples [280]. Hierarchical clustering was performed on the expression matrix via hclust, and clusters were assigned via cutree [281]. The optimal number of clusters was determined via silhouette analysis via the cluster package [282]. GO enrichment analysis was conducted on clustered genes to generate GO term-based row annotations.

LINCS-based identification of discordant perturbagens

To identify small-molecule perturbagens that are predicted to reverse transcriptional alterations in astrocytes associated with MDD, we queried the Library of Integrated Network-based Cellular Signatures (LINCS). DEGs between R vs. HC-iA and NR vs. HC-iA conditions were used to generate discordant perturbagen lists. LINCS similarity scores were calculated to rank compounds on the basis of their potential to induce gene expression profiles opposing those observed in the astrocyte subtypes. LINCS similarity data for R and NR discordant perturbagens were processed to filter for compounds unique to each condition. Overlapping discordant perturbagens between LINCS analysis and FDA-approved antidepressants were determined. The top-ranked discordant perturbagens were selected on the basis of absolute similarity scores, and a Venn diagram was generated to visualize overlaps between R and NR discordant perturbagens

and FDA-approved antidepressants. A bar plot was created to depict the overlap between R discordant perturbagens and FDA-approved antidepressants.

To identify perturbagens with discordant R and NR targeting key regulatory genes, we performed a network-based core node analysis. The DEGs in R and NR relative to HC were used to retrieve PPI data on curated biological networks. The network topology was then constructed, and rich-club analysis was performed to determine whether a subset of nodes displayed higher-than-expected connectivity, as previously described [283] (Supplementary Table S13, Supplementary Table S14). The genes most highly connected in the network on the basis of degree, betweenness, and clustering coefficients were extracted and compared against LINCS-predicted discordant perturbagen targets to determine whether their modulation might explain the transcriptional reversal effects observed in R and NR astrocytes. To prioritize perturbagens predicted to influence these key astrocytic targets, LINCS discordant perturbagen lists were filtered to retain only those targeting core nodes. The resulting core node-targeting perturbagens were further classified into FDA-approved drugs and preclinical small molecules. Bar plots were generated to visualize the top 10 FDA-approved and top 10 preclinical perturbagens targeting core nodes, which were ranked by the absolute similarity score.

Statistical analysis and data visualization

All data processing and statistical analyses were performed in R [281, 284-286]. Statistical significance was assessed using independent two-sample t-tests to compare group means, evaluating differences between SSRI responder and nonresponder patients versus healthy controls. Welch's correction was applied when variances were unequal. Pearson's correlation coefficient (r) was calculated to assess the strength and direction of linear. The significance of

correlations was determined using corresponding p values, with multiple testing corrections applied where necessary. Values are presented as the mean with the standard error of the mean (SEM). A p value threshold of 0.05 was used for general statistical tests, while an adjusted p value of 0.05 was applied for genomic analyses to account for multiple comparisons.

Results

Astrocytic molecular signatures linked to SSRI responsiveness in MDD

To delineate the cell-type-resolved molecular signatures associated with MDD with differential SSRI treatment responses, we used a transcription factor-induction approach [259] (Figure 1.1A) to differentiate astrocytes from hiPSC lines derived from three SSRI responder MDD patients (R), three SSRI nonresponder MDD patients, and three healthy control individuals (HC), who were participants in the PGRN-AMPS study at Mayo Clinic [256]. SSRI-Rs and -NRs were selected on the basis of treatment outcomes, which were determined via the HAMD-17 and QIDS-C16 [257] depression rating scales before the start of SSRI (20 mg of citalopram or 10 mg of escitalopram) treatment and 8 weeks after SSRI treatment. Immunofluorescence analysis of the resulting cells revealed the expression of glial fibrillary acidic protein (GFAP) and vimentin (VIM), both canonical astrocyte markers (Figure 1.1B). RNA sequencing of hiPSC and isogenic hiPSC-derived astrocytes followed by differential expression analysis indicated that the expression of canonical astrocyte markers was significantly upregulated in hiPSC-derived astrocytes relative to parental hiPSCs ($\log_2\text{FoldChange} > 1.2$, adjusted p value < 0.05) (Figure 1.1C, Supplementary Table S1), further validating their astrocytic identity.

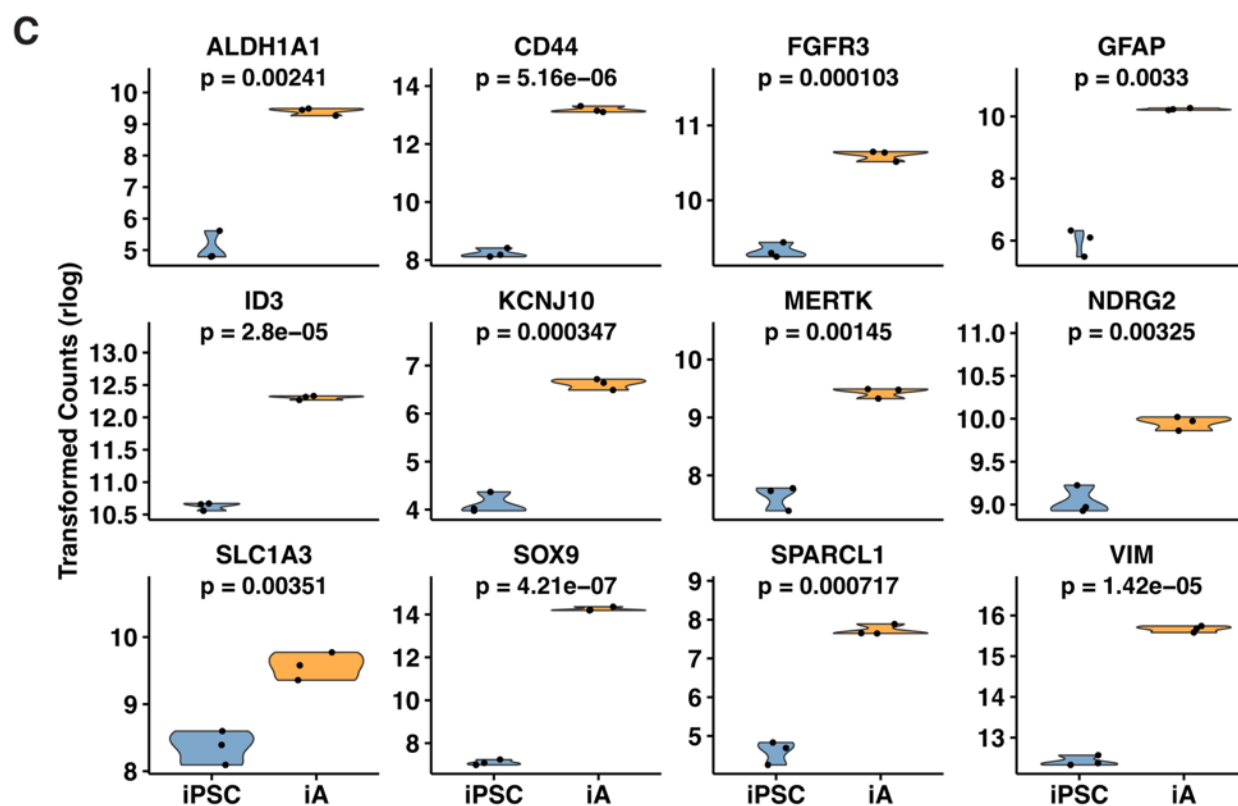
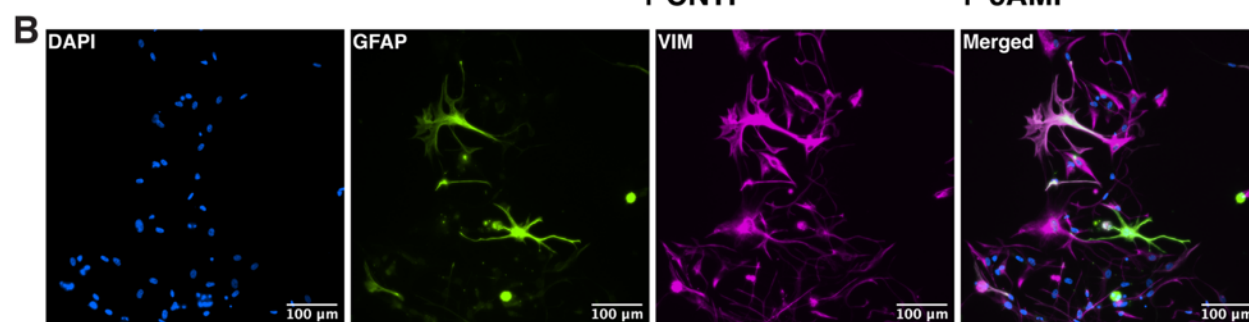
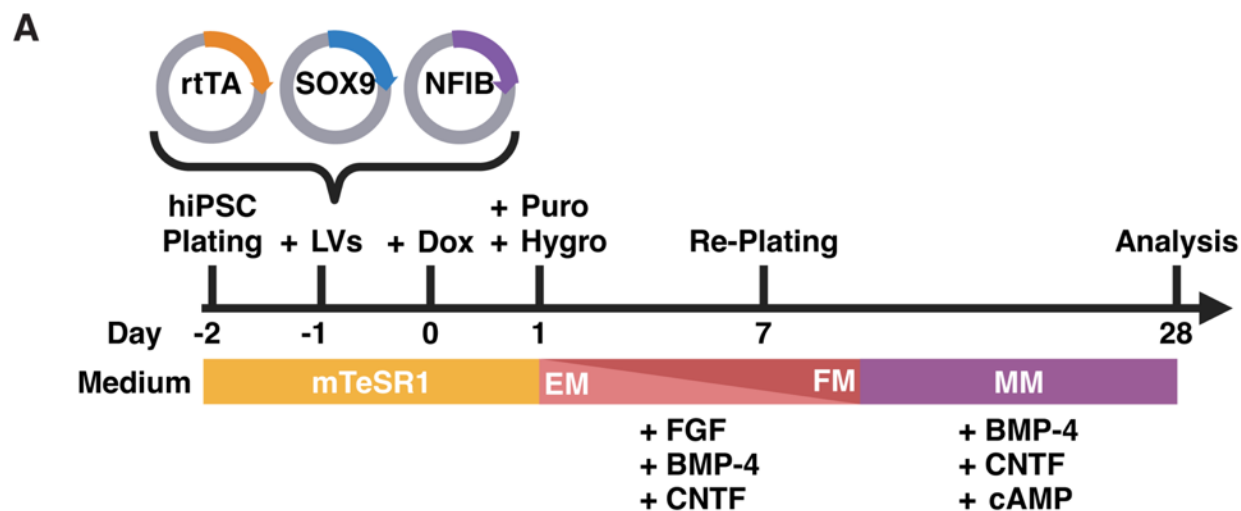


Figure 2.1. Transcription factor-based differentiation of astrocytes from human induced pluripotent stem cells. (A) Overexpression of the SOX9 and NFIB transcription factors was used to induce astrocyte differentiation as previously described [259]. (B) Immunofluorescence staining of hiPSC-derived astrocytes at 20x magnification showing GFAP (green) and VIM (magenta) expression. (C) Violin plots of rlog-transformed gene expression data from RNA sequencing illustrating the expression of canonical astrocyte markers in hiPSC and isogenic hiPSC-derived astrocyte samples.

To investigate the transcriptional differences associated with SSRI response in hiPSC-derived astrocytes, we performed RNA sequencing and differential gene expression analyses (Figure 1.2A). Pairwise differential expression comparisons were conducted between the SSRI-R, SSRI-NR, and HC groups. In the R vs. HC comparison, 160 genes were significantly upregulated, whereas 306 genes were downregulated (Figure 1.2B, Supplementary Table S2). The top 10 upregulated genes included SLC2A7, VPS52, TDRD1, CTSE, PHF1, NF1P8, FGL1, PSPHP1, ZNF676, and RNF39, whereas the top 10 downregulated genes included SAGE1, HSPA1B, NOC2LP1, PEG3, MAGEA4, DDX3Y, RPS4Y1, PHRF1, UTY, and MAGEA2 (Figure 1.2B). GO enrichment analysis identified seven GO terms were enriched among the upregulated genes, whereas 251 GO terms were enriched among the downregulated genes (Supplementary Table S5). The upregulated genes were primarily associated with “collagen-containing extracellular matrix” (GO:0062023), “modulation of chemical synaptic transmission” (GO:0050804), “synapse organization” (GO:0050808), “regulation of transsynaptic signaling” (GO:0099177), and “positive regulation of excitatory postsynaptic potential” (GO:2000463) (Figure 1.2C, Supplementary Table S5). The downregulated genes were associated primarily

with extracellular matrix organization, including “extracellular matrix structural constituent” (GO:0005201), “extracellular structure organization” (GO:0043062), and “external encapsulating structure organization” (GO:0045229) (Figure 1.2C, Supplementary Table S5).

On the other hand, in the NR vs. HC comparison, 266 genes were upregulated, and 325 were downregulated, with VPS52, AIF1, CTSF, LCN9, ADGRG7, LDC1P, PSPHP1, GSTT4, CLEC2A, and MTCO2P22 identified among the top significantly upregulated genes, whereas MAGEA4, PEG3, CSAG3, MICA, REN, PKD1P2, OR3A2, OTOL1, DCAF12L1, and GPSM3 were the most significantly downregulated (Figure 1.2D, Supplementary Table S3). 39 GO terms were enriched for upregulated genes, whereas 185 GO terms were enriched for downregulated genes (Supplementary Table S6). The upregulated genes were associated with immune-related functions such as “chemotaxis” (GO:0006935), “cell chemotaxis” (GO:0060326), and “leukocyte migration” (GO:0050900), along with “positive regulation of the MAPK cascade” (GO:0043410) (Figure 1.2E, Supplementary Table S6). The downregulated genes were related primarily to mitotic functions, including “nuclear division” (GO:0000280), “nuclear chromosome segregation” (GO:0098813), and “sister chromatid segregation” (GO:0000819) (Figure 1.2E, Supplementary Table S6).

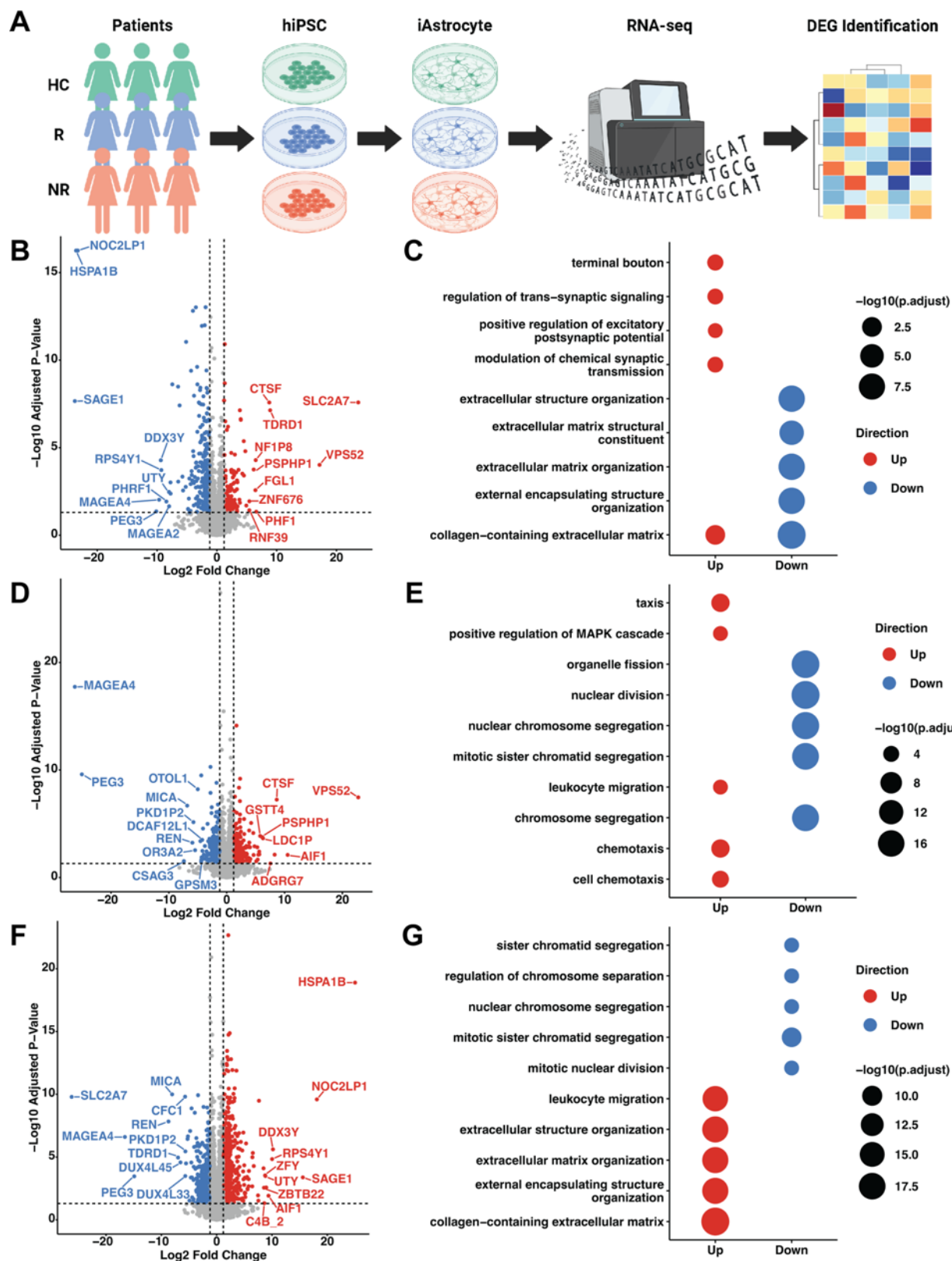


Figure 2.2. Astrocytic gene expression signatures associated with depression with differential antidepressant responses. (A) Schematic overview of the study design and analysis workflow. Volcano plots showing differentially expressed genes (DEGs) for R vs. HC (B), NR vs. HC (C), and NR vs. R (D). Upregulated genes (red) and downregulated genes (blue) are highlighted based on significant \log_2 fold-change ($\log_2\text{FoldChange} > 1.2$) and adjusted p values ($\text{padj} < 0.05$). The top 10 upregulated and downregulated genes are labeled. Dot plots of Gene Ontology (GO) enrichment analysis for the top 10 upregulated (red) and downregulated (blue) Biological Processes (BP), Molecular Functions (MF), and Cellular Components (CC) in R vs. HC (E), NR vs. HC (F), and NR vs. R (G). Dot sizes are scaled according to the $-\log_{10}$ adjusted p value.

Intriguingly, the NR vs. R comparison revealed the most extensive transcriptional changes, with 687 upregulated and 571 downregulated genes (Supplementary Table S4). Among the most highly upregulated genes in NR relative to R were HSPA1B, NOC2LP1, SAGE1, DDX3Y, RPS4Y1, AIF1, ZBTB22, UTY, ZFY, and C4B_2, whereas SLC2A7, MAGEA4, PEG3, REN, MICA, TDRD1, DUX4L45, CFC1, DUX4L33, and PKD1P2 were significantly downregulated (Figure 1.2F). The upregulated genes were significantly enriched in extracellular matrix-related pathways, including “collagen-containing extracellular matrix” (GO:0062023), “extracellular matrix organization” (GO:0030198), and “extracellular structure organization” (GO:0043062), alongside “leukocyte migration” (GO:0050900) (Figure 1.2G, Supplementary Table S7). Conversely, the downregulated genes were predominantly associated with mitotic processes, including “mitotic sister chromatid segregation” (GO:0000070), “mitotic nuclear

division” (GO:0140014), and “regulation of chromosome separation” (GO:1905818) (Figure 1.2G, Supplementary Table S7).

Further hierarchical cluster analysis revealed that a cluster of genes associated with “regulation of chromosome separation” (GO:1905818) was significantly upregulated in R and HC relative to NR (Figure 1.3). In contrast, a gene cluster linked to “extracellular matrix organization” (GO:0030198) was upregulated in NR vs. HC, with an even stronger increase observed in the NR vs. R comparison (Figure 1.3). These results highlight distinct transcriptional and biological process differences between SSRI responders and nonresponders, as well as alterations relative to healthy controls.

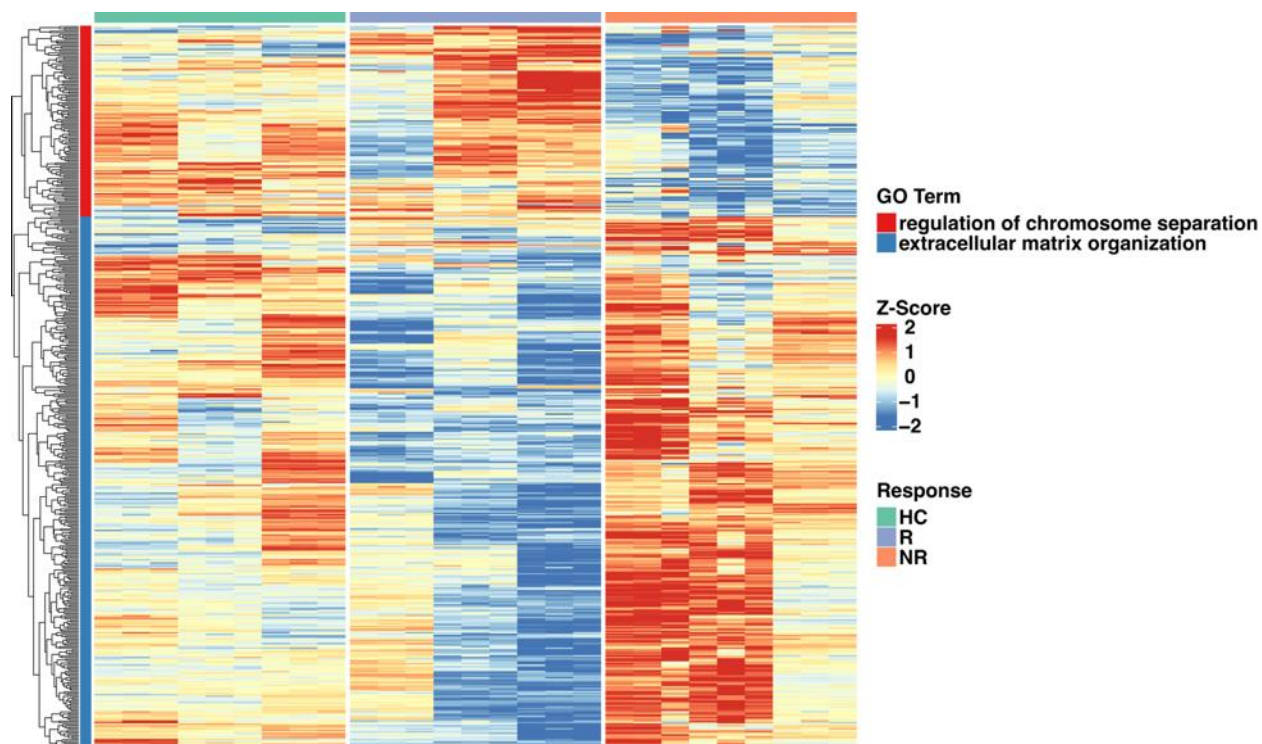


Figure 2.3. Differentially expressed gene clustering in healthy control, responder, and non-responder hiPSC-derived astrocytes. Heatmap of differentially expressed genes ($\log_2FC > 1.2$, $padj < 0.05$) with low within-group variability (standard deviation < 1.0) and high between-

group variability (mean difference > 1.0) across healthy controls (HC), responders (R), and non-responders (NR). Rows represent individual genes, clustered based on hierarchical clustering, and columns are grouped by response category. The row annotation on the right indicates two top Gene Ontology (GO) terms: “regulation of chromosome separation” (GO:1905818) and “extracellular matrix organization” (GO:0030198). The heatmap colors represent Z-score--normalized expression values.

Gene co-expression networks associated with the SSRI response in MDD astrocytes

To further identify the specific gene modules associated with SSRI-responsive and nonresponsive MDD in astrocytes, we performed weighted gene co-expression network analysis (WGCNA) followed by gene set enrichment analysis GSEA (Figure 1.4, Supplementary Table S8).

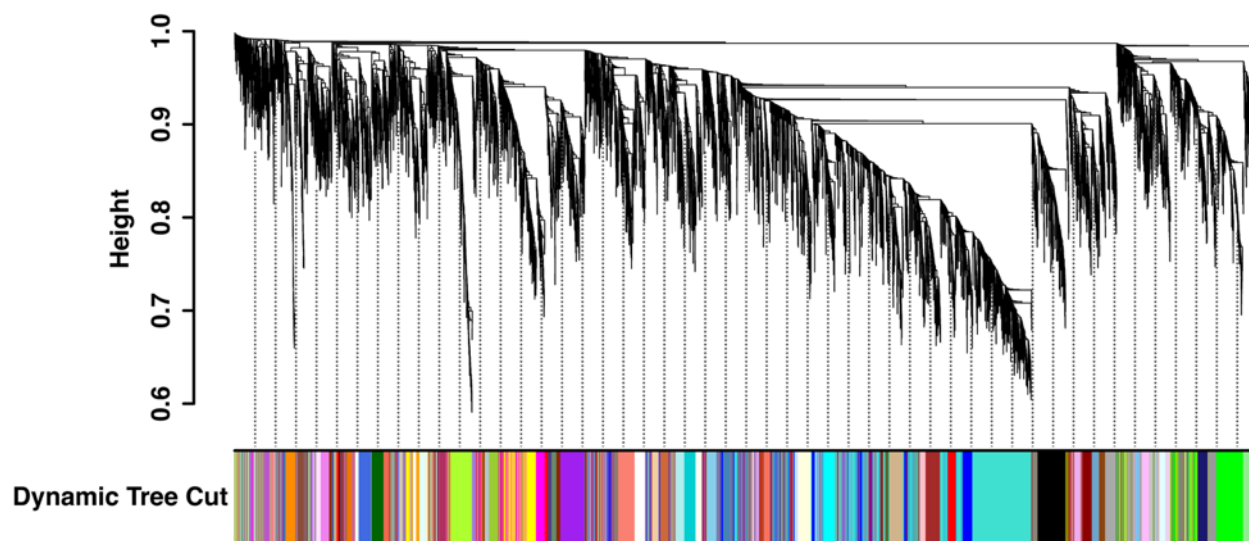


Figure 2.4. Hierarchical clustering of genes and module detection in hiPSC-derived astrocytes. Hierarchical clustering dendrogram of genes expressed in hiPSC-derived astrocytes from healthy controls (HC), responders (R), and non-responders (NR), based on topological overlap. Each branch in the dendrogram groups genes with similar expression patterns, while the

colored bar below indicates module assignments (each color represents a distinct co-expression module). The analysis was performed with a soft-thresholding power of 7 and a minimum module size of 30, as determined by the dynamic tree cut algorithm.

The average difference in eigengene values between R and HC revealed three significantly enriched modules that were upregulated: "PI3K-GTPase Signaling and TF Binding," "Oxidative Phosphorylation and Antioxidant Activity," and "Oxidative Phosphorylation, Proteostasis, and Cell Cycle Control" (Figure 1.5A, Supplementary Table S8). In contrast, five modules were significantly downregulated in R patients compared with HCs, including "ECM/Integrin Interactions and Tyrosine Phosphorylation," "Myogenesis and Calcium Channel Activity," "Neuroactive Ligand-Receptor Interaction," "Lipid Metabolism and Immune Regulation," and "Immune Activation and ECM/Glycosaminoglycan Metabolism" (Figure 1.5A, Supplementary Table S8).

In contrast, the upregulated in NR astrocytes compared to HC primarily associated with immune activation, stress response, and cell motility, including "Stress, Immune, and Circadian Regulation," "MET Signaling, DNA Repair, and Cell Motility," "TNF-NF κ B and T/B Lymphocyte-Mediated Immune Response," and "Cell Stress and Cell Adhesion" (Figure 1.5B); while downregulated modules are linked to intracellular trafficking, cell cycle regulation, and structural remodeling, including "Endosomal Recycling and Trafficking," "Cell Cycle, G2M Checkpoint, and DNA Replication," "Focal Adhesion and Cell Adhesion Dynamics," and "Estrogen Response and ECM/Cell Junction Remodeling" (Figure 1.5B, Supplementary Table S8).

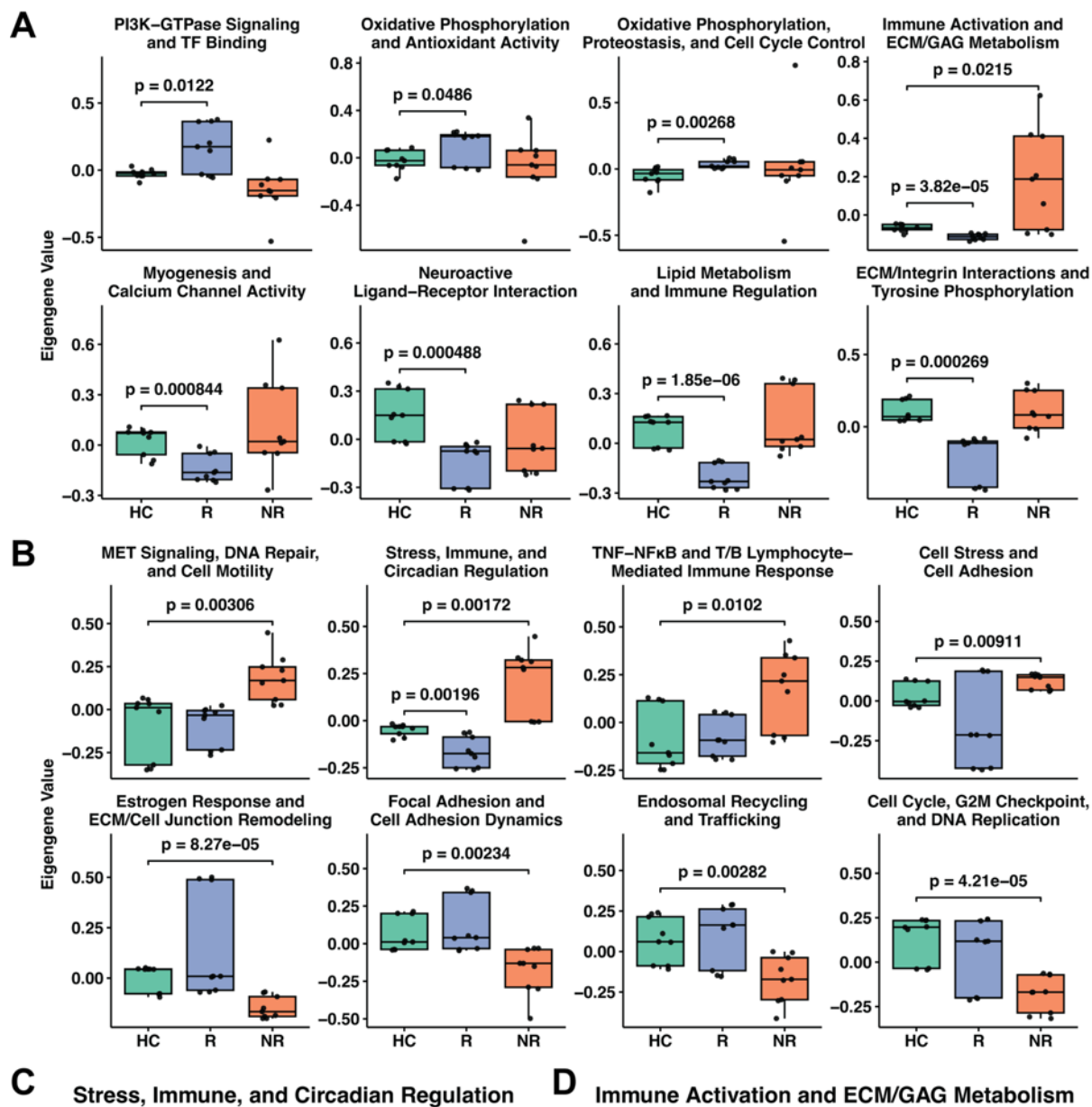


Figure 2.5. Identification of significant modules in hiPSC-derived astrocytes from SSRI-responders and nonresponders. (A) Boxplots of eigenvalues for HC, R, and NR hiPSC-derived astrocytes for significantly enriched modules ($p < 0.05$) between R and HC hiPSC-derived astrocytes. (B) Boxplots of eigenvalues for HC, R, and NR hiPSC-derived astrocytes for significantly enriched modules ($p < 0.05$) between NR and HC hiPSC-derived astrocytes. Module annotations represent pathway enrichment identified through Gene Set Enrichment Analysis (GSEA) using annotated gene sets from the Molecular Signatures Database (MSigDB). (C) Protein-protein interaction (PPI) network of genes in the "Stress, Immune, and Circadian Regulation" module. (D) PPI network of genes in the "Immune Activation and Extracellular Matrix/Glycosaminoglycan Metabolism" module. Node color indicates the direction of gene expression changes, with orange nodes indicating significantly upregulated genes ($p < 0.05$) and blue nodes representing significantly downregulated genes ($p < 0.05$). The size of each node is proportional to the significance of the adjusted p value, with larger nodes representing more statistically significant changes in gene expression.

Two transcriptional modules, "Stress, Immune, and Circadian Regulation" and "Immune Activation and ECM/Glycosaminoglycan Metabolism," exhibited opposing eigengene expression patterns in SSRI R and NR compared with HC. In the R vs. HC comparison, both modules were significantly downregulated, whereas in the NR vs. HC comparison, they were significantly upregulated (Figure 1.5A, Figure 1.5B, Supplementary Table S8). PPI network analysis of the "Stress, Immune, and Circadian Regulation" module revealed a cluster of differentially expressed genes, with upregulated nodes primarily involving inflammatory and circadian regulatory factors (Figure 1.5C). The top differentially expressed genes in NR vs. R

included MT1X ($\log_2FC = 3.573$), G0S2 ($\log_2FC = 3.392$), MT2A ($\log_2FC = 3.196$), IRF8 ($\log_2FC = 2.597$), and THBS1 ($\log_2FC = 2.555$). The most interconnected nodes in this module included PER1 (degree = 6), PIK3R3 (degree = 6), CUL1 (degree = 6), SYNJ2 (degree = 6), and PTEN (degree = 6), indicating a central role for these genes in network connectivity (Figure 1.5C). Similarly, the PPI network for the "Immune Activation and Extracellular Matrix/Glycosaminoglycan Metabolism" module displayed a distinct set of differentially expressed genes, with significantly upregulated genes predominantly associated with immune signaling and ECM remodeling (Figure 1.5D). The top differentially expressed genes in NR vs. R included HLA-DPB1 ($\log_2FC = 5.107$), ACTA1 ($\log_2FC = 4.056$), HLA-DQB1 ($\log_2FC = 3.900$), HLA-DQA1 ($\log_2FC = 3.306$), and HSD17B6 ($\log_2FC = 1.349$). The most interconnected nodes in this module included HSPG2 (degree = 10), ITGB1 (degree = 6), XYLT2 (degree = 4), BCAN (degree = 4), and HLA-DQA1 (degree = 4) (Figure 1.5D). These modules were enriched in pathways related to immune function, extracellular matrix remodeling, and circadian regulation, highlighting distinct transcriptional signatures between responders and non-responders.

Key genes driving the distinct transcriptional signatures between SSRI responders and non-responders in astrocytes

To investigate transcriptional regulation differences and identify the driver genes in R and NR compared to HC, transcription factor (TF) activity scores were inferred using the univariate linear model (ULM) based on differentially expressed genes. In the R vs. HC comparison, the most significantly activated TFs included HIF3A, KLF17, TGIF1, NR1D1, CIITA, ZNF219, ZMYND8, SOX9, FOXJ1, and ZNF202 (Figure 3A, Supplementary Table S9), while the most

significantly deactivated TFs were SP1, HIF1A, AP1, JUN, SMAD3, NFKB, MYC, CEBPB, NFKB1, and CREB1 (Figure 3A, Supplementary Table S9). Conversely, in the NR vs. HC comparison, the most activated TFs were TP53, JUN, TP73, E4F1, BMAL1, FOS, EPAS1, ETS1, NPAS2, and RELA (Figure 3B, Supplementary Table S10), while the most deactivated TFs included E2F4, E2F1, E2F2, E2F3, HCFC1, TFDP1, E2F5, ARID3A, STOX1, and SRSF2 (Figure 3B, Supplementary Table S10). These findings highlight distinct transcription factor activity patterns between responders and non-responders, with differing sets of activated and deactivated TFs relative to healthy controls.

To further characterize the differences in transcription factor activity between responders and non-responders, the number and overlap of significantly activated and deactivated TFs were examined. The total number of significantly activated TFs was 12 in R vs. HC and 109 in NR vs. HC, while the total number of significantly deactivated TFs was 248 in R vs. HC and 24 in NR vs. HC (Figure 1.6C). Notably, there was no overlap between the activated TFs in R vs. HC and any other group (Figure 1.6C). The largest pairwise intersection was between activated TFs in NR vs. HC and deactivated TFs in R vs. HC ($n = 70$), suggesting a group of TFs with inverse regulatory patterns across conditions (Figure 1.6C). Smaller overlaps included 8 TFs shared between deactivated TFs in both R vs. HC and NR vs. HC (Figure 1.6C). These results indicate distinct and largely non-overlapping transcriptional regulatory changes in responders and non-responders compared to healthy controls.

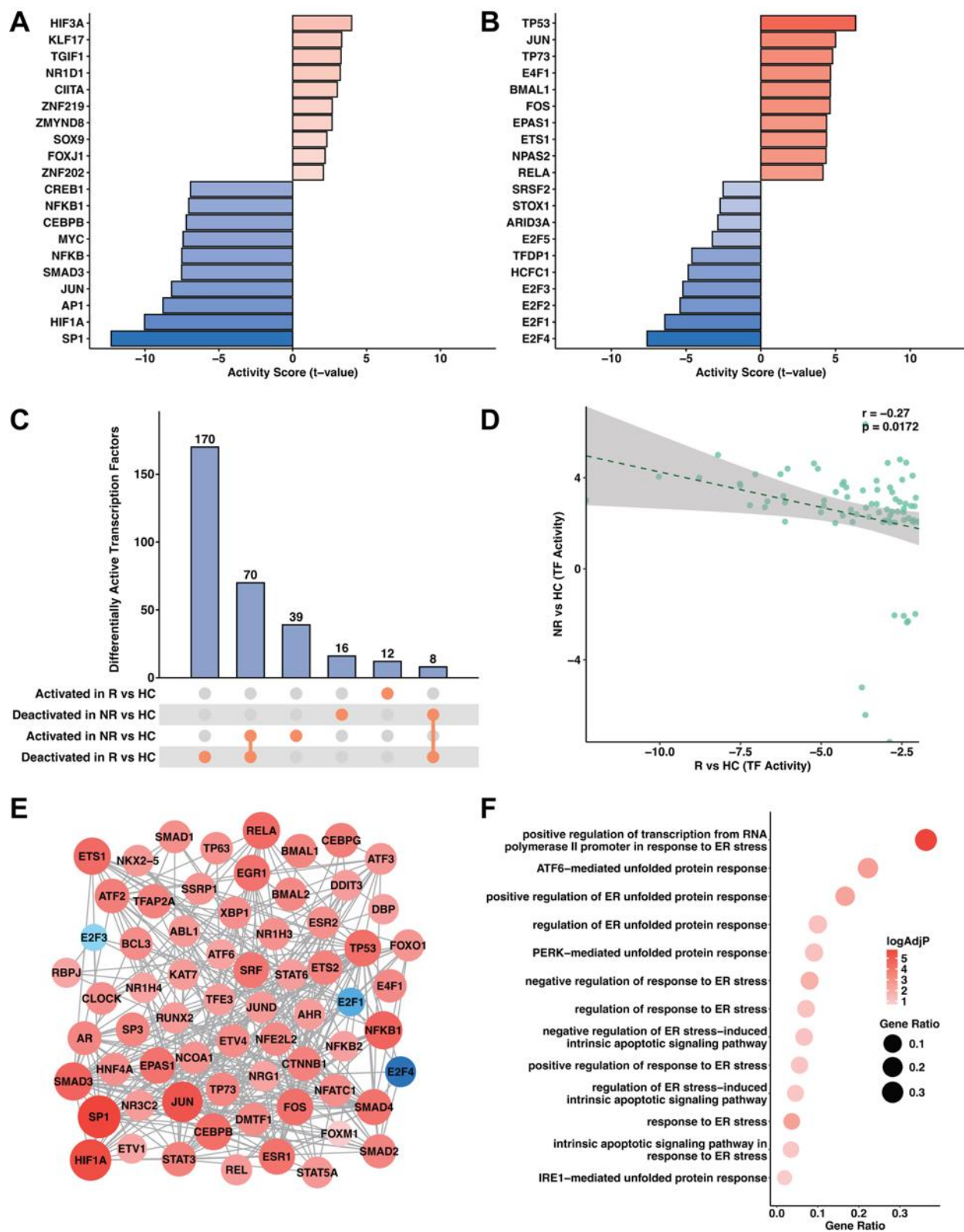


Figure 2.6. Key transcription factors driving the astrocytic signatures of SSRI-responders and non-responders. Bar plots of inferred TF activity scores from Univariate Linear Model (ULM) analysis of differentially expressed genes in R vs. HC (A) and NR vs. HC (B). Positive scores indicate activation, while negative scores indicate deactivation. (C) UpSet plot illustrating the intersections of significantly activated and deactivated TFs across R vs. HC and NR vs. HC. (D) Pearson correlation analysis of TF activity scores between R vs. HC and NR vs. HC, with a fitted regression line. The correlation coefficient (r) and p value indicate the degree of similarity in TF regulation between groups. (E) Protein-protein interaction (PPI) network of TFs with significantly different activity between NR and R. Node colors represent activation (red) or deactivation (blue) in NR relative to R, and node size corresponds to absolute differential activity score. (F) Dot plot of UPR-related GO terms enriched in the PPI network, where dot size reflects the gene ratio and color represents the $-\log_{10}$ of the adjusted p value.

To assess the global similarity in TF activity patterns between R vs. HC and NR vs. HC, Pearson correlation analysis was performed (Figure 1.6D). The resulting correlation suggests an inverse relationship between TF activity changes in responders and non-responders relative to healthy controls ($r = -0.27$, p value = 0.0172) (Figure 1.6D). These findings indicate that TF activity patterns in R and NR exhibit opposing regulatory trends when compared to HC. To further examine the connectivity and centrality of these TFs, a PPI network analysis was conducted for TFs with differential activity between NR vs. R relative to HC (Figure 1.6E). The PPI network consisted of 67 nodes and 590 edges, with a relatively compact structure with multiple key hubs. Several TFs exhibited high centrality across different network metrics, including degree, betweenness centrality, closeness centrality, and eigenvector centrality

(Supplementary Table S15). Among these, TP53, JUN, FOS, SMAD3, SP1, and STAT3 consistently ranked high across all centrality measures, suggesting their prominent role in TF network connectivity and regulation. These results highlight a highly interconnected transcriptional network in non-responders, with these key TFs emerging as central regulators based on multiple network topology measures.

GO and pathway enrichment analysis of TFs with differential activity in NR versus R identified a significant overrepresentation of biological processes related to unfolded protein response (UPR) in NR astrocytes (Figure 1.6F). GO terms revealed enrichment in positive regulation of transcription from RNA polymerase II promoter in response to ER stress (adj. $p = 1.62e-06$, Gene Ratio = 0.364), ATF6-mediated UPR (adj. $p = 0.0034$, Gene Ratio = 0.222), and response to ER stress (adj. $p = 0.0040$, Gene Ratio = 0.036), among others. Additional enriched terms included positive regulation of ER UPR (adj. $p = 0.0052$, Gene Ratio = 0.167), negative regulation of response to ER stress (adj. $p = 0.0167$, Gene Ratio = 0.08), and PERK-mediated UPR (adj. $p = 0.0752$, Gene Ratio = 0.091) (Figure 1.6F). Notably, IRE1-mediated UPR also appeared in the results (adj. $p = 0.1924$, Gene Ratio = 0.019), indicating the involvement of multiple branches of the UPR (Figure 1.6F). Network centrality analysis of key UPR-related TFs revealed CEBPB (degree = 36, betweenness = 62.13, eigenvector = 0.662) as a major hub in the PPI network (Supplementary Table S15). Other UPR-associated TFs, including XBP1 (degree = 10, betweenness = 61.58, eigenvector = 0.151), NFE2L2 (degree = 8, betweenness = 3.57, eigenvector = 0.193), and NR1H3 (degree = 8, betweenness = 0.73, eigenvector = 0.176), exhibited moderate connectivity but notable regulatory influence (Supplementary Table S15). The enrichment of these TFs in multiple branches of UPR signaling, combined with their

centrality in the network, suggests a critical role for ER stress responses in differentiating transcriptional activity between SSRI responders and non-responders.

Altered XBP1 signaling in SSRI-nonresponder astrocytes

XBP1 signaling plays a key role in UPR through alternative splicing mediated by IRE1, a process modulated by SIGMAR1 (Figure 4A) [287-295]. To investigate potential alterations in XBP1 signaling in hiPSC-derived astrocytes from individuals with depression, we first examined the relative expression levels of unspliced XBP1 (uXBP1) and spliced XBP1 (sXBP1) across diagnostic groups. RT-qPCR analysis revealed a statistically significant increase in sXBP1 expression in NRs compared with HCs, whereas uXBP1 levels remained unchanged (Figure 4B). The ratio of sXBP1 to uXBP1 did not significantly differ across the diagnostic groups (Figure 4B). These results indicate differential expression of XBP1 isoforms across diagnostic groups, with a significant increase in spliced XBP1 in nonresponders compared to healthy controls.

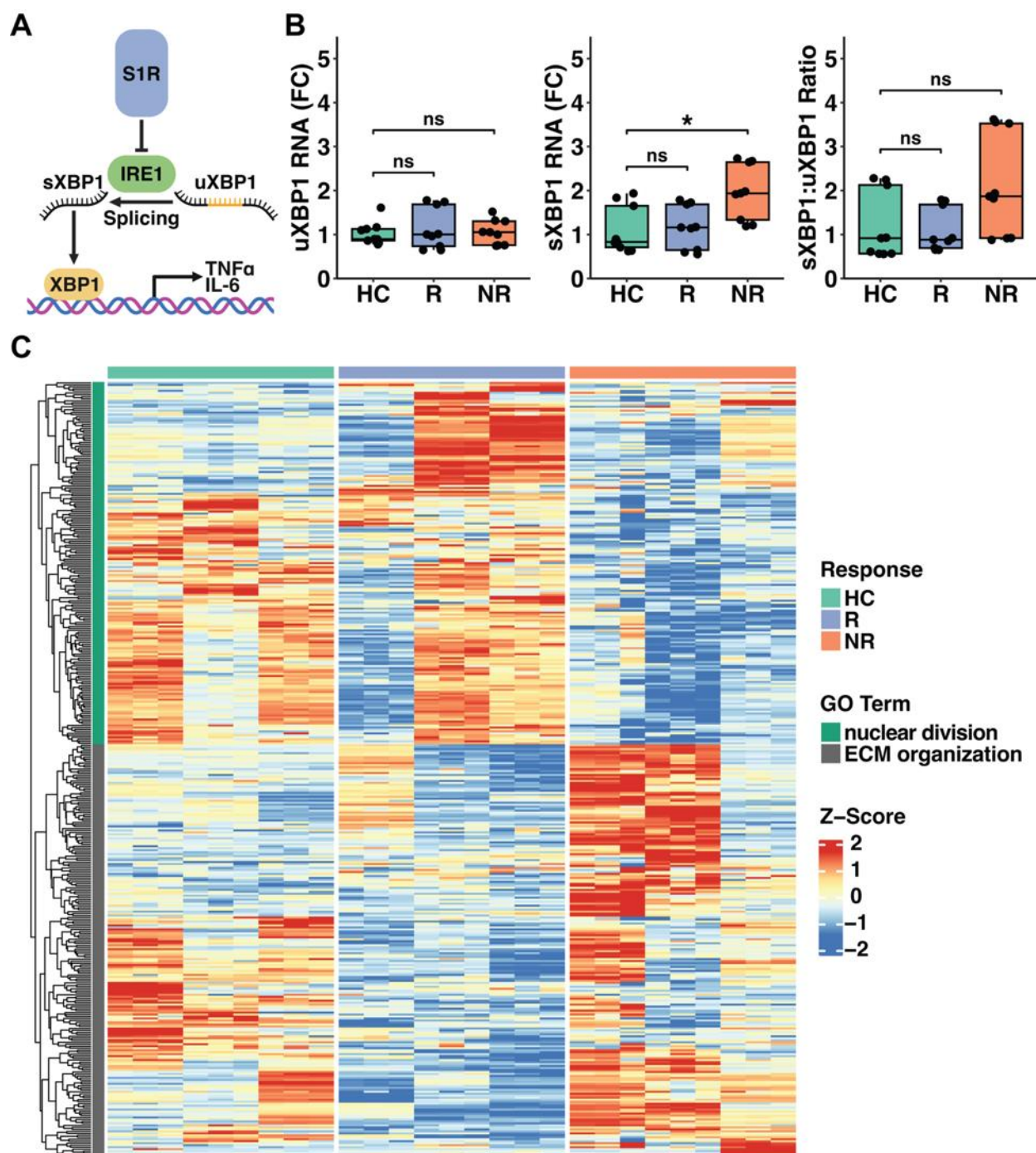


Figure 2.7. Alterations in XBP1 signaling and XBP1 target genes in hiPSC-derived astrocytes. (A) Schematic representation of SIGMAR1 regulation of IRE1 activity and the production of spliced XBP1 (sXBP1). **(B)** RT-qPCR analysis of XBP1 isoforms across diagnostic groups. Bar graphs show fold change (FC) expression levels of unspliced XBP1 (uXBP1),

spliced XBP1 (sXBP1), and the sXBP1:uXBP1 ratio in iPSC-derived astrocytes from healthy controls (HC), responders (R), and non-responders (NR). FC values were calculated using the $\Delta\Delta\text{Ct}$ method with GAPDH as the reference gene. Data are represented as mean \pm SEM. Asterisks (*) indicate statistically significant differences ($p < 0.05$). (C) Heatmap of differentially expressed XBP1 target genes in NR and R compared to HC. Genes are hierarchically clustered based on Z-score normalized expression values, with annotation for diagnostic groups (HC, R, and NR) and enriched biological processes (GO terms) associated with each gene cluster.

To further explore the downstream effects of altered XBP1 signaling, we analyzed the expression of XBP1 target genes in hiPSC-derived astrocytes. A heatmap of differentially expressed genes revealed distinct clustering patterns between diagnostic groups, with NR and R displaying unique transcriptional profiles compared with those of HCs (Figure 4C). Functional enrichment analysis revealed two primary clusters of differentially expressed genes associated with extracellular matrix (ECM) organization and nuclear division (Figure 4C). Compared with that in HCs, the ECM organization gene cluster was upregulated in NRs but downregulated in R patients, suggesting differential regulation of astrocytic ECM remodeling in response to treatment (Figure 4C). Conversely, the nuclear division cluster was upregulated in R patients compared with HCs and downregulated in NR patients compared with HCs, indicating potential alterations in cell cycle-related processes across diagnostic groups (Figure 4C). These findings highlight distinct transcriptional programs associated with XBP1 target genes in astrocytes from individuals with depression.

Identification of discordant perturbagens in SSRI-responder and nonresponder astrocytes

To identify small molecule perturbagens that may modulate astrocyte signatures in MDD and TRD, we queried the LINCS database for compounds that induce gene expression profiles discordant from those observed in response to R and NR states (Figure 1.8A, Supplementary Table S11, Supplementary Table S12). Among the predicted discordant perturbagens, 17 FDA-approved antidepressants overlapped with R discordants, while only two overlapped with NR discordants, with tranylcypromine appearing in both groups (Figure 1.8B). The antidepressants discordant with the R transcriptional signature included four tricyclic antidepressants (TCAs; protriptyline, amitriptyline, desipramine, and imipramine), three monoamine oxidase inhibitors (MAOIs; tranylcypromine, isocarboxazid, moclobemide), two SSRIs (paroxetine, sertraline), one norepinephrine-dopamine reuptake inhibitors (NDRI; bupropion), two serotonin-norepinephrine reuptake inhibitors (SNRI; duloxetine, venlafaxine), two serotonin antagonist and reuptake inhibitors (SARIs; nefazodone, trazodone), two tetracyclic antidepressants (TeCAs; mianserin, maprotiline), one noradrenergic and specific serotonergic antidepressant (NaSSA; mirtazapine). The similarity scores of these antidepressants indicate their degree of transcriptional opposition to the R state, suggesting that astrocyte-associated gene expression changes in responders correspond to established antidepressant mechanisms (Figure 1.8C). The predicted discordant compounds include many FDA-approved antidepressants, which support the connection between gene expression changes in responder astrocytes and known antidepressant mechanisms. However, only MAOI antidepressants, tranylcypromine and phenelzine, showed discordance with the NR state. Importantly, no SSRIs appeared among the predicted compounds for NR astrocytes, which aligns with the lack of clinical response to escitalopram or citalopram in these patients.

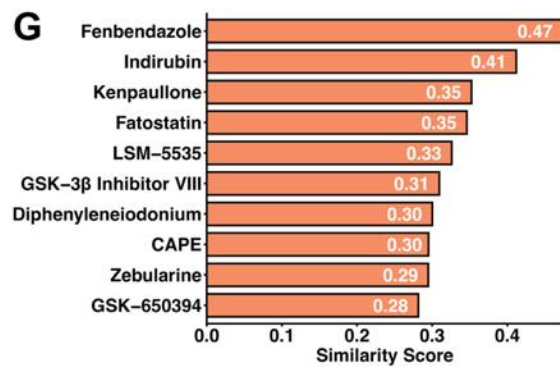
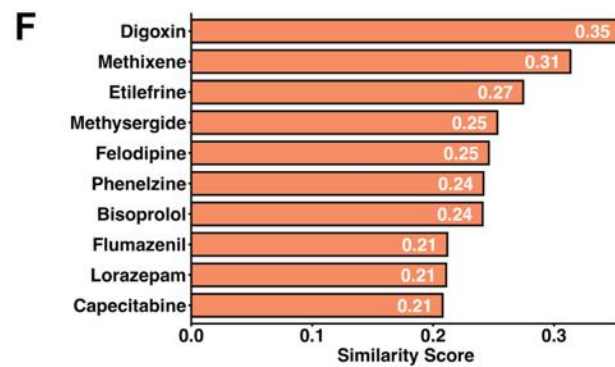
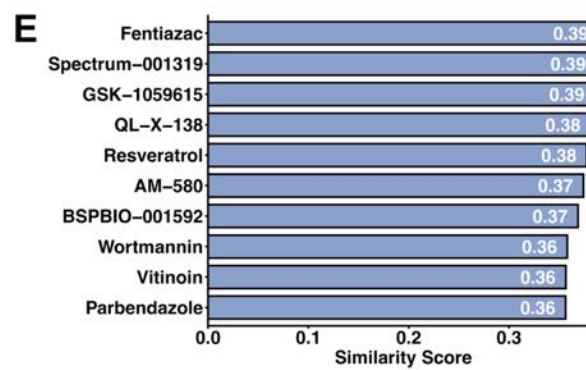
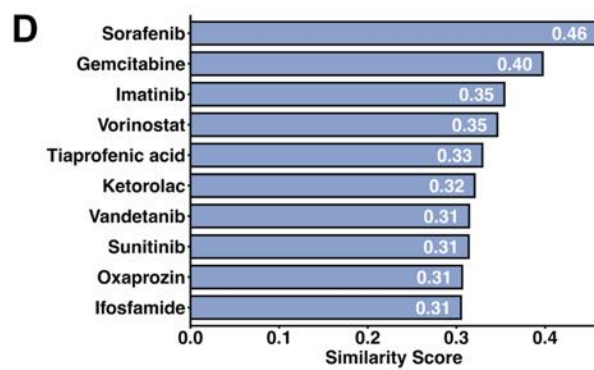
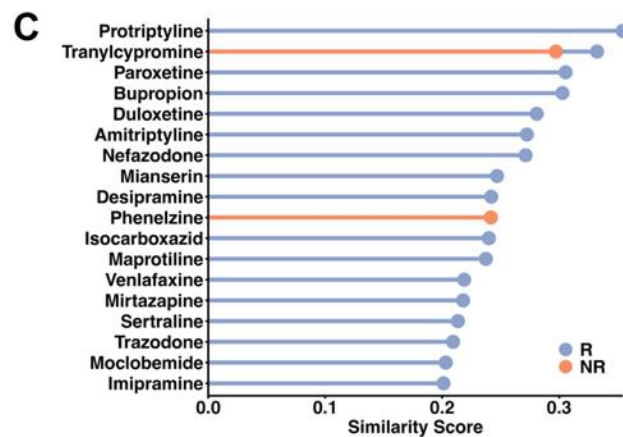
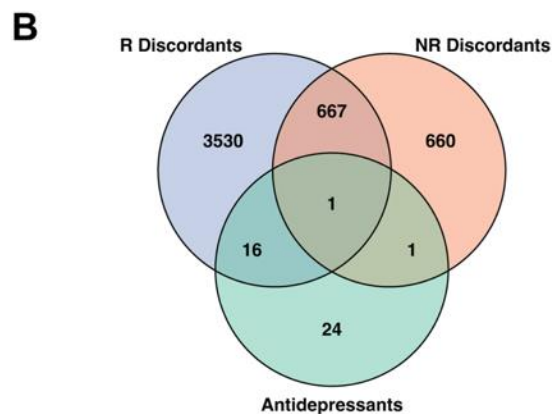
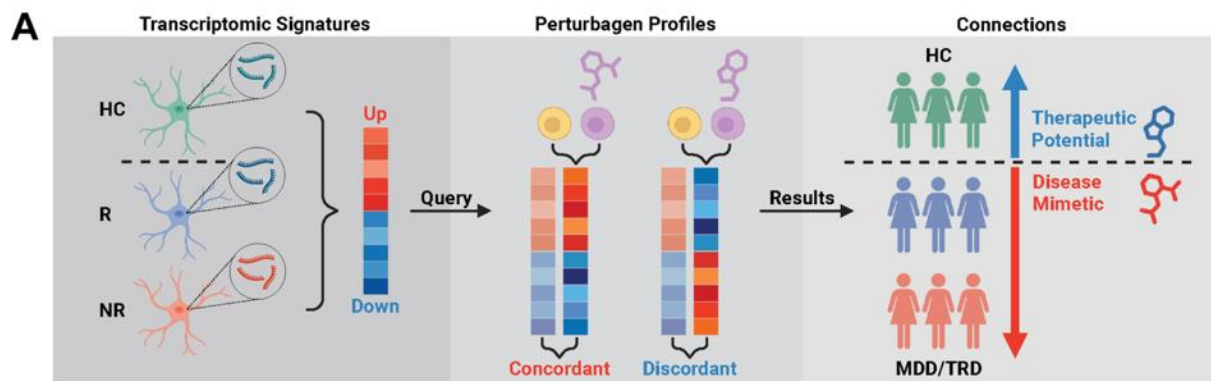


Figure 2.8. Identification of potential therapeutics using LINCS analysis. (A) Schematic representation of the workflow for querying the Library of Integrated Network-based Cellular Signatures (LINCS) to identify discordant perturbagens. (B) Venn diagram showing the overlap between FDA-approved antidepressants and discordant perturbagens for R and NR predicted by LINCS analysis. (C) Similarity scores of FDA-approved antidepressants that overlap with R and NR discordant perturbagens. Similarity scores of FDA-approved discordant perturbagens (D) and preclinical discordant perturbagens (E) specific to R. Similarity scores of FDA-approved discordant perturbagens (F) and preclinical discordant perturbagens (G) specific to NR.

To identify small-molecule perturbagens for potential repurposing in MDD and TRD, FDA-approved drugs and preclinical compounds that exhibited discordant transcriptional profiles specific to R astrocytes were analyzed (Supplementary Table S11). The FDA-approved discordant perturbagens included sorafenib (FLT3/KIT/PDGFR/RAF/RET/VEGFR inhibitor), gemcitabine (ribonucleotide reductase inhibitor), imatinib (Bcr-Abl/KIT/PDGFR inhibitor), vorinostat (histone deacetylase inhibitor), tiaprofenic acid (cyclooxygenase inhibitor), ketorolac (cyclooxygenase inhibitor), vandetanib (ephrin receptor/EGFR/tyrosine kinase inhibitor), sunitinib (CSF1R/PDGFR/SCFR/FLT3/RET/VEGFR inhibitor), oxaprozin (cyclooxygenase inhibitor), and ifosfamide (DNA alkylating agent) (Figure 1.8D). Additionally, the preclinical discordant small molecules targeting included fentiazac (cyclooxygenase inhibitor), Spectrum-001319 (11-beta-HSD1 inhibitor), GSK-1059615 (PI3K inhibitor), QL-X-138 (mTOR inhibitor), resveratrol (cytochrome P450 inhibitor, SIRT activator), AM-580 (retinoid receptor agonist), BSPBIO-001592 (COX/HAT/LOX inhibitor, NF- κ B pathway inhibitor), wortmannin (PI3K inhibitor), vitinoin (retinoid receptor agonist), and parbendazole (tubulin inhibitor) (Figure 1.8E).

These findings define a set of FDA-approved and investigational compounds with discordant transcriptional profiles relative to R astrocytes.

To further investigate perturbagens relevant to treatment-resistant depression, a complementary analysis was conducted to identify FDA-approved drugs and preclinical compounds discordant with NR astrocytes (Supplementary Table S12). The FDA-approved discordant perturbagens ranked included digoxin (sodium/potassium-transporting ATPase inhibitor), methixene (acetylcholine receptor antagonist), etilefrine (adrenergic receptor agonist), methysergide (serotonin receptor antagonist), felodipine (mineralocorticoid receptor antagonist, voltage-gated L-type calcium channel blocker), phenelzine (monoamine oxidase inhibitor), bisoprolol (adrenergic receptor antagonist), flumazenil (benzodiazepine receptor antagonist), lorazepam (benzodiazepine receptor agonist), and capecitabine (DNA synthesis inhibitor, thymidylate synthase inhibitor) (Figure 1.8F). Additionally, the preclinical discordant compounds included fenbendazole (tubulin inhibitor), indirubin (CDK/GSK inhibitor), kenpaullone (CDK inhibitor/GSK inhibitor), fatostatin (SREBP inhibitor), LSM-5535 (tubulin inhibitor), GSK-3 β inhibitor VIII (GSK inhibitor), diphenyleneiodonium (nitric oxide synthase inhibitor), caffeic acid phenethyl ester (HIV integrase, inhibitor, lipoxygenase inhibitor, NF-kB pathway inhibitor, NO/TNF production inhibitor, PPAR receptor modulator), zebularine (DNA methyltransferase inhibitor), and GSK-650394 (serum/glucocorticoid-regulated kinase inhibitor) (Figure 1.8G). These findings showcase the use of iPSC-derived astrocytes to identify FDA-approved drugs and preclinical compounds exhibiting opposite transcriptional signatures to those found in NR astrocytes. By integrating patient-specific, hiPSC-derived astrocytes with computational drug discovery, this approach enhances disease relevance, patient stratification, and translational potential while laying the foundation for future implementation of fully personalized psychiatry.

Discussion

In this study, we compared hiPSC-derived astrocytes from R and NR patients against age- and sex-matched HC individuals. Our transcriptomic analyses revealed notable differences in immune signaling, ECM regulation, and cell cycle processes between NR, R, and HC donors. WGNCA complemented these findings by uncovering distinct modules of coexpressed genes in both R and NR astrocytes. Notably, modules tied to oxidative phosphorylation, antioxidant activity, and proteostasis were upregulated in R compared to HC, whereas ECM/Integrin interactions, lipid metabolism, and immune regulation modules were downregulated. In contrast, NR astrocytes showed upregulated modules related to stress, immune and circadian regulation, and TNF–NF κ B immune signaling, while downregulated modules involved cell cycle functions and ECM/cell junction remodeling. TF activity analysis revealed distinct regulatory patterns between groups: R astrocytes showed increased activity of HIF3A and KLF17, while NR astrocytes exhibited elevated activity of TP53, JUN, and BMAL1. We also detected enhanced XBP1 splicing in NR astrocytes, suggesting that the IRE1–XBP1 branch of the UPR may be disrupted in these cells [292], potentially contributing to maladaptive stress responses and impaired proteostasis [296]. XBP1 signaling has been linked to the regulation of ECM components and remodeling pathways [297]; thus, dysregulated UPR signaling could affect astrocyte function and the integrity of the extracellular environment [298]. Finally, we leveraged the LINCS database to identify small molecules with contrasting transcriptomic signatures relative to the pathological gene expression profiles observed in R and NR hiPSC-derived astrocytes. This approach identified FDA-approved and preclinical compounds, including kinase, epigenetic modulators, and anti-inflammatory agents, that may represent promising candidates

for drug repurposing and antidepressant drug development. Overall, these findings highlight the neuroimmune dysfunction and extracellular matrix remodeling as astrocyte-specific contributors to SSRI resistance, underscoring the need for further investigation into novel therapeutic strategies targeting these pathways.

These results reinforce the psychoneuroimmune hypothesis of depression, which posits that inflammatory mediators, including IL-6 and TNF, contribute to behavioral and physiological depressive symptoms resembling sickness syndrome [299-302]. While astrocytes are known to both regulate and react to immune system activity [124, 172, 198, 253, 255, 303-306], the immunoinflammatory differences identified in our R and NR patient-derived astrocytes bridge the gap between this knowledge and the mounting evidence of dysregulated immunity and inflammation in MDD and, to an even greater extent, in TRD [226, 307-313]. The resultant disparity in inflammatory transcript expression between our NR and R patient-derived astrocytes suggests that these cells may be potential drivers of the elevated inflammatory markers that have been observed in TRD patients. Mechanistically, several pathways highlighted by our WGCNA and GO enrichment analyses, most notably TNF–NF κ B signaling, chemotaxis, and ECM organization, may contribute to SSRI resistance by disrupting neuronal and, more specifically, synaptic function [314]. Given the critical role of astrocytes in serotonin uptake and metabolism, chronic inflammatory activation in these cells could impair serotonergic neurotransmission, thereby handicapping SSRI efficacy [198, 226, 315, 316]. The concurrent ECM-related gene expression changes we observed in NR patient-derived astrocytes mirror previous observations that stress and immune activation can negatively impact synaptic stability and neuronal plasticity via ECM remodeling [317-319]. Together, these insights imply that astrocyte-driven crosstalk between inflammation and ECM modulation may drive SSRI resistance, advancing our

mechanistic understanding of TRD. Additionally, the differential splicing of XBP1 in NR patient-derived astrocytes and the resultant alterations in the expression of XBP1 gene targets suggest dysregulation of UPR pathways [292, 320], which prior studies have linked to both ECM remodeling [297, 298] and inflammatory cascades [321]. Collectively, these findings uncover multifaceted interactions between inflammatory responses, ECM dynamics, and UPR activity in SSRI-resistant MDD, highlighting the promise of therapies targeting astrocyte-centric disease mechanisms to address TRD.

An important translational extension of our findings comes from querying the LINCS database for compounds whose transcriptional signatures oppose those observed in our hiPSC-derived astrocyte model. This analysis confirmed that gene expression trends in R astrocytes were discordant with the transcriptomic signatures of 17 FDA-approved antidepressants, including 2 SSRIs: paroxetine and sertraline. In contrast, only two FDA-approved antidepressants showed discordance with the NR astrocyte signature: tranylcypromine and phenelzine. The discordance between the gene expression profiles of NR astrocytes and those of tranylcypromine and phenelzine, both MAOIs typically reserved for cases where standard therapies fail [322], suggests that broad-spectrum monoamine modulation may uniquely counter the astrocyte-specific transcriptional disturbances linked to SSRI resistance in these patients. However, whether the increased likelihood of antidepressant effect outweighs the risks of MAOI side effects and drug-drug interactions may depend on individualized risk-reward assessments. Overall, this analysis supports the classifications of these donors and suggests that the genetic factors that determine antidepressant responses are preserved through the iPSC reprogramming process.

To identify additional small-molecule perturbagens for potential repurposing in MDD and TRD, we assessed both FDA-approved drugs and preclinical compounds. Among the discordant perturbagens for R astrocytes were drugs inhibiting tyrosine kinases (sorafenib, imatinib), histone deacetylases (vorinostat), cyclooxygenases (tiaprofenic acid, ketorolac), and DNA alkylation (ifosfamide). Preclinical agents such as GSK-1059615 (PI3K inhibitor), QL-X-138 (mTOR inhibitor), and wortmannin (PI3K inhibitor) also emerged. Notably, the mechanisms of these compounds intersect with inflammation, epigenetic regulation, and metabolic processes, which are increasingly implicated in mood disorders. For instance, cyclooxygenase inhibitors have been explored for their anti-inflammatory properties in MDD [323], histone deacetylase inhibitors can modify gene expression involved in stress responses [324], and PI3K/Akt/mTOR pathway regulation is known to affect synaptic plasticity and glial function [325]. These diverse targets suggest that multiple molecular pathways could modulate astrocyte phenotypes akin to R astrocyte states and potentially reinforce the effects of traditional antidepressants.

On the other hand, NR-specific discordant FDA-approved compounds included sodium/potassium-transporting ATPase inhibitors (digoxin), serotonin receptor antagonists (methysergide), and MAOIs (tranylcypromine, phenelzine), pharmacologic strategies that have been explored in other neuropsychiatric contexts [322, 326, 327]. Preclinical molecules targeting cell-cycle kinases (kenpaullone, indirubin), lipid regulators (fatostatin), and epigenetic modulators (zebularine) also emerged, aligning with growing evidence that metabolic, cell-cycle, and epigenetic mechanisms can influence depressive phenotypes [328-330]. Together, these results illustrate how computational screening via LINCS can complement functional genomics data, unveiling both established antidepressants and novel agents that may help restore or preserve astrocyte health in MDD. Among the preclinical compounds identified, GSK-3 β

inhibitors such as kenpaullone and indirubin stand out for their potential relevance to TRD-related astrocyte dysfunction. GSK-3 β has been implicated in neuroinflammation, synaptic remodeling, and neuronal plasticity, and its inhibition has been shown to alleviate depressive-like behaviors in preclinical models [331, 332]. Additionally, kenpaullone was identified in a large-scale screen as a KCC2-enhancing compound, where it promoted neuronal chloride homeostasis and inhibitory neurotransmission through GSK-3 β inhibition in pain models [333]. Given that astrocytes regulate both inhibitory neurotransmission and synaptic integrity, it is plausible that GSK-3 β inhibition may have broader effects on glial-neuronal interactions in TRD. However, there is currently no direct evidence linking GSK-3 β inhibition to ECM remodeling or UPR dysfunction in this context, and further research is needed to validate whether targeting GSK-3 β could restore astrocyte homeostasis and neuroimmune balance in TRD.

Despite these promising findings, there are several limitations to consider. First, the sample size and potential heterogeneity among patient-derived hiPSCs may limit the generalizability of our results. Second, hiPSC-derived astrocytes cultured *in vitro* may not completely capture the intricacies of the *in vivo* brain environment, where cell-cell interactions among astrocytes, neurons, and microglia are critical. Third, the time point at which astrocytes were profiled was cross-sectional, making it difficult to capture dynamic transcriptomic changes that might occur over the course of the disease or treatment. Fourth, while the LINCS-based screening identified numerous perturbagens, extensive functional validation will be crucial to confirm their therapeutic potential and explore optimal dosing schedules. Finally, although we see a potential link between astrocyte-specific pathways and SSRI resistance, additional mechanistic work is required to show causality.

Our findings highlight the importance of investigating astrocyte-mediated processes in MDD and TRD, but additional research is needed to validate and expand these results. Longitudinal studies that track changes in astrocyte gene expression before and after antidepressant treatment could clarify whether the identified transcriptional signatures shift with the clinical response. Coculture or organoid-based models incorporating neurons, microglia, and astrocytes would also provide a more physiologically relevant system to validate the role of immune and ECM pathways in SSRI resistance. Additionally, more functional analyses, including gene knockdown, overexpression, or targeted pharmacological modulation of high-centrality TFs, such as TP53, JUN, SMAD3, and STAT3, are needed to establish causal links between specific dysregulated pathways, such as TNF–NF κ B, UPR, and ECM remodeling, and the antidepressant response. Finally, exploring combinatorial therapies, such as immune-modulating agents alongside SSRIs, may yield novel strategies to overcome resistance in patients with TRD.

Conclusions

By integrating transcriptomic profiling, TF activity assessments, coexpression network analyses, and LINCS-based computational approaches, we reveal a complex astrocyte-specific landscape in MDD that diverges between SSRI responders and non-responders. Immune modulation, circadian rhythms, oxidative metabolism, and proteostasis emerge as critical processes potentially dictating antidepressant efficacy. Moreover, our LINCS data highlight both FDA-approved antidepressants and repurposing candidates whose signatures oppose pathological gene expression states in astrocytes. While additional *in vivo* validation, expanded sample sizes, and longitudinal assays are crucial next steps, these findings underscore how targeting astrocyte-

focused pathways may yield more effective treatments for individuals facing treatment-resistant depression.

Chapter 3: Proinflammatory transcriptomic and kinomic alterations in astrocytes derived from patients with familial Alzheimer's disease

Abstract

AD is a progressive neurodegenerative disorder characterized by profound neuronal and cognitive decline, with increasing evidence implicating astrocyte dysfunction in disease pathology. While traditional therapeutic approaches have primarily targeted neurons, the crucial role of astrocytes in metabolism, neurotransmission, amyloid-beta clearance, and neuroinflammation underscores their potential as therapeutic targets. In this study, we employed a multiomic integrative analysis combining transcriptomic and kinomic profiling of hiPSC-derived astrocytes from patients with fAD compared to healthy controls. Our transcriptomic analysis identified 1249 significantly differentially expressed genes, highlighting a pronounced upregulation of inflammatory genes (SERPINA3, IL6R, IL1RAP, TNFRSF11A) and a concomitant downregulation of genes essential for synaptic support and ion channel function (STMN2, NMNAT2, SCN2A, GRIN1). Kinomic profiling revealed dysregulated kinase activities within DYRK, GSK, and MAPK families, further implicating altered kinase signaling pathways in astrocyte dysfunction. Integration of these datasets pinpointed critical molecular hubs, notably within the PI3K signaling and inflammatory pathways, highlighting targets such as JAK2, STAT3, and AKT1 as potential modulators of disease progression. Furthermore, leveraging the LINCS platform, we identified chemical perturbagens, including fluticasone propionate and Akt inhibitors, capable of reversing the transcriptomic signatures associated with fAD astrocytes. This integrative multiomic approach not only enhances our understanding of

astrocyte-specific molecular mechanisms in AD but also provides novel targets for therapeutic intervention aimed at mitigating astrocyte-driven neurodegeneration.

Introduction

AD, a leading cause of dementia, was the sixth leading cause of death in the United States in 2019 and the fifth leading cause of death in 2021 among individuals aged 65 and older [334]. Alzheimer's disease is a progressive neurodegenerative disorder characterized by significant neuronal damage that leads to cognitive decline, loss of function, and eventually death. The economic impact of AD is also substantial, with projected costs of \$360 billion for 2024 [334]. Symptomatic medications for AD have been used for decades; however, their benefit is modest. Recently, amyloid monoclonal antibodies have been shown to demonstrate strong disease-modifying properties with amyloid removal and slowing of cognitive decline, but side effects that require close monitoring and efficacy for individual patients vary [335-340]. Ongoing research and clinical trials continue to seek more effective treatments for both the disease and its symptoms, highlighting AD as a significant focus of global scientific efforts.

Astrocytes are critical to the pathophysiology of AD because of their role in metabolism, neurotransmission, and A β clearance [335, 336]. For example, astrocytes upregulate EAAT2/GLT-1 to regulate neurotransmission and mitigate excitotoxicity [341-343] while suppressing neuroinflammation through C3/STAT3 pathway downregulation [344]. However, drug development efforts for neurodegenerative diseases have traditionally focused on neuronal targets, frequently neglecting the significant contributions of astrocytes to disease progression and pathology [345]. The development of astrocyte-specific therapeutic interventions that

support astrocyte function could significantly advance the treatment of AD, offering new avenues to mitigate disease progression and improve patient outcomes.

Kinases orchestrate an array of cellular processes, including neuroinflammation in AD [346, 347]. Novel markers have been linked to neurotoxic astrocytes that drive AD progression, particularly those associated with proinflammatory responses [348-350]. Previous transcriptomic studies have identified critical roles for astrocytes and protein kinases in AD pathogenesis. Specific mutations in protein kinases may drive cognitive decline in AD, independent of A β metabolism, load, and clearance [351-353]. Notably, quantitative phosphoproteomic studies have revealed differential phosphorylation of protein kinases and small heat shock proteins [354-357]. These studies also revealed increases in the phosphorylation of astrocyte-specific proteins such as GFAP, suggesting gliosis or astrocyte proliferation in AD [356, 357]. However, the kinase signaling pathways that specifically regulate astrocyte functions in AD remain poorly characterized. To enhance our understanding of AD and develop more effective interventions, it is crucial to delve deeper into astrocyte-specific kinases, phosphoproteins, and kinase-phosphosite networks in AD.

fAD, an early-onset form of AD, arises from autosomal-dominant mutations in genes such as *APP*, *PSEN1*, and *PSEN2* [358]. These mutations offer a genetically controlled model that is ideal for dissecting the molecular mechanisms underlying AD. iPSC-derived astrocytes from fAD patients may provide insights into astrocytic dysfunction and offer a platform for exploring astrocyte-specific therapeutic targets.

In this study, we employed an integrative analysis of differential transcriptomic and kinomic signatures to identify molecular alterations associated with fAD, the hereditary form of AD, in hiPSC-derived astrocytes. We used RNA sequencing and PamGene kinomic profiling to

identify key differentially expressed genes and dysregulated kinase activities in hiPSC-derived astrocytes from patients with fAD compared with age- and sex-matched healthy controls. The integration of RNA-seq and kinome array analyses provides a detailed view of both global gene expression changes and kinase activity alterations in AD. This combined approach enhances our understanding of the transcriptional changes and their functional implications in kinase signaling, specifically within astrocytes involved in AD progression. By correlating gene expression profiles with kinase activity, this methodology facilitates a more precise identification of potential therapeutic targets and contributes to deeper insight into the molecular mechanisms underlying astrocyte dysfunction in AD. The integration of these datasets enables the mapping of critical protein-protein interaction networks, uncovering central nodes and disrupted pathways that may serve as potential therapeutic targets. These integrative multiomic insights provide a deeper understanding of the molecular mechanisms underlying astrocyte dysfunction in fAD and suggest potential therapeutic targets for modulating disease progression.

Materials and methods

Culture of human iPSCs and differentiation into astrocytes

Three fAD human iPSC lines (AD-001: male, APOE3/3, PSEN1 Y155H; AD-002: male, APOE4/4, APP V717I; AD-003: female, APOE3/3, PSEN1 intron 4 deletion) and three healthy control human iPSC lines (HC-001: male, APOE3/3; HC-002: male, APOE3/3; HC-003: female, APOE2/3) were previously generated and fully characterized [359]. The control and fAD subjects from which our iPSCs were derived were matched for age and sex. For our analyses, fAD cells were compared with nonisogenic healthy controls. All experiments were performed in compliance with the relevant laws and institutional guidelines. Human iPSCs were cultured in

mTeSR1 medium (Stemcell Technologies, 85850) in cell culture dishes coated with Geltrex LDEV-Free Reduced Growth Factor Basement Membrane Matrix (Gibco, A1413201) diluted 1:100 in DMEM/F-12 (Gibco, 11320033). Briefly, mTeSR1 was replaced every other day or every day once the cells reached 50% confluence. When 80–90% confluent, the cells were passaged as follows: aspirating media, washing with DPBS, incubating with ReLeSR (STEMCELL Technologies, 100–0484) at RT for 3 minutes, aspirating ReLeSR, incubating at 37°C for 10 minutes, resuspending in mTeSR1 supplemented with 10 nM Y-27632 dihydrochloride ROCK inhibitor (Tocris, 125410), counting, and plating onto Matrigel-coated plates at the desired number.

Human iPSC-derived astrocytes were generated as previously described [259]. Briefly, iPSCs were plated on Matrigel-coated 6-well plates and infected with rtTA, SOX9, or NFIB lentivirus. On Day 0, the medium was replaced with fresh mTeSR-1 media containing 2.5 µg/mL doxycycline. From Days 1-7, the cells were cultured in expansion medium (DMEM/F12, 10% FBS, 1% N2, 1.25 µg/mL puromycin, and 200 µg/mL hygromycin) and gradually transitioned to FGF medium (Neurobasal, 2% B27, 1% NEAA, 1% GlutaMax, 1% FBS, 8 ng/mL FGF, 5 ng/mL CNTF, 10 ng/mL BMP4, and 200 µg/mL hygromycin) by Day 7. On Day 7, the cells were dissociated via Accutase for 10 minutes and then replated on Matrigel-coated 6-well plates in FGF medium. From Day 9, the FGF medium was changed to maturation medium (1:1 DMEM/F12 and neurobasal medium, 1% N2, 1% Na pyruvate, 10 µg/µL NAC, 10 µg/µL hbEGF, 10 ng/mL CNTF, 10 ng/mL BMP4, and 500 µg/mL cAMP), and half of the medium was changed every 2-3 days.

For immunocytochemistry, astrocytes were fixed with 4% paraformaldehyde for 15 min at room temperature. The samples were permeabilized and blocked with 0.25% Triton X-100 and

10% donkey serum in PBS for 20 min, as previously described [260]. The samples were then incubated with anti-GFAP (rat, 1:500; Invitrogen 13-0300) and anti-S100B (mouse, 1:500; Sigma–Aldrich AMAB91038) primary antibodies at 4°C overnight, followed by incubation with secondary antibodies (donkey anti-rat Alexa Fluor 488, 1:1000; Invitrogen A-21208; donkey anti-mouse Alexa Fluor 568, 1:1000; Invitrogen A10037) for 2 hours at room temperature. Coverslips were mounted with Fluoromount-G (Southern Biotech, 0100-01) and imaged via a Nikon Eclipse Ti-E microscope.

Sample preparation and processing for transcriptomics

For RNA-seq, total RNA samples from the six cell lines were prepared with TRIzol reagent (Invitrogen). Total RNA was treated with DNase I (Zymo Research) and concentrated via the Clean & Concentrator Kit (Zymo Research). A NanoDrop One/OneC Microvolume UV–Vis Spectrophotometer (Thermo Scientific) was used to determine the RNA yield. For mRNA-enriched RNA-seq in all six cell lines, 150-cycle PE sequencing via the Illumina HiSeq2500 platform was performed with 1 µg of RNase-free RNA (>10 ng/µL, RIN > 7) per technical triplicate. Transcript abundances were quantified from paired-end reads (raw FASTQ files) against the *Homo sapiens* reference transcriptome (hg19) via kallisto [360]. Transcriptome-wide gene counts were obtained through gene-level transcript summarization with the tximport R package [361]. DGE analysis was performed after filtering for genes with low expression using the *filterByExpr* function via the edgeR R package [362].

Sample preparation and processing for kinomics

For kinomics, each of the six iPSC samples (three HC and three fAD patients) was homogenized in mammalian protein extraction reagent (Thermo Fisher, 78501) containing 1× Halt phosphatase and protease inhibitor cocktail (Thermo Fisher, 78443). The samples were incubated on ice for 30 minutes and subsequently run through the Fisherbrand Bead Mill 24 Homogenizer (Thermo Fisher, 15340163) for 5 minutes at 14000 × g. The supernatant was collected and quantified via the Pierce BCA protein assay (Thermo Fisher, 23225). All the samples in each group were pooled according to total protein content and diluted with the same lysis buffer to 0.2 μg/μL. The six sample groups were then loaded on a single STK PamChip array (PamGene) and run in technical triplicate using three separate chips. Two micrograms of total protein were loaded into each array, followed by 30 minutes of blocking with 2% bovine serum albumin (BSA), with a master mixture containing a final concentration of 90.91 μM adenosine triphosphate (ATP), 0.1× BSA solution, 1× protein kinase buffer, water, and a primary proprietary antibody mixture (PamGene). The sample and master mixture are incubated within the PamStation 12 (PamGene) for 80 minutes and pumped through the well to facilitate the phosphorylation of the immobilized peptides. In the subsequent step, FITC-labeled, anti-phosphoserine-threonine antibodies (PamGene) were added to each array. Each array was washed using PBS-T buffer (1× PBS, 0.1% Triton-X100), and Evolve2 (PamGene) kinetic image capture software was used to capture peptide phosphorylation on each PamChip. During the post-wash phase, the intensity of peptide spots was recorded at 10, 20, 50, 100, and 200 ms, then Bionavigator software was used to convert the captured images and their signal intensity to numerical values used for data analysis.

Transcriptomic analysis

The ggplot2 R package was used for volcano plots to depict differential expression profiles. The volcano plots display the difference in gene expression ($\log_2\text{FoldChange}$) between experimental comparisons and significance values ($-\log_{10}$ adjusted p value), with dashed lines indicating the significance thresholds of adjusted p values < 0.05 and absolute \log_2 -fold change values > 1 . For the heatmaps, the pheatmap R package was used, and the differentially expressed genes were filtered by AD risk-associated genes identified through Multimarker Analysis of GenoMic Annotation (MAGMA) of genome-wide association studies (GWAS) in late-onset AD [363]. Z scores were calculated via the scale function in R, ensuring normalized values for comparison across samples.

Transcriptomic pathway analysis

We utilized the 3PodReports package to conduct gene set enrichment analysis (GSEA) with the entire set of genes ranked by $\log_2\text{FC} \times -\log_{10}(p \text{ value})$ and ORA of genes in the top and bottom 10% of genes ranked by $\log_2\text{FoldChange}$ [364, 365]. We then analyzed the overlap between GSEA and ORA.

Protein-protein interaction network analysis

To construct PPI networks, we used STRINGdb for Homo sapiens to map DEGs to known interactors. Significant DEGs (adjusted p value < 0.05 , $|\log_2\text{FC}| > 1$) were filtered for specific GO terms, as annotated by the GO knowledgebase [366, 367], and STRINGdb was used to retrieve interaction data for mapped genes [368]. The network was visualized via igraph [369]. Node sizes were scaled inversely to the adjusted p value, node colors were determined by $\log_2\text{FC}$

(red for upregulated genes and blue for downregulated genes), and the layout was generated via the Graphopt algorithm.

Transcription factor activity inference

TF activity was inferred from bulk RNA-seq data via the decoupleR package [370]. The input gene-level statistics, derived from differential gene expression analysis with edgeR, included *t* values and log2FC values for each gene. TF activities were inferred via the ULM method, which fits a linear model to predict observed gene expression on the basis solely of TF–gene interaction weights from the CollecTRI network [371]. The resulting *t* value from the fitted model was used as the TF activity score, where positive scores indicate TF activation, and negative scores represent TF inhibition.

Kinomic analysis

We utilized the BioNavigator software tool (PamGene) to preprocess kinome data, conduct image analysis, interpret output measurements, and visualize, store, and share results from the sample screen. The processed data yielded a list of differentially phosphorylated reporter peptides, which served as raw data for subsequent analyses. To increase confidence in predicting upstream kinases influencing substrate phosphorylation differences, we employed four distinct kinase substrate mapping tools, namely, a kinome random sampling analyzer (KRSA) as the primary analysis tool, PamGene upstream kinase analysis (UKA), kinase enrichment analysis version 3 (KEA3), and posttranslational modification signature enrichment analysis (PTM-SEA). Using the Creedenzymatic R package, we converted the analysis outputs into percentile rankings, divided them into quartiles, and visually summarized the quartiles. High confidence candidate

kinases were those detected in the top quartile of the results from all four analyses, whereas medium confidence candidates appeared in the top quartile of the KRSA results and at least the top two quartiles of the UKA, PTM-SEA, and KEA3 results.

Multiomic integration

We employed the Kinograte R package, which utilizes an optimized version of the PCSF algorithm, to construct an integrated multiomic PPI network. This network included transcriptomic hits ($FDR < 0.05$) and Creedenzymatic-predicted kinomic hits. Node prizes were assigned on the basis of the percentile rank of $\log_2\text{FoldChange}$ or mean Creedenzymatic score, whereas edge costs were determined by the inverse STRING database interaction confidence. The PPI network nodes were subsequently ranked using the average of their node prize and eigencentrality for gene-set enrichment analysis with the fgsea R package, and the top 10% of these nodes were also tested for overrepresentation analysis with the enrichR R package via Gene Ontology. Subnetworks of gene members from dysregulated pathways ($FDR < 0.05$) identified in the primary PPI network were visualized. Pathways exhibiting dysregulation ($FDR < 0.05$) were subjected to functional clustering and visualization via Pathway Analysis Visualization with Embedding Representations (PAVER), a meta-clustering method specifically designed for pathways [364, 365]. PAVER identifies the most representative terms (MRTs) for hierarchically clustered pathway embeddings by selecting the term with the highest cosine similarity to its respective cluster's average embedding. UMAP scatter plots were created, portraying individual pathways with colors indicating their cluster affiliation and shapes denoting the pathway analysis.

Sample size and statistical analyses

For RNA-seq, 3 familial AD iPSC-derived astrocyte lines and 3 nonisogenic matched control lines were used with 3 technical replicates each. For kinomics, 3 familial AD iPSC-derived astrocyte lines and 3 nonisogenic matched control lines were used with 3 technical replicates each. All genes and pathways analyzed had FDR <0.05 and $\log_2FC > 1$.

Results

Characterization of hiPSC-derived astrocytes

To identify astrocyte-specific dysregulated molecular pathways in AD, transcriptomic and kinomic signatures were obtained from hiPSC-derived astrocytes from patients with fAD (n=3) and age- and sex-matched nonisogenic HC individuals (n=3) and subjected to network-based multiomic integration (Figure 2.1A). hiPSC-derived astrocytes were generated as previously described [259] and astrocyte differentiation was verified through RNA sequencing and immunocytochemistry (Figure 2.1B). Heatmap analysis of differential gene expression in hiPSC-derived astrocytes relative to isogenic undifferentiated hiPSCs revealed increased expression of canonical astrocyte transcripts, including GFAP and S100B (Figure 2.1C). Immunofluorescent analysis of hiPSC-derived astrocytes analysis further validated the astrocytic phenotype, with strong staining for GFAP and S100B (Figure 2.1D). Following astrocytic differentiation and verification, RNA was extracted from the 3 familial AD iPSC-derived astrocyte lines and the 3 healthy control lines, and RNA sequencing was performed to investigate the molecular alterations in fAD astrocytes relative to controls.

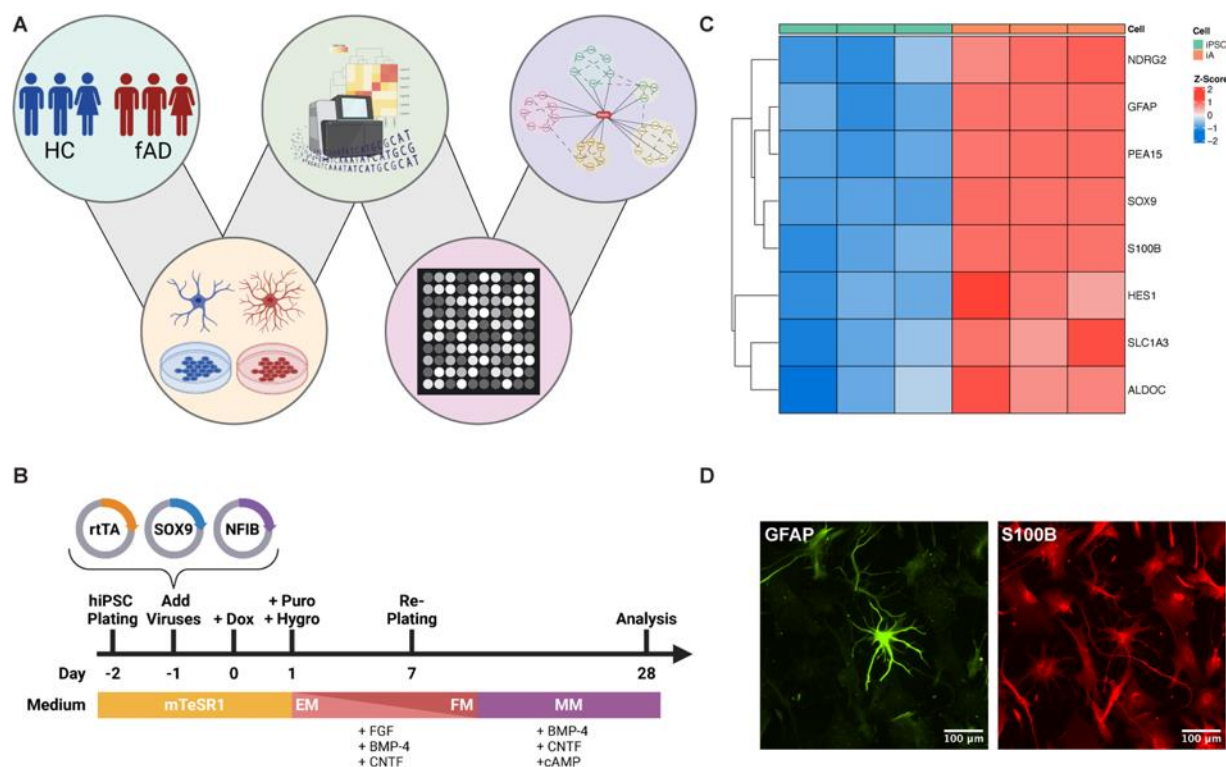


Figure 3.1. Study design and characterization of hiPSC-derived astrocytes. (A) Differential transcriptomic and kinomic signatures from iPSC-derived astrocytes from patients with familial Alzheimer’s disease (n=3) and age- and sex-matched nonisogenic healthy controls (n=3) were subjected to network-based multiomic integration to identify dysregulated molecular pathways. (B) Human iPSC-derived astrocytes were generated as previously described [259]. (C) Heatmap showing the differential expression of canonical astrocyte markers in astrocytes relative to iPSCs. (D) Immunofluorescence staining of hiPSC-derived astrocytes at 20x magnification showing GFAP (green) and S100B (red) expression.

Transcriptomic profiling reveals key dysregulated pathways in fAD astrocytes

To elucidate the molecular mechanisms underlying astrocyte dysfunction in fAD, a comprehensive transcriptomic analysis was conducted to compare the gene expression profiles of

fAD astrocytes with those of healthy controls. This analysis identified 1249 significantly differentially expressed genes (adjusted p value < 0.05 , $|\logFC| > 1$). Among these genes, 307 were downregulated and 942 were upregulated in fAD astrocytes compared with healthy controls. The transcript levels of genes related to the inflammatory response, synaptic function, and ion channel activity were significantly altered. Inflammatory response genes such as SERPINA3, IL7R, IL6R, MMP12, IL1RAP, TNFRSF11A, TNFSF10, and CXCL14 were significantly upregulated, whereas synaptic function and ion channel activity genes such as STMN2, NMNAT2, SCN2A, GRIN1, and KIF1A were significantly downregulated (Figure 2.2A). These results suggest a shift toward a more reactive, inflammatory state in fAD astrocytes, alongside a reduction in synaptic support functions.

To investigate the relevance of transcriptomic signatures in fAD astrocytes, we determined whether the differentially expressed genes in our model were enriched for known AD genetic risk factors identified by GWAS analyses in humans. We probed the MAGMA study, a GWAS analysis of late-onset AD, to determine whether our differentially expressed fAD genes were among those identified as AD risk-associated genes. The expression of MEF2C, OAS1, and SORL1 was significantly altered, among other genes (Figure 2.2B). The integration of GWAS analyses into our study supported the relevance of our fAD astrocyte model.

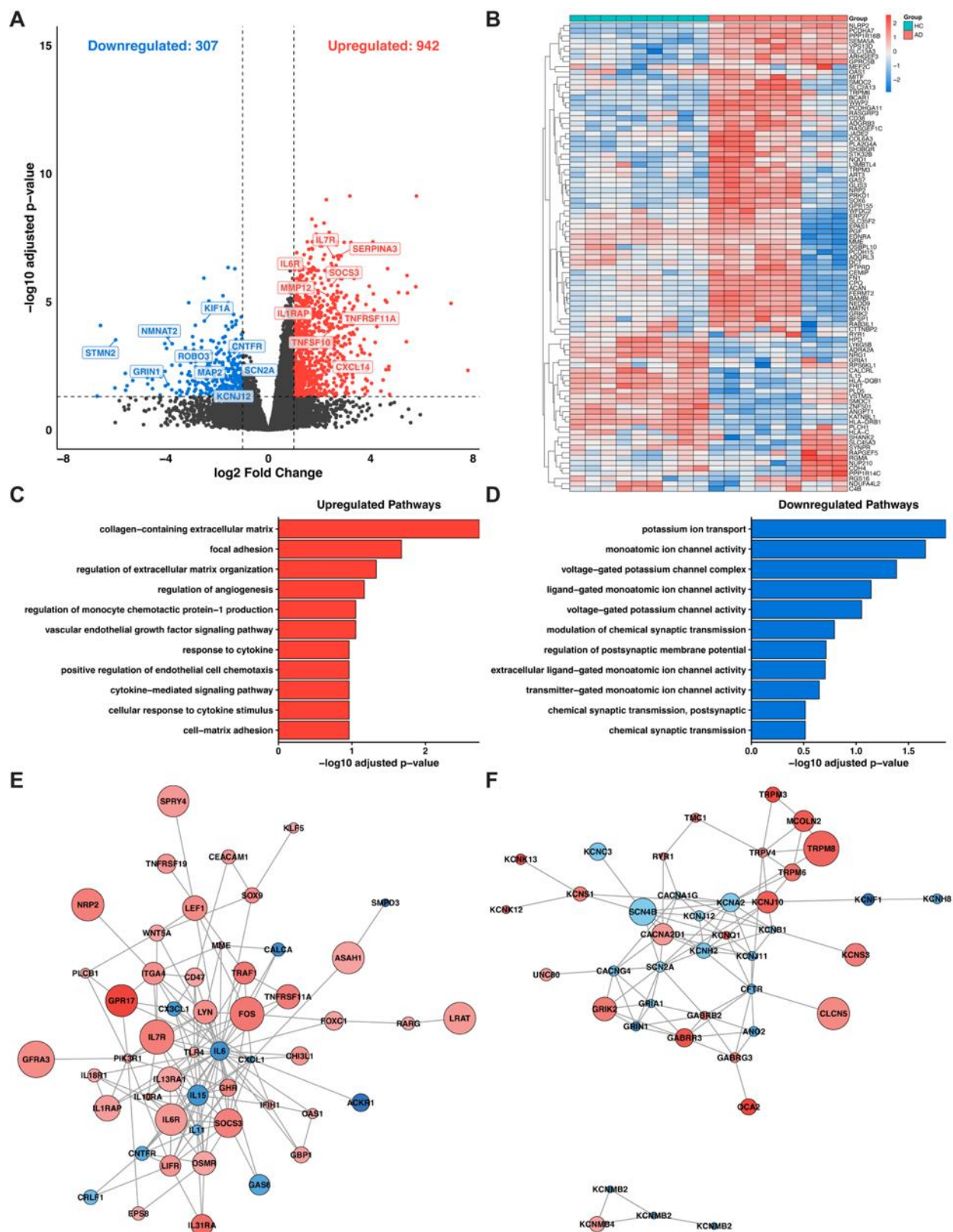


Figure 3.2. Transcriptomic analysis of fAD versus HC hiPSC-derived astrocytes. (A)

Volcano plot of differential gene expression analysis comparing hiPSCs from HC and fAD astrocytes, plotted as a function of the log₂-fold change in gene expression and the inverse log₁₀ of the adjusted *p* value. The dashed lines demarcate adjusted *p* values less than 0.05 and absolute values of log₂-fold change greater than 1. (B) Heatmap showing the differential expression of AD-associated GWAS hits in fAD astrocytes. (C) Top 10 upregulated and (D) top 10 downregulated pathways in fAD astrocytes identified via both rank-based GSEA and ORA analysis. (E) PPI network of genes associated with the cellular response to cytokine stimulus (GO:0071345) and (F) PPI network of genes associated with monoatomic ion channel activity (GO:0005216), with the node color and size indicating the direction and significance of gene expression changes. Red nodes indicate significantly upregulated genes (log₂-fold change > 1, *p* < 0.05), whereas blue nodes represent significantly downregulated genes (log₂-fold change < -1, *p* < 0.05). The size of each node is proportional to the significance of the adjusted *p* value, with larger nodes representing more statistically significant changes in gene expression.

To elucidate the molecular dynamics in fAD astrocytes and their impact on disease progression, GSEA and ORA were conducted to identify pathways that are significantly altered [364, 365]. The pathways reported were present in both the GSEA and ORA results, thus providing greater confidence in their relevance to fAD astrocytes. The upregulated pathways included those related to the extracellular matrix, such as the collagen-containing extracellular matrix and cytokine-mediated signaling pathways, suggesting enhanced inflammatory and structural remodeling in fAD astrocytes (Figure 2.2C). On the other hand, downregulated pathways involve crucial neuronal functions, including potassium ion transport, synapse

organization, and voltage-gated potassium channel activity, which may contribute to the impaired neuronal communication observed in AD (Figure 2.2D). Overall, these findings illustrate a multifaceted disruption in cellular pathways within fAD astrocytes, underscoring their potential role in exacerbating AD pathology through both inflammatory processes and neuronal dysfunction.

We then examined established PPI networks to explore how changes in gene expression affect functional cellular pathways in fAD astrocytes. The PPI network associated with the cellular response to cytokine stimuli features upregulated genes such as IL6R, IL1RAP, IL7R, FOS, and GPR17, further supporting the inflammatory shift in fAD astrocytes (Figure 2.2E). In contrast, the network associated with monoatomic ion channel activity in fAD astrocytes revealed reduced expression of genes such as SCN2A, GRIN1, KCNB1, KCNA2, and GRIA1 (Figure 2.2F), suggesting a diminished function of ion channels, which is critical for maintaining neuronal excitability and communication.

Together, these findings suggest that fAD astrocytes are characterized by increased inflammation and structural remodeling coupled with diminished support for neuronal function, providing key insights into the cellular mechanisms driving AD pathology in astrocytes.

Identification of astrocyte-specific molecular targets in fAD

To elucidate the molecular mechanisms driving astrocyte dysfunction in fAD, an analysis of TF activity was conducted via the gene expression profiles of fAD astrocytes and healthy control astrocytes. This analysis aimed to identify the key transcription factors that are either activated or deactivated in fAD astrocytes, providing insight into their roles in the progression of AD pathology. TF activity was inferred via the ULM method, where t values were derived to

predict the impact of TFs on gene expression [370, 371]. Positive t values indicate activated TFs, reflecting increased target gene expression, whereas negative t values indicate deactivated TFs, which are associated with reduced gene expression. TF activity analysis revealed both activated and deactivated TFs in fAD astrocytes. Activated TFs include STAT3, NF κ B, and MYC, which are critical regulators of inflammation and cellular stress responses (Figure 2.3A). Conversely, deactivated TFs such as SREBF1, MAML1, and YAP1 are implicated in cellular repair and metabolic regulation, and their suppression suggests a loss of protective functions in fAD astrocytes (Figure 2.3A). The deactivation of these TFs may exacerbate cellular dysfunction and contribute to the progression of AD pathology in astrocytes.

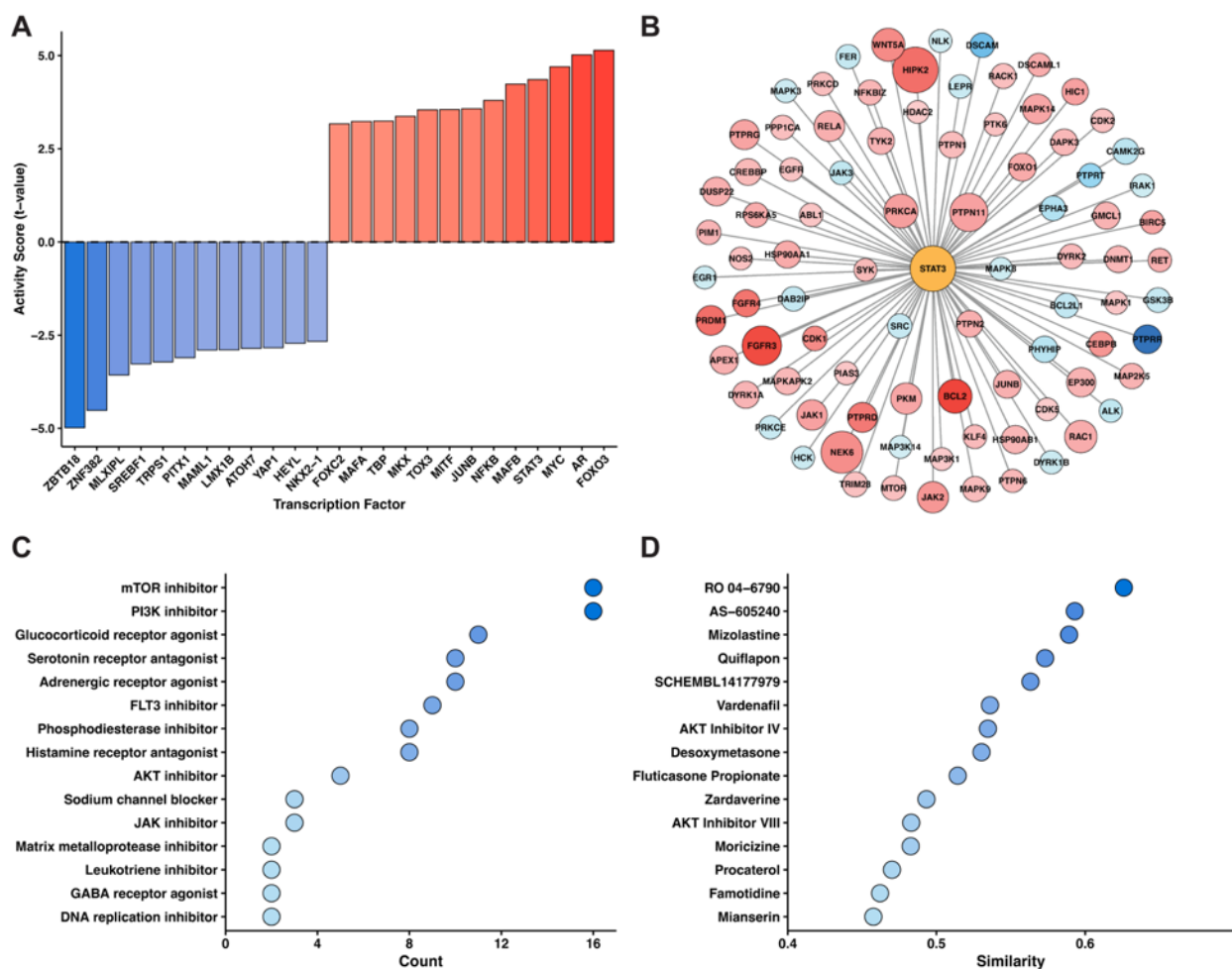


Figure 3.3. Identification of astrocyte-specific molecular targets in fAD. (A) The results of TF activity inference. Positive scores (red bars) indicate active TFs, whereas negative scores (blue bars) reflect inactive TFs. (B) A STAT3-centered PPI network in which nodes represent genes interacting with STAT3; red represents significantly upregulated genes (\log_2 -fold change > 1 , $p < 0.05$), and blue represents significantly downregulated genes (\log_2 -fold change < -1 , $p < 0.05$). The size of each node is proportional to the significance of the adjusted p value, with larger nodes reflecting greater significance. (C) The discordant mechanisms of action identified through LINCS. The color of each point is proportional to the number of perturbations, with darker nodes reflecting a greater number of perturbations. (D) The top discordant perturbagens identified through LINCS. The color of each point is proportional to the similarity score, with darker nodes reflecting greater similarity.

To further explore the molecular interactions contributing to astrocyte dysfunction in fAD, a STAT3-centered PPI network was analyzed via interaction data retrieved from the STRING database. This PPI network highlights interactions with several upregulated genes critical in AD pathology, particularly those linked with neuroinflammatory and stress responses (Figure 2.3B). In addition to the previously mentioned genes, such as JAK1, JAK2, and SRC, this analysis also revealed significant upregulation of HDAC2 and PRKCD, which are involved in epigenetic regulation and signaling pathways relevant to AD (Figure 2.3B). Targeting these key nodes, especially STAT3 and its direct interactors, presents viable therapeutic avenues to mitigate inflammation and restore cellular function in astrocytes, addressing core aspects of AD pathology.

To advance our understanding of fAD and explore potential therapeutic interventions, the LINCS platform was employed. The LINCS platform utilizes the log₂-transformed fold change and *p* values for landmark genes from the LINCS L1000 project to identify and cluster chemical perturbations by their mechanisms of action [372, 373]. In this study, the LINCS platform was used to identify small molecules and mechanisms of action that counteract the transcriptomic alterations observed in fAD astrocytes compared with those in control astrocytes. Discordant MOAs, such as PI3K inhibitors, mTOR inhibitors, JAK inhibitors, and matrix metalloprotease (MMP) inhibitors, were identified as potential therapeutic targets that may counteract these pathological shifts (Figure 2.3C). Additionally, discordant perturbagens such as fluticasone propionate, a glucocorticoid receptor agonist, Akt inhibitor VIII and Akt inhibitor IV, and AS-605240, a PI3K γ inhibitor; Vardenafil, a PDE5 inhibitor; Zardaverine, a dual PDE3/PDE4 inhibitor; and mianserin, an antagonist of multiple adrenergic, histaminergic, and serotonergic receptors, suggest therapeutic strategies that may reverse these transcriptomic changes (Figure 2.3D). These discordant perturbagens offer a promising avenue for treatment by targeting astrocyte-driven processes, which have been largely overlooked in traditional AD therapies that focus primarily on neuronal dysfunction.

Kinomic profiling reveals dysregulated kinase activity in fAD astrocytes

To better understand the role of kinases in fAD astrocyte dysfunction, we analyzed kinase activity and peptide phosphorylation patterns. The use of the PamGene12 Kinome Array enabled comprehensive coverage of the human kinome by analyzing a biological sample's phosphorylation profile through bioinformatic permutation with extensive validation of the phosphorylation patterns observed. This analysis revealed significant changes in peptide

phosphorylation patterns in fAD astrocytes compared with healthy controls (Figure 2.4A). Compared with that in healthy controls, the global peptide phosphorylation signal in fAD astrocytes was lower (Figure 2.4B). Furthermore, specific peptides exhibited differential phosphorylation, suggesting targeted disruptions in signaling pathways (Figure 2.4C). We used three analytical modalities (KRSA, KEA3, and UKA) to identify specific protein kinases implicated in our fAD astrocytes. (Figure 2.4D). We identified kinases in the dual-specificity tyrosine phosphorylation-regulated kinase (DYRK), glycogen synthase kinase (GSK), and mitogen-activated protein kinase (MAPK) families as hit kinases in our disease model (Figure 2.4D). These kinases were consistently detected with three distinct peptide-to-kinase mapping tools, emphasizing their importance in pathological signaling pathways in fAD astrocytes.

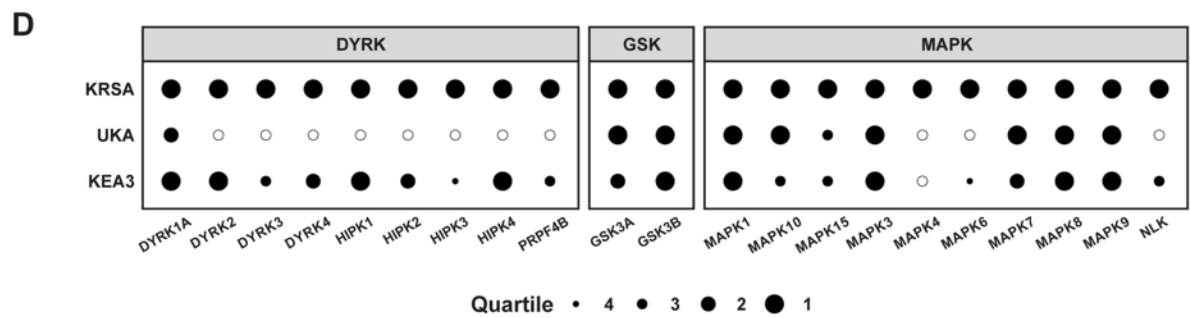
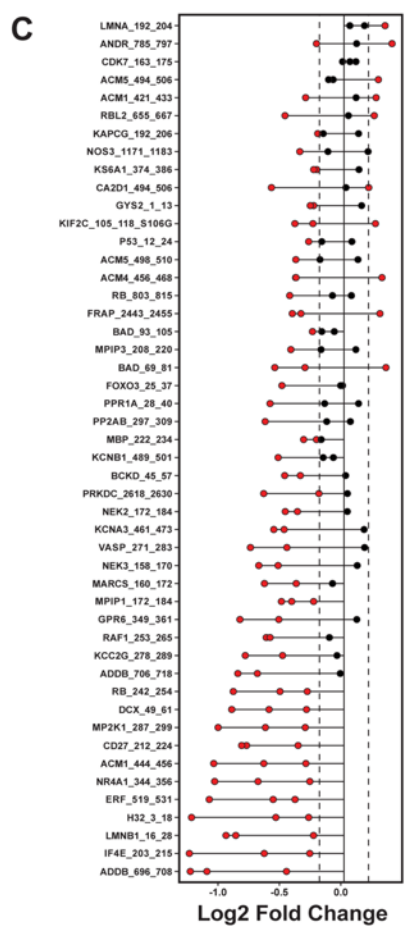
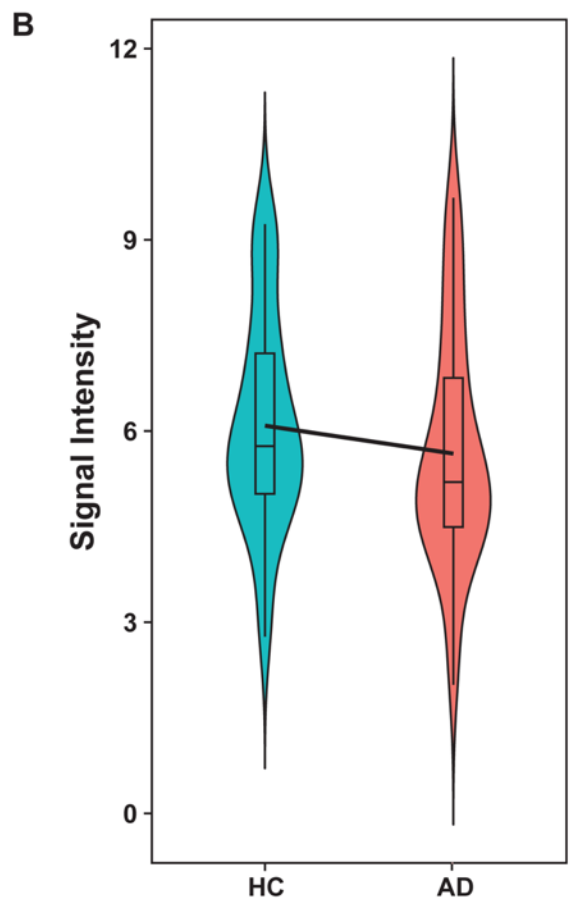
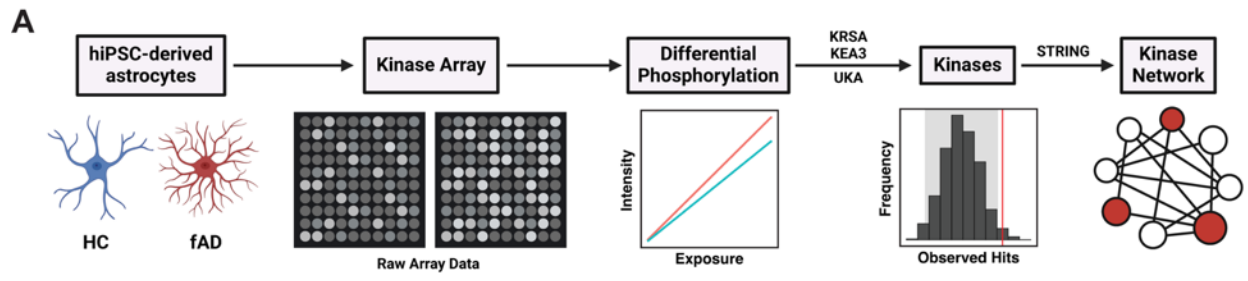


Figure 3.4. Differential kinase activity in fAD astrocytes versus healthy control astrocytes.

(A) Peptides were initially selected on the basis of differences in phosphorylation between groups, and the upstream kinases that most likely drive these effects were identified via four different analyses of peptide phosphorylation. The emerging kinase hits were integrated into a larger kinase-to-kinase interaction network model. (B) Violin plot showing global peptide phosphorylation in familial AD patients versus HCs via KRSA. (C) Waterfall plot showing differentially phosphorylated peptides between AD and WT strains on serine–threonine chips. (D) Bubble plot showing the differentially active kinases utilizing four different analyses packages of peptide phosphorylation: KRSA, KEA3, and UKA. Column headers represent kinase families, whereas single kinases are represented within the columns. Circles denote kinases whose activity was detected by the analyses. Kinases are present within black filled-in circles and absent in black outlined circles. The size of the circles (1-4) denotes the quartile in which the result appears in each analysis, with the 1st quartile being the lowest and the 4th quartile being the highest confidence results.

Multiomics integration highlights dysregulated pathways in fAD astrocytes

To identify key dysregulated molecular pathways involved in astrocyte dysfunction and AD progression, we conducted an integrative multiomics analysis that combined transcriptomic and kinome array data. This integrated approach provides a more comprehensive understanding of how alterations in gene expression impact kinase activity and signaling pathways in fAD astrocytes. Our analysis revealed significant dysregulation of key molecular pathways, particularly those involved in inflammatory responses and phosphatidylinositol 3-kinase (PI3K) signaling. The UMAP plot (Figure 2.5A) visually represents the clustering of these gene sets,

highlighting distinct functional pathways with notable emphasis on the regulation of inflammatory responses and PI3K signaling. These pathways were identified as critical areas of dysregulation in fAD astrocytes. PPI network analysis further elucidated these findings by mapping the interactions within these pathways. PPI network analysis of proteins in the PI3K signaling network revealed key nodes, including PIK3R1, IGF1, and AKT1. These nodes are central to this pathway and show substantial changes in connectivity and activity in fAD astrocytes (Figure 2.5B). Similarly, protein-protein interaction (PPI) network analysis of proteins in the inflammatory response network highlighted the central roles of IL6, JAK2, and STAT3 in mediating the inflammatory processes that are upregulated in the disease state (Figure 2.5C). The integrative approach of this analysis revealed multiple multiomic hits in both networks, such as JAK2, indicating both transcriptomic dysregulation and kinomic changes in these targets. These results provide a comprehensive view of the molecular mechanisms underlying astrocyte dysfunction in AD, pinpointing specific pathways that may serve as potential therapeutic targets.

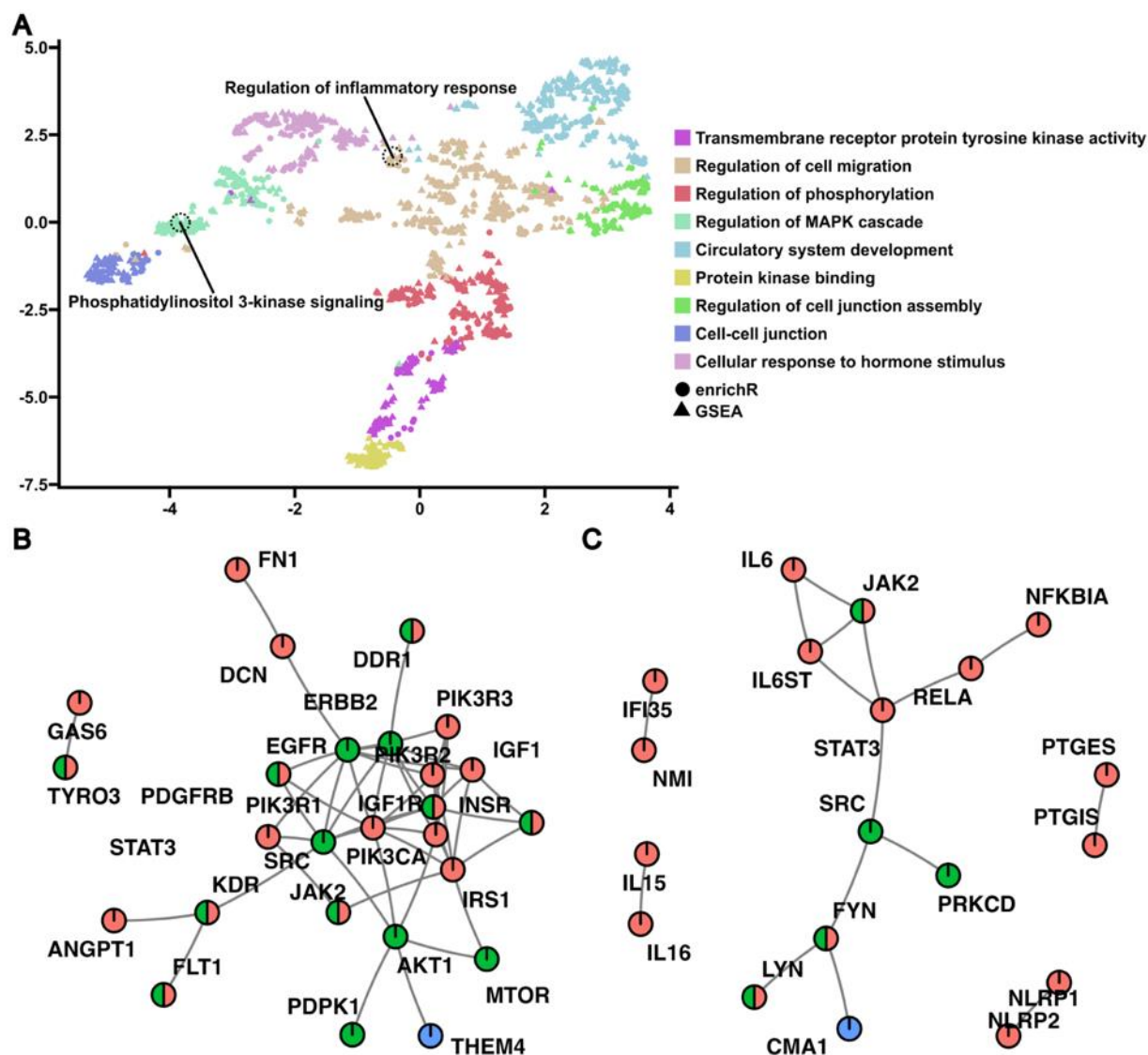


Figure 3.5. Identification of molecular pathways altered in fAD astrocytes via multiomic integration. (A) PAVER analysis of dysregulated molecular pathways revealed 10 functionally distinct gene set clusters in nonlinear UMAP space. (B) PPI network showing the subnetwork of genes involved in the PI3K pathway. (C) PPI network showing the subnetwork of genes involved in inflammatory pathways. Node color indicates omic hits, with red nodes indicating RNA, green nodes indicating kinases, and blue nodes indicating algorithmically interpolated hidden nodes.

Discussion

The results of this study offer valuable insights into the molecular changes associated with astrocyte dysfunction in fAD. By leveraging a multiomic approach that integrates transcriptomic and kinomic analyses, we identified key pathways and molecular hubs that are dysregulated in fAD astrocytes compared with healthy controls. The distinct gene expression and kinase activity profiles we observed suggest that astrocytes may play a role in disease pathophysiology.

Transcriptomic analysis revealed the upregulation of genes involved in inflammation, such as SERPINA3, IL6R, IL1RAP, and TNFRSF11A, indicating a shift toward a reactive, inflammatory astrocyte phenotype. Recent studies have highlighted the roles of these genes in exacerbating the inflammatory processes central to AD pathogenesis [374]. SERPINA3 transcript and protein expression is increased in senescent astrocytes, leading to the upregulation of proinflammatory factors and the downregulation of neurotrophic growth factors, which ultimately diminishes the neuroprotective functions of astrocytes and exacerbates neurodegenerative processes, such as the upregulation of proinflammatory cytokines and the downregulation of neurotrophin production [375-379]. Additionally, the p.D358A variant of IL6R increases soluble IL-6R levels, enhancing IL-6 trans-signaling in astrocytes, which contributes to neuroinflammatory processes and is associated with an earlier onset of AD, especially in APOE ϵ 4 carriers [380, 381]. Moreover, genetic variants in IL1RAP are associated with increased cerebrospinal fluid tau levels, accelerated amyloid accumulation, and cognitive decline in AD [382, 383]. Furthermore, GPR17 has been identified as a key mediator of neuroinflammation, particularly in response to A β exposure, where its inhibition has been shown to ameliorate cognitive deficits, reduce neuroinflammation, and promote synaptic function

through the modulation of the NF- κ B, Nrf2/HO-1, and BDNF signaling pathways [384, 385].

Taken together, these findings underscore the critical impact of inflammatory gene expression in astrocytes on the onset and progression of AD, revealing potential molecular targets for therapeutic intervention.

Conversely, genes involved in synaptic function and ion channel activity, such as STMN2, NMNAT2, SCN2A, GRIN1, and KIF1A, were significantly downregulated, suggesting diminished neuronal support (Figure 2.2A). Additionally, genes that have been shown to be associated with AD risk via large-scale GWAS [386-388], such as MEF2C, OAS1, and SORL1, presented altered expression in fAD astrocytes relative to healthy controls (Figure 2.2B). This finding substantiates the translational relevance of this study's model and supports the validity of using this model to explore pathophysiological mechanisms in AD. Research into these genes has revealed their critical roles in neuronal health and function. STMN2, a key target of TDP-43, is aberrantly spliced in patients with AD, and its partial loss results in motor deficits, detectable neuropathology, and abnormal mitochondrial morphology in mice [389]. The overexpression of NMNAT2, a key enzyme in energy metabolism that is reduced in AD, has been shown to reduce A β production and tau phosphorylation in Tg2576 mice via the upregulation of ADAM10 and PP2A, respectively [390, 391]. The downregulation of these genes suggests that astrocytes may contribute to the loss of synaptic integrity in AD.

Comprehensive pathway analysis further emphasized the dual role of enhanced inflammatory pathways and diminished neuronal support functions. This analysis revealed that extracellular matrix remodeling and cytokine-mediated signaling were significantly upregulated (Figure 2.2C), whereas pathways involved in potassium ion transport and synapse organization were downregulated (Figure 2.2D). These findings are consistent with previous studies

suggesting that astrocytes contribute to the neuroinflammatory environment observed in AD and are involved in the disruption of neuronal support mechanisms, potentially exacerbating neurodegeneration [392, 393].

Additional TF activity analysis identified key molecular drivers of astrocyte dysfunction in fAD. This analysis revealed inferred activation of the transcription factors STAT3, NFKB, and MYC and inferred deactivation of SREBF1, MAML1, and YAP1 (Figure 2.3A). Activation of the STAT3 pathway in astrocytes has been shown to increase the production of proinflammatory cytokines and neuroinflammation, contributing to neuronal death, exacerbating A β deposition, and impairing neuronal function [348, 394]. On the other hand, inhibition of STAT3 has been shown to reduce neuroinflammation, decrease A β levels, and improve cognitive function in AD models [349, 395-399]. Additionally, SREBF1 is downregulated in AD oligodendrocytes, potentially contributing to neurodegeneration by disrupting cholesterol synthesis and affecting oligodendrocyte function [400, 401]. Our results also suggest that SREBF1 is dysregulated in astrocytes. Furthermore, the loss of YAP1 in astrocytes promotes senescence and contributes to neurodegenerative processes in AD [402]. Taken together, these findings suggest that STAT3, SREBF1, and YAP1 promote astrocyte-driven inflammation, senescence, and lipid metabolism dysfunction in AD.

The LINCS platform identifies small molecules that may reverse the molecular alterations we described in fAD astrocytes. Our application of this platform revealed that discordant perturbagens, such as fluticasone propionate, Akt inhibitor VIII, Akt inhibitor IV, and AS-605240, may offer therapeutic potential by reversing these dysregulated processes (Figure 2.3B). Notably, the discordant perturbagens align with findings from pathway analysis and TF activity inference, both of which pointed toward increased inflammation in fAD astrocytes.

Previous studies have revealed an association between the use of fluticasone, an FDA-approved glucocorticoid receptor agonist, and a significantly reduced risk of AD, indicating its potential for lowering the incidence of AD through anti-inflammatory mechanisms [403-405].

Additionally, pretreatment with the Akt inhibitor VIII significantly reduces LPS-induced MMP-9 overexpression, which has been implicated in extracellular matrix breakdown and blood-brain barrier disruption in neuroinflammatory and neurodegenerative diseases [406]. However, specific investigations into the effects of fluticasone or Akt inhibitor VIII on AD astrocytes have yet to be conducted. These small molecules could be further explored for their ability to modulate the dysregulated genes and kinases identified in this study, potentially leading to the development of more effective treatments for Alzheimer's disease.

The kinomic analysis further supported these observations by identifying significant changes in kinase activity, particularly among the DYRK, GSK, and MAPK families. These kinase families have been previously implicated in AD, notably their role in regulating neuroinflammation and synaptic function in astrocytes. DYRK1A and GSK-3 β , for example, are known to influence tau phosphorylation and neuroinflammatory responses, both of which are critical in AD progression [407, 408]. MAPK signaling pathways, including the ERK and p38 MAPK pathways, are also involved in mediating cellular stress responses and inflammation [409, 410]. The PamGene platform allowed comprehensive kinomic profiling, which corroborated our neuroinflammatory findings.

The integration of kinomic and transcriptomic data through network-based approaches has pinpointed critical molecular hubs such as PIK3R1, IGF1, and AKT1 in the PI3K signaling pathway, as well as IL6, JAK2, and STAT3 in the inflammatory response pathway. These hubs represent potential therapeutic targets, and modulating these hubs may mitigate the progression

of AD [411, 412]. Notably, JAK2 has been identified across multiple omics platforms, reflecting both transcriptomic dysregulation and kinomic changes, further validating its critical role in fAD pathology. These findings provide a comprehensive overview of the molecular mechanisms driving astrocyte dysfunction in AD.

This study offers key insights into astrocyte dysfunction in fAD, highlighting novel therapeutic targets. The integrative multiomic approach employed here offers a comprehensive view of the molecular landscape in fAD astrocytes, providing a foundation for future research aimed at developing targeted therapies that address both the contributions of neurons and glia to AD.

Conclusions

In conclusion, this study elucidates the intricate molecular alterations underlying astrocyte dysfunction in fAD through a comprehensive multiomic approach. By integrating transcriptomic and kinomic analyses, we identified critical dysregulated pathways, including those related to neuroinflammation, synaptic function, lipid metabolism, and kinase activity, that are likely driving the pathophysiology of fAD in astrocytes. The consistent dysregulation of key molecular hubs, such as those in the PI3K signaling and inflammatory response pathways, underscores the central role of astrocytes in the progression of AD. Moreover, the identification of chemical perturbagens offers promising avenues for therapeutic intervention, targeting the specific molecular abnormalities revealed in this study. These findings not only enhance our understanding of the molecular mechanisms contributing to Alzheimer's disease but also provide a valuable foundation for developing targeted therapies aimed at modulating astrocyte function to slow or halt disease progression.

Chapter 4: Shared and distinct psychoneuroimmune dysregulation in hiPSC astrocyte transcriptomes across depressive and neurodegenerative disorders

Abstract

MDD and AD represent significant clinical challenges, imposing considerable burdens on patients, caregivers, and healthcare systems. Emerging evidence highlights a complex, bidirectional relationship between these disorders, suggesting shared pathophysiological mechanisms involving astrocyte dysfunction, neuroimmune signaling, and ECM remodeling. Utilizing hiPSC-derived astrocytes from healthy controls, treatment-responsive MDD, treatment-nonresponsive MDD, and familial Alzheimer's disease patients, this study systematically characterized transcriptomic alterations to identify both overlapping and distinct molecular signatures. Differential gene expression analyses revealed significant transcriptional dysregulation across conditions, with key functional clusters identified through gene ontology enrichment, including ECM organization, immune regulation, chemotaxis, and cell cycle pathways. Integrated analysis of transcription factor and kinase activities demonstrated distinct regulatory landscapes, with notable involvement of TFs such as SP1, TP53, and STAT3 and kinases including DDR2, TTBK1, and BRSK2. Leveraging the LINCS database, pharmacological profiling identified concordant and discordant perturbagens and mechanisms, notably highlighting HDAC, mTOR, and tyrosine kinase inhibitors, suggesting novel therapeutic targets for modulating astrocyte function. These findings underscore astrocyte-mediated mechanisms linking neuropsychiatric and neurodegenerative disorders and provide critical insights into potential precision medicine strategies for MDD and AD.

Introduction

MDD and AD are highly prevalent conditions that place a significant clinical and economic strain on individuals and society. MDD, characterized by persistent sadness, loss of interest, and impaired cognitive function, has been estimated to affect more than 21 million American adults annually and approximately 5% of adults globally [413-415]. The lifetime prevalence of MDD is estimated to be between 10% and 20% [416-419]. AD, the most common form of dementia, is estimated to affect 6.9 million Americans aged 65 and older [31]. This number is projected to rise significantly with the aging population, potentially reaching 13.8 million by 2060 [31]. AD is characterized by gradual memory loss, behavioral changes, and cognitive decline, ultimately leading to profound functional impairment and death [420-423]. The clinical burden of AD includes a high mortality rate, substantial healthcare costs, and a significant impact on caregivers [424-427]. Furthermore, AD is associated with an increased incidence of comorbidities like hypertension, diabetes, and stroke [425, 428].

Emerging evidence suggests a complex and bidirectional relationship between MDD and AD, with depression both contributing to and resulting from neurodegenerative processes [429-431]. Research indicates that 38–40% of individuals with dementia experience depressive symptoms, and 16% are diagnosed with MDD [432-434]. Depression has been recognized as both a potential risk factor for dementia and a frequent symptom in individuals living with dementia [64, 429, 435-442]. Studies have shown that depression can hasten cognitive decline and elevate one's risk of dementia, while dementia can trigger or exacerbate depressive symptoms [430, 442-444]. Importantly, it appears that depression in later life, rather than early life, is a stronger predictor of dementia risk [57, 445-447]. This two-way relationship between

depression and dementia points to common underlying mechanisms and highlights the importance of gaining a more comprehensive understanding of their interconnectedness. Astrocytes, the most ubiquitous cells in the human brain, play an indispensable role in the regulation of numerous neurological processes and the maintenance of neural homeostasis [448]. These star-shaped cells play critical roles in neuroinflammation, immune regulation, ECM maintenance, BBB integrity, synaptic transmission modulation, and metabolic support for neurons [448]. Additionally, astrocytes interact with the blood-brain barrier to detect molecules, such as cytokines, produced by peripheral immune cells [163]. In response to injury or disease, astrocytes become reactive, undergoing morphological and functional changes that can either protect against or worsen neuronal damage [449]. Reactive astrocytes are known to influence both innate and adaptive immune responses [450]. Astrocyte dysfunction has been linked to both neuropsychiatric and neurodegenerative disorders, including MDD and AD [451]. In MDD, astrocytes display disrupted calcium signaling, impaired glutamate homeostasis, and dysregulated inflammatory responses [452]. In AD, they contribute to amyloid-beta plaque formation, tau pathology, and chronic neuroinflammation [453]. By interacting with the immune system, astrocytes act as central mediators of neuroimmune signaling, bridging PNI mechanisms with the pathophysiology of both neuropsychiatric and neurodegenerative disorders.

hiPSC models offer a powerful tool for studying human-specific disease mechanisms [454, 455]. These cells, derived from adult somatic cells, can be reprogrammed to a pluripotent state and differentiated into various cell types, including astrocytes [456, 457]. hiPSC models provide several advantages over traditional animal models, including the ability to recapitulate human genetic and epigenetic backgrounds, study disease progression in a controlled environment, and test potential therapeutic interventions [458-462]. Importantly, it has been

shown that iPSCs retain the epigenetic signature of their starting somatic cells, which can affect their differentiation potential [455, 463]. These unique properties make hiPSC models an invaluable platform for investigating disease mechanisms, modeling patient-specific pathophysiology, and developing targeted therapeutic strategies.

hiPSC-derived astrocytes have been used to investigate the cellular and molecular mechanisms underlying MDD and AD [90, 95, 210, 213]. Studies using hiPSC-derived astrocytes from MDD patients have revealed alterations in gene expression, calcium signaling, and mitochondrial function [210, 464]. These findings provide insights into the role of astrocytes in MDD pathogenesis and potential therapeutic targets. Similarly, hiPSC-derived astrocytes from AD patients have shown altered responses to amyloid-beta and tau, as well as dysregulated inflammatory pathways [213, 465, 466]. These studies highlight the utility of hiPSC-derived astrocytes as a translational platform for elucidating disease-specific astrocyte dysfunction in MDD and AD, paving the way for novel therapeutic interventions.

By systematically comparing the transcriptomic landscapes of hiPSC-derived astrocytes from MDD and fAD patients, this study seeks to uncover both shared and condition-specific molecular alterations that contribute to disease pathology. Identifying common dysregulated pathways may reveal convergent mechanisms underlying astrocyte dysfunction in neuropsychiatric and neurodegenerative disorders, while distinct signatures could provide insights into their divergent pathophysiology. Furthermore, elucidating these transcriptomic changes may highlight novel therapeutic targets, offering a foundation for precision medicine approaches aimed at modulating astrocyte function to improve clinical outcomes in MDD and AD.

Materials and methods

Data acquisition and processing

Normalized gene expression data for three comparisons, non-responders versus healthy controls (NR vs. HC), responders versus healthy controls (R vs. HC), and familial Alzheimer's disease versus healthy controls (fAD vs. HC), were obtained from RNA-sequencing differential expression analysis as previously described.

Differential gene expression analysis

Significant DEGs were identified using the DESeq2 [265] and limma-voom pipelines [467, 468]. DEGs were identified using an adjusted p value threshold ($\text{padj} < 0.05$) and an absolute \log_2 fold-change threshold ($|\log_2\text{FC}| > 1.2$). To identify patterns of gene expression changes, hierarchical clustering was performed using Euclidean distance and Ward's method (ward.D2) with the cluster R package [282]. The optimal number of clusters was determined by maximizing the average silhouette width across k -values ranging from 2 to 10 using the factoextra package [469]. Genes within each cluster were subjected to GO enrichment analysis using the clusterProfiler package [267-270], and BP terms were identified at an adjusted p value threshold of 0.05. A heatmap of clustered genes was generated using the pheatmap package [280], with rows representing individual genes and columns representing the three comparisons (R, NR, and fAD). Z-score normalization was applied to standardize \log_2 fold-change values. To assess shared and unique DEGs across the three comparisons, an UpSet plot was generated using the UpSetR package to visualize DEG intersections across conditions [470].

Correlation analysis of differential gene expression

To evaluate transcriptional similarities between conditions, Pearson correlation coefficients of log₂ fold-change values were computed using the stats package for genes meeting the significance threshold in at least one condition. Correlations were calculated for NR vs. HC vs. fAD, R vs. HC vs. fAD, and NR vs. HC vs. R. Linear regression models with 95% confidence intervals were fitted using the ggplot2 package to visualize relationships.

Functional enrichment analysis

To determine shared biological processes affected across conditions, GO enrichment analysis was performed separately for NR, R, and fAD DEGs using clusterProfiler. Enriched terms were compared across conditions using the compareCluster function. A dot plot visualization was generated with ggplot2 to highlight overlapping and unique biological processes among conditions.

Clustering of differentially expressed genes in overlapping biological processes

To identify DEGs associated with overlapping biological processes, we retrieved genes annotated with extracellular matrix organization (GO:0030198), extracellular structure organization (GO:0045229), and apoptotic processes (GO:0043062) from the org.Hs.eg.db database using the AnnotationDbi package in R. Gene symbols corresponding to these GO terms were mapped to the RNA-sequencing dataset, and expression data were subset to include only these genes. Hierarchical clustering was performed on the filtered dataset using a distance matrix defined as 1 - Pearson correlation coefficient, computed with the cor() function from the stats package, and the minimum variance method (Ward.D2) implemented in the cluster R package.

To calculate the optimal number of clusters, silhouette width analysis was performed for k values ranging from 2 to 10 using the factoextra R package. The k value maximizing the average silhouette width was selected, and a minimum cluster size threshold of five genes was enforced to avoid over-fragmentation. Genes were clustered based on the optimal k value. Expression patterns were visualized using ggplot2 and ggrepel, with condition-specific trends highlighted by fitting locally estimated scatterplot smoothing (LOESS) regression lines using the geom_smooth() function.

Transcription factor activity inference

To systematically infer TF activities from differential expression data, we employed the decoupleR package [370]. First, we retrieved the human CollecTRI network via get_collectri, then applied the Universal-Literate Model (ULM) to each contrast's DEG t statistic (e.g., NR vs. HC, R vs. HC, fAD vs. HC). The ULM output was filtered for TFs with $p < 0.05$, and the resulting significant TF scores were merged across the three conditions. We scaled these scores row-wise to generate a Z-score matrix and visualized the results with the pheatmap R package, creating a heatmap of relative TF activity patterns. Overlap in significantly active TFs among NR, R, and fAD was examined using VennDiagram [471].

Kinase enrichment analysis

To determine potential kinase regulators of DEGs, we submitted both up and downregulated gene sets to KEA3 [472, 473] via its API. Each query provided gene lists in JSON format, returning enriched kinases for each condition (NR vs. HC, R vs. HC, fAD vs. HC) in both up and downregulated directions. We filtered the STRING-based output by false

discovery rate ($FDR < 0.05$) and selected the top ten kinases, ranked by odds ratio (OR). We generated separate plots for up- and downregulated kinases in each contrast, distinguishing up and down sets by color and point shape. We visualized the overlaps among the significantly enriched kinases in up- and downregulated gene sets across NR, R, and fAD using the UpSetR package. Next, we merged kinase results meeting the FDR threshold for all contrasts, computed the mean OR for any duplicate entries, and illustrated the data as a heatmap generated using the pheatmap R package.

Results

Differential gene expression and functional enrichment in hiPSC-derived astrocytes

To assess transcriptional differences in astrocytes derived from distinct patient groups and healthy controls, we first identified significant DEGs. A total of 675 DEGs were detected in NR vs. HC astrocytes, 555 DEGs in R vs. HC, and 949 DEGs in fAD vs. HC (adjusted p value < 0.05 , $|\log_2FC| > 1.2$) (Figure 3.1A). Pairwise intersections revealed that 68 DEGs were shared between NR and R, 66 DEGs were shared between NR and fAD, and 94 DEGs were shared between R and fAD; six DEGs were commonly differentially expressed across all three comparisons (Figure 3.1A).

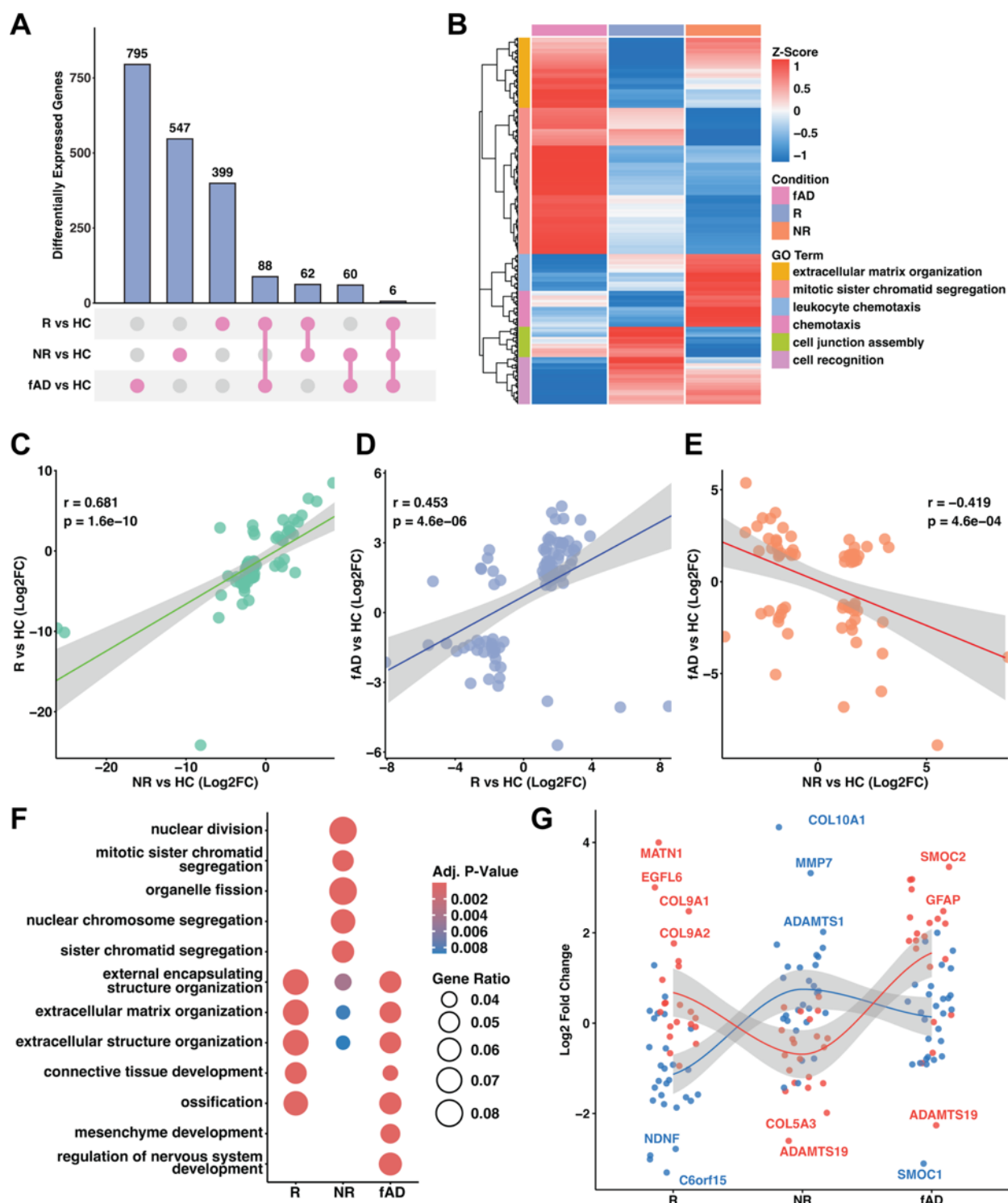


Figure 4.1. Comparative analysis of differential gene expression and functional enrichment in NR, R, and fAD hiPSC-derived astrocytes. (A) A hierarchical clustering heatmap of DEGs common to NR vs. HC, R vs. HC, and fAD vs. HC, using row-wise Z-score normalization of

log₂ fold changes. Rows are genes, columns represent each condition, and annotated rows indicate the top GO-BP term per gene cluster. **(B)** An UpSet plot depicting the overlap of significant DEGs ($p_{adj} < 0.05$, $|\log_2FC| > 1.2$) across NR, R, and fAD. **(C–E)** Scatter plots comparing log₂ fold changes in R vs. NR **(C)**, fAD vs. R **(D)**, and fAD vs. NR **(E)**. Each point represents a DEG shared between two contrasts, with regression lines added for clarity and inset annotations of Pearson's correlation (r) and p value. **(F)** Functional Enrichment Dot Plot. A dot plot showing significantly enriched GO Biological Processes among DEGs from R, NR, and fAD, highlighting representative terms such as extracellular matrix organization and encapsulating structure organization. Dot size corresponds to the gene ratio within each term, and color reflects statistical significance. **(G)** A silhouette-informed clustering of genes associated with external encapsulating structure organization (GO:0045229), extracellular matrix organization (GO:0030198), and extracellular structure organization (GO:0043062), with points representing expression measurements across R, NR, and fAD and loess curves indicating overall expression trends within each cluster.

Hierarchical clustering of the union set of 1957 DEGs from these three contrasts identified six clusters based on silhouette analysis (Figure 3.1B). Cluster 1 (707 genes), enriched in cell cycle processes with “mitotic sister chromatid segregation” as the top GO term, was upregulated in fAD and R compared to NR (Figure 3.1B). Cluster 2 (173 genes), associated with “chemotaxis,” and Cluster 5 (178 genes), associated with “leukocyte chemotaxis,” were both more highly expressed in NR relative to fAD and R (Figure 3.1B). Cluster 3 (147 genes), centered on “cell junction assembly,” showed elevated expression in R relative to NR and fAD (Figure 3.1B). Cluster 4 (227 genes), linked to “cell recognition,” was upregulated in R and NR

relative to fAD (Figure 3.1B). Lastly, Cluster 6 (339 genes), highlighting “extracellular matrix organization,” was more abundant in fAD and NR than in R (Figure 3.1B). These results reflect both unique and overlapping gene expression changes among NR, R, and fAD astrocytes relative to healthy controls.

Scatter plot analyses were performed on shared DEGs to evaluate the relationships in gene expression across these groups further. The correlation coefficient of $r = 0.681$ ($p = 1.6e-10$) for NR vs. R indicated a strong and highly significant positive correlation (Figure 3.1C), while $r = 0.453$ ($p = 4.6e-06$) for R vs. fAD represented a moderate (Figure 3.1D), statistically significant positive correlation. In contrast, $r = -0.419$ ($p = 4.6e-04$) for NR vs. fAD reflected a moderate and significant negative correlation (Figure 3.1E). Overall, these analyses highlight distinct levels of correlation in shared gene expression changes across the three comparisons, with R and NR displaying opposite relationships with fAD.

To clarify the functional roles of these DEGs, we performed gene set enrichment analyses in each experimental condition. Gene set enrichment analyses in each patient group highlighted significantly enriched GO-BP terms. For R, the top five terms were “extracellular matrix organization” ($p = 6.14e-13$), “extracellular structure organization” ($p = 6.73e-13$), “external encapsulating structure organization” ($p = 7.37e-13$), “connective tissue development” ($p = 2.65e-08$), and “ossification” ($p = 1.79e-07$) (Figure 3.1F). In NR, the top five were “nuclear division” ($p = 3.01e-14$), “mitotic sister chromatid segregation” ($p = 7.28e-14$), “organelle fission” ($p = 3.51e-13$), “nuclear chromosome segregation” ($p = 4.96e-13$), and “sister chromatid segregation” ($p = 5.24e-13$) (Figure 3.1F). For fAD, “external encapsulating structure organization” ($p = 4.67e-12$), “extracellular matrix organization” ($p = 1.38e-11$), “extracellular structure organization” ($p = 1.54e-11$), “mesenchyme development” ($p = 1.08e-08$), and

“regulation of nervous system development” ($p = 1.36e-08$) emerged as the top five (Figure 3.1F). The GO terms “external encapsulating structure organization,” “extracellular matrix organization,” and “extracellular structure organization” were shared among these conditions (Figure 3.1F). In summary, these analyses identified distinct top-ranked biological processes in each condition, with three extracellular-related terms appearing across R, NR, and fAD.

To investigate whether identical or distinct subsets of genes contributed to the enrichment of “external encapsulating structure organization” (GO:0045229), “extracellular matrix organization” (GO:0030198), and “extracellular structure organization” (GO:0043062) in both R, NR, and fAD, a silhouette-based clustering was performed on 49 genes mapping to these GO terms. The silhouette analysis indicated an optimal partition of $k = 2$, yielding a first cluster with 28 genes and a second cluster with 21 genes. Cluster 1, comprising COL10A1, MMP7, ADAMTS1, NDNF, C6ORF15, and SMOC1, showed elevated expression in NR compared to R and fAD. Conversely, Cluster 2, which included MATN1, EGFL6, COL9A1, COL9A2, SMOC2, GFAP, COL5A3, and ADAMTS19), was upregulated in the R and fAD lines but downregulated in the NR lines. This partition allowed closer inspection of which genes drove the enrichment in each line, providing insight into how both R, NR, and fAD can exhibit functional overlap in extracellular organization pathways while displaying opposite overall correlations in gene expression.

Integrated transcription factor and kinase activity analysis in hiPSC-derived astrocytes

To identify differences in TF activity across astrocytes from R, NR, and fAD patients relative to HCs, we first determined the number of significantly active TFs in each comparison ($p < 0.05$). A total of 212 TFs were detected in R vs. HC, 140 in NR vs. HC, and 117 in fAD vs. HC

(Figure 3.2A). To determine which TFs were significantly active in each astrocyte line relative to healthy controls, a three-way Venn diagram was generated (Figure 3.2A). This comparison revealed the degree of overlap among TFs displaying significant activity ($p < 0.05$) in R vs. HC, NR vs. HC, and fAD vs. HC, indicating both shared and unique TFs across conditions. Intersection counts revealed 68 TFs in R vs. HC and NR vs. HC, 42 in R vs. HC and fAD vs. HC, 28 in NR vs. HC and fAD vs. HC, and 17 in all three contrasts (Figure 3.2A). Overall, this analysis demonstrated both distinct and intersecting TF activity profiles in each group.

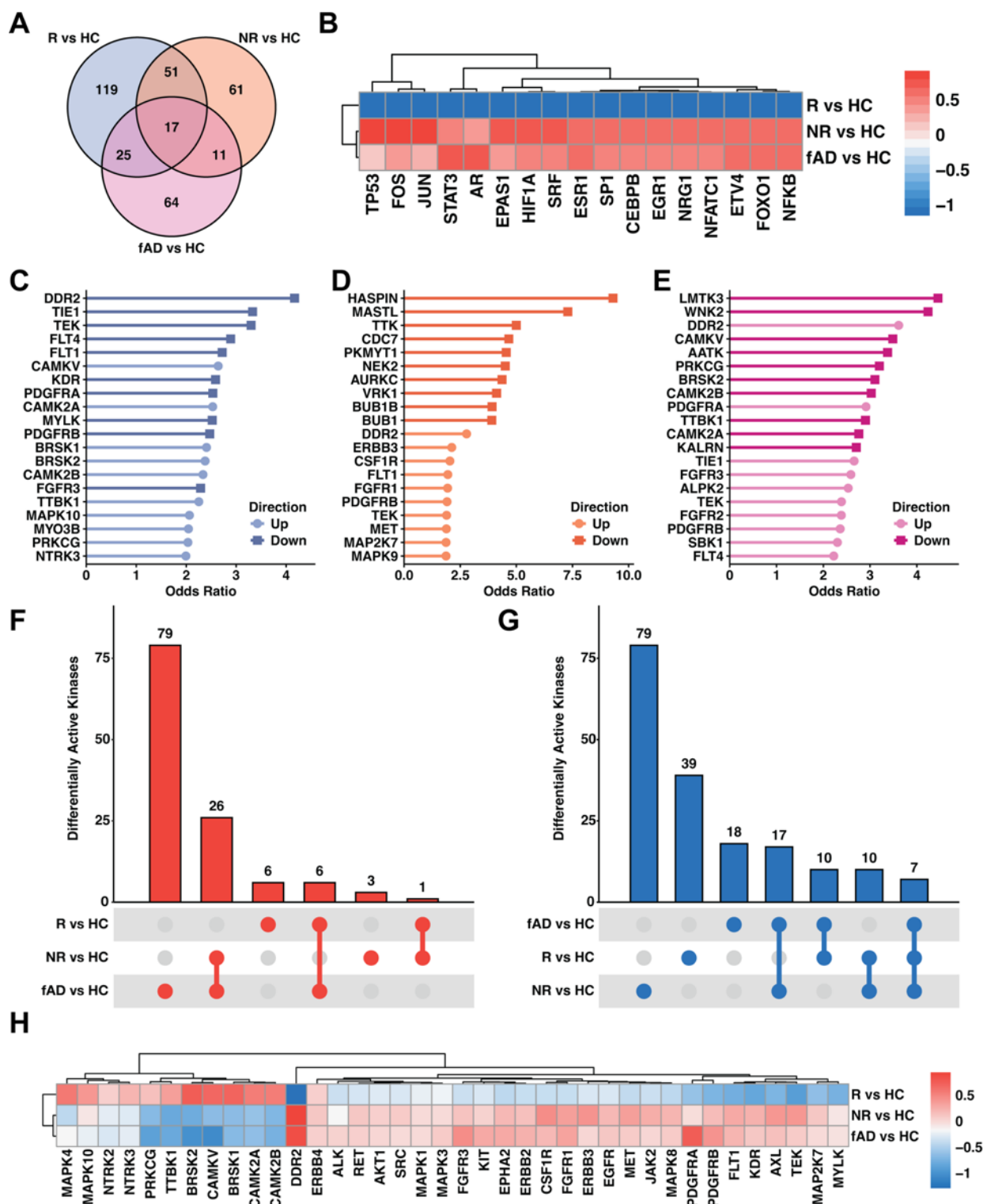


Figure 4.2. Integrated analysis of transcription factor and kinase activities in R, NR, and fAD hiPSC-derived astrocytes. (A) A three-way Venn diagram illustrating overlap among

significantly active transcription factors (TFs) identified in R vs. HC, NR vs. HC, and fAD vs. HC ($p < 0.05$). **(B)** A heatmap of TF activity z-scores (rows: R, NR, fAD; columns: TFs) retained in all three contrasts ($p < 0.05$). Each row is clustered to highlight similar TF activity profiles across conditions, with a diverging color palette indicating relative activation (red) or deactivation (blue). **(C-E)** Bar plots showing the top ten kinases enriched in upregulated and downregulated gene sets for R vs. HC **(C)**, NR vs. HC **(D)**, and fAD vs. HC **(E)**. The bars represent the odds ratio (OR). **(F-G)** UpSet plots displaying overlaps of significantly active kinases ($FDR < 0.05$) in upregulated **(F)** and downregulated **(G)** sets across NR vs. HC, R vs. HC, and fAD vs. HC. **(H)** A heatmap of kinases enriched in all three contrasts (NR vs. HC, R vs. HC, fAD vs. HC). Kinases enriched in downregulated gene sets for a given comparison are shown in blue, while kinases enriched in upregulated gene sets are shown in red.

To explore these TFs in more detail, we examined the 17 TFs common to all three comparisons. Among these shared TFs, some showed mixed directions of association across R, NR, and fAD, such as SP1 (-11.090 in R vs. HC, 3.124 in NR vs. HC, and 2.573 in fAD vs. HC) and TP53 (-3.561 in R vs. HC, 6.622 in NR vs. HC, and 2.754 in fAD vs. HC) (Figure 3.2B). Examination of the highest overall TF scores per contrast indicated that NRG1 had the most extreme value in R vs. HC (-2.106), TP53 in NR vs. HC (6.622), and AR in fAD vs. HC (4.888). These results highlight a distinct distribution of TF activity in each group relative to healthy controls.

To investigate potential kinase-driven regulation, we next identified kinases enriched in upregulated and downregulated gene sets for each group (Figures 3.2C–E). In R vs. HC, upregulated kinases were led by CAMKV, CAMK2A, BRSK1, BRSK2, CAMK2B, TTBK1,

MAPK10, MYO3B, PRKCG, and NTRK3, whereas downregulated kinases included DDR2, TIE1, TEK, FLT4, FLT1, KDR, PDGFRA, MYLK, PDGFRB, and FGFR3 (Figure 3.2C). For NR vs. HC, the top ten upregulated kinases included DDR2, ERBB3, CSF1R, FLT1, FGFR1, PDGFRB, TEK, MET, MAP2K7, and MAPK9, while the top ten downregulated kinases included HASPIN, MASTL, TTK, CDC7, PKMYT1, NEK2, AURKC, VRK1, BUB1B, and BUB1 (Figure 3.2D). For fAD vs. HC, the top ten upregulated kinases comprised DDR2, PDGFRA, TIE1, FGFR3, ALPK2, TEK, FGFR2, PDGFRB, SBK1, and FLT4, while downregulated kinases included LMTK3, WNK2, CAMKV, AATK, PRKCG, BRSK2, CAMK2B, TTBK1, CAMK2A, and KALRN (Figure 3.2E). These findings revealed distinct sets of enriched kinases in each comparison.

To evaluate the overlap of significantly active kinases ($FDR < 0.05$) in up- and downregulated gene sets, UpSet plots were generated for NR vs. HC, R vs. HC, and fAD vs. HC. For upregulated kinases, 30 were detected in NR vs. HC, 13 in R vs. HC, and 111 in fAD vs. HC, with pairwise intersections of one kinase between NR vs. HC and R vs. HC, 26 between NR vs. HC and fAD vs. HC, six between R vs. HC and fAD vs. HC, and none were common to all three (Figure 3.2F). Downregulated kinases numbered 113 in NR vs. HC, 66 in R vs. HC, and 52 in fAD vs. HC, with 17 shared by NR vs. HC and R vs. HC, 24 by NR vs. HC, and fAD vs. HC, 17 by R vs. HC and fAD vs. HC, and seven shared among all three (Figure 3.2G). Finally, a heatmap of overlapping kinases showed contrasting enrichment patterns, such as DDR2 having a positive association ($OR = 0.935$) in NR vs. HC and ($OR = 0.848$) in fAD vs. HC but a negative association ($OR = -1.293$) in R vs. HC (Figure 3.2H). Notably, the highest odds ratio per contrast indicated that DDR2 was most strongly activated in NR vs. HC and fAD vs. HC, while TTBK1 was most strongly inhibited in NR vs. HC, BRSK2 was most strongly activated in R vs. HC, and

DDR2 was most strongly inhibited in R vs. HC (Figure 3.2H). Finally, several kinases exhibited different directions of association across the three groups, including AKT1, AXL, BRSK1, CAMKV, and FGFR3 (Figure 3.2H). Overall, these findings reveal both unique and overlapping kinase enrichment patterns in NR, R, and fAD astrocytes.

LINCS-derived mechanisms of action and perturbagens in R, NR, and fAD hiPSC-derived astrocytes

To analyze shared transcriptomic signatures among R, NR, and fAD hiPSC-derived astrocytes, we used LINCS to identify overlapping mechanisms underlying MDD and AD. By examining concordant MOAs and perturbagens that mimicked disease states, we identified key molecular pathways driving astrocyte dysfunction in both disorders. This approach not only elucidated common pathogenic mechanisms but also highlighted potential pharmacological agents for modeling disease states and identifying therapeutic targets. Analysis of concordant MOAs revealed HDAC inhibitors as the most frequently identified pharmacological class across all disease groups (Fig. 3.3A). Other prominent concordant MOAs included mTOR inhibitors, topoisomerase inhibitors, and HSP inhibitors. Notably, several neurotransmitter-related mechanisms were identified, including potassium channel blockers, AChR agonists, and GluR antagonists. Additional concordant MOAs included IGF-1 inhibitors, ATPase inhibitors, and tubulin inhibitors. Examining specific perturbagens that mimic disease signatures, we identified several compounds with distinct MOAs (Fig. 3.3B). Geldanamycin, an HSP inhibitor, displayed the strongest concordance with the NR phenotype. AZD-8055, an MTOR inhibitor, showed the highest overall similarity score among all concordant perturbagens, particularly in NR samples. BMS-536924, an IGF-1 inhibitor, demonstrated notable concordance with NR and moderate

effects in R and fAD samples. Elliptecine, a topoisomerase inhibitor, showed strong mimicry of the NR phenotype (0.504). Tacedinaline, an HDAC inhibitor, exhibited consistent concordance across all groups with a slightly higher effect in NR samples (0.387). Piplartine, a glutathione transferase inhibitor, showed the strongest effect in NR samples (0.352). WZ3105, a CLK2 inhibitor, demonstrated relatively balanced concordance across all groups (R: 0.270, NR: 0.279, fAD: 0.332). PG-9 CPD, an acetylcholine receptor agonist, had its strongest effect in fAD samples (0.390). Plumbagin, an apoptosis stimulant, similarly showed the highest concordance with fAD (0.350).

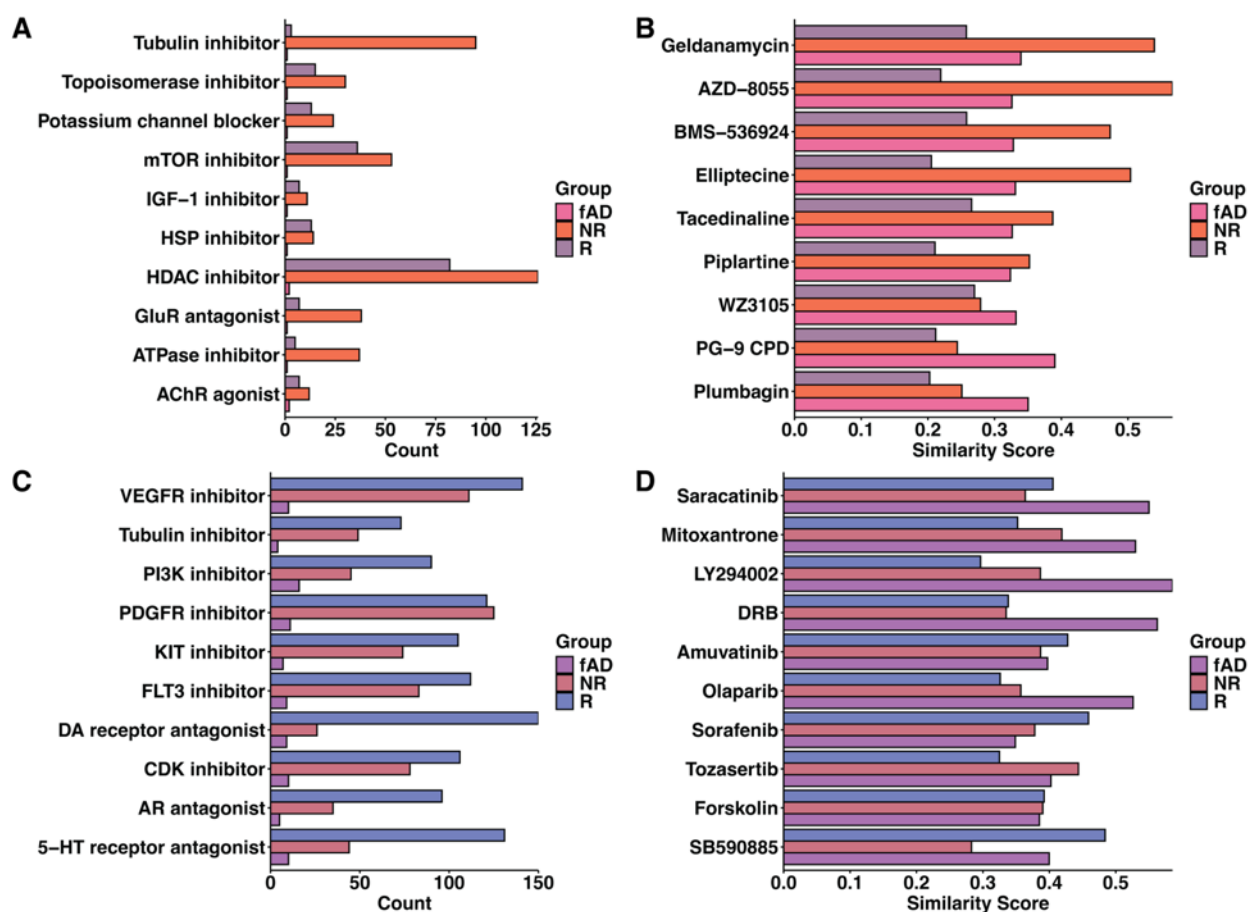


Figure 4.3. LINCIS-derived MOAs and perturbagens in R, NR, and fAD hiPSC-derived astrocytes. (A) Top 10 MOAs most frequently associated with small molecules showing

transcriptomic concordance with the DEG signatures of R, NR, and fAD compared to HC. Bar lengths represent the frequency (count) of each MOA, with colors indicating the respective groups. (B) Top 10 perturbagens most strongly concordant with the DEG signatures of R, NR, and fAD astrocytes. Higher absolute similarity scores indicate greater concordance with disease signatures, with colors corresponding to the groups. (C) Top 10 MOAs most frequently associated with small molecules showing transcriptomic discordance with the DEG signatures of R, NR, and fAD astrocytes. (D) Top 10 perturbagens most strongly discordant with the DEG signatures of R, NR, and fAD astrocytes, based on similarity scores. All signatures were derived using the LINCS database,

To identify pharmacological mechanisms and compounds that may counteract disease-associated molecular changes in MDD and AD, we analyzed discordant MOAs and perturbagens, those that reversed the transcriptomic signatures of R, NR, and fAD astrocytes. This approach aimed to identify key pharmacological classes that oppose disease-associated astrocyte dysfunction across these conditions. Analysis of discordant MOAs, which may represent counteractive pharmacological strategies, identified dopamine receptor antagonists as the most frequent in R samples (150 counts) but less represented in NR (26 counts) and fAD (9 counts) (Fig. 3.3C). Other prominent discordant MOAs included VEGFR inhibitors (R: 141, NR: 111, fAD: 10), 5-HT receptor antagonists (R: 131, NR: 44, fAD: 10), and PDGFR inhibitors (R: 121, NR: 125, fAD: 11). Additional discordant MOAs encompassed FLT3 inhibitors (R: 112, NR: 83, fAD: 9), CDK inhibitors (R: 106, NR: 78, fAD: 10), KIT inhibitors (R: 105, NR: 74, fAD: 7), AR antagonists (R: 96, NR: 35, fAD: 5), PI3K inhibitors (R: 90, NR: 45, fAD: 16), and tubulin inhibitors (R: 73, NR: 49, fAD: 4). For discordant perturbagens, which potentially counteract

disease-associated molecular changes, several compounds with distinct MOAs were identified (Fig. 3.3D). Saracatinib, a Src inhibitor, demonstrated the strongest effect in fAD samples (similarity score 0.550). Mitoxantrone, a DNA topoisomerase II alpha inhibitor, also showed substantial discordance with fAD (0.530). LY294002, with multiple MOAs including MTOR inhibitor, DNA-dependent protein kinase inhibitor, phosphodiesterase inhibitor, and PLK inhibitor, exhibited the highest overall discordance score in fAD samples (0.585). DRB, a casein kinase inhibitor, similarly showed strong discordance with fAD (0.563). Amuvatinib, with multiple tyrosine kinase-related MOAs (FLT3 inhibitor, KIT inhibitor, PDGFR tyrosine kinase receptor inhibitor, RAD51 inhibitor, and RET tyrosine kinase inhibitor), had its strongest effect in R samples (0.428). Olaparib, a PARP inhibitor, showed the greatest discordance with fAD (0.526). Sorafenib, with multiple MOAs including FLT3 inhibitor, KIT inhibitor, PDGFR tyrosine kinase receptor inhibitor, RAF inhibitor, RET tyrosine kinase inhibitor, and VEGFR inhibitor, demonstrated strongest discordance with R samples (0.459). Tozasertib, an Aurora kinase inhibitor with additional activities as a Bcr-Abl kinase inhibitor, FLT3 inhibitor, and JAK inhibitor, showed the highest discordance with NR samples (0.444). Forskolin, an adenylyl cyclase activator, displayed similar discordance across all groups with a slightly higher effect in R samples (0.392). SB590885, an RAF inhibitor, showed the strongest discordance with R samples (0.484). These findings highlight distinct pharmacological mechanisms and compounds that were most strongly associated with the reversal of disease-associated transcriptomic signatures in MDD and AD astrocytes.

Discussion

The present study sought to elucidate both shared and condition-specific transcriptional changes in hiPSC-derived astrocytes from R, NR, and fAD patients. By coupling differential gene expression profiling with functional enrichment analyses, TF activity assessment, kinase pathway exploration, and LINCS-derived pharmacological signature analysis, we identified unique and overlapping molecular signatures within each group. In doing so, this work adds to the growing literature emphasizing the pivotal contribution of astrocytes to the pathophysiology of both neuropsychiatric and neurodegenerative disorders.

A key finding was the clustering of DEGs into distinct biological processes, many reflecting critical astrocytic functions (Figure 3.1B). Chemotaxis-related clusters (Cluster 2) were significantly enriched in NR astrocytes, while ECM and external encapsulating structure organization genes (Cluster 6) showed substantial dysregulation predominantly in fAD astrocytes and, to a lesser extent, in R astrocytes. Notably, cell cycle-related processes (Cluster 1) were elevated prominently in fAD and R astrocytes, whereas leukocyte chemotaxis and immune pathways (Cluster 5) exhibited enrichment predominantly in NR astrocytes.

The observed clustering of DEGs into processes such as chemotaxis, ECM organization, cell cycle regulation, and leukocyte chemotaxis aligns with previous evidence linking these pathways to MDD and AD. Prior studies have demonstrated that astrocytes play a central role in neuroimmune signaling and ECM remodeling, both of which are critical components of the PNI framework [474-476]. Moreover, astrocyte dysfunction in MDD has been linked to altered neuroinflammatory responses and dysregulated chemotaxis that together may enhance inflammatory cell recruitment and exacerbate depression-associated inflammation [171, 174, 197, 198]. In parallel, dysregulation of ECM components, including those involved in

extracellular and external encapsulating structure organization, has been implicated in synaptic dysfunction and neurodegeneration in AD [477-481]. Moreover, recent studies indicate that astrocyte dysfunction, characterized by altered immune modulation and glial activation, significantly contributes to neuroinflammation in both Alzheimer's disease and depressive disorders [171, 202, 482, 483]. These converging lines of evidence expand upon the existing literature by emphasizing that differential regulation of these pathways in astrocytes may underlie distinct disease phenotypes in MDD and AD and further support the role of astrocytes as key mediators in the interface between neural, immune, and ECM processes.

A notable extension of our findings comes from the overlap between our DEG lists and previously identified causal mRNAs for psychiatric traits and 64 for neurodegenerative diseases [484]. Several genes implicated in MDD and AD were also found in our analyses. Specifically, among MDD-associated DEGs, BMP8B and MYRIP were present in the R vs. HC comparison; ZNF804A, RASD2, HLA-DQB1, and HLA-DQA1 were identified in the NR vs. HC dataset; and HLA-DQB1, ZNF501, ARHGAP19, HIBADH, PRPH2, CDH6, and PCDH18 appeared in the fAD vs. HC group. For AD-associated genes, three genes (ACOT1, PLCE1, and HNMT) were observed in the fAD vs. HC DEGs. This overlap reinforces the notion that astrocyte-mediated processes, including neuroimmune signaling and ECM remodeling, play a critical role in the pathophysiology of both MDD and AD, and it expands upon existing literature by linking our hiPSC-derived astrocyte model to causal molecular mechanisms identified across major psychiatric and neurodegenerative disorders.

Evidence from previous studies supports the association of these DEGs with both MDD and AD, particularly in the context of astrocyte function, psychoneuroimmunology, and ECM remodeling. For example, in the R vs. HC comparison, BMP signaling is known to regulate

astrocytic differentiation, ECM integrity, and neuroimmune communication, though BMP8B's specific role in astrocyte development remains to be fully elucidated [485-487]. In the NR vs. HC dataset, the detection of HLA-DQB1 and HLA-DQA1, key immune signaling genes implicated in autoimmune disorders [488, 489], reinforces the notion that aberrant immune signaling and transcriptional dysregulation in astrocytes may contribute to the pathophysiology of MDD. Among AD-associated DEGs, PLCE1 upregulation and HNMT's role in histamine degradation suggest that disruptions in phospholipid signaling and histamine metabolism may affect neuroinflammation and astrocyte function in Alzheimer's disease [490, 491]. Together, these findings extend the literature by linking causal mRNAs identified in large-scale genomic studies [484] with distinct astrocyte-specific transcriptional profiles, thereby underscoring the contribution of astrocyte-mediated ECM remodeling and immune regulation in both MDD and AD.

Building on these DEG findings, our integrated analysis of TFs and kinases provided additional insight into the regulatory mechanisms underlying these expression profiles. TFs such as SP1, TP53, and STAT3 exhibited mixed or opposite directions of modulation across groups. For instance, SP1 was markedly downregulated in R vs. HC (-11.090) but upregulated in NR vs. HC (3.124) and fAD vs. HC (2.573), while TP53 and STAT3 also showed similar divergent patterns. The highest TF scores per contrast further underscored these differences, with NRG1 showing the most extreme value in R vs. HC, TP53 in NR vs. HC, and AR in fAD vs. HC. These data suggest that astrocytes from MDD and AD patients engage distinct transcriptional programs that may be linked to disease-specific alterations in neuroimmune and ECM-associated pathways. Moreover, existing literature supports the involvement of these genes in MDD and AD through multiple mechanisms. SP1 regulates the expression of genes involved in neuronal

development, synaptic modulation, and inflammatory processes in astrocytes, influencing both extracellular matrix organization and neuroinflammation [475, 492, 493]. TP53, primarily known for its roles in cell cycle control and apoptosis, has been implicated in glial cell function, neuroprotection, and the pathogenesis of neurodegenerative diseases such as Alzheimer's and Parkinson's [494-496]. STAT3 plays a central role in cytokine signaling and astrocyte reactivity, with studies demonstrating its activation in reactive astrocytes in models of Alzheimer's disease and its involvement in regulating inflammatory processes that may contribute to both neurodegenerative and mood disorders [394, 396, 497]. Notably, these associations are well aligned with the PNI framework, which emphasizes the interplay between immune function, neural processes, and extracellular matrix dynamics in disease.

Similarly, kinase analysis revealed that regulators, including DDR2, TTBK1, and BRSK2, varied significantly in both their odds ratios and directionality between conditions. DDR2, for example, exhibited a positive association in NR vs. HC (OR = 0.935) and fAD vs. HC (OR = 0.848) but a negative association in R vs. HC (OR = -1.293). Notably, the highest odds ratios identified DDR2 as the most strongly activated kinase in NR and fAD astrocytes, whereas TTBK1 and BRSK2 emerged as prominent in NR and R, respectively. Notably, the enrichment of inflammation-associated kinases in NR vs. HC astrocytes complements the immunological signatures observed in the GO analyses, whereas ECM-related pathways and associated kinases were particularly pronounced in fAD astrocytes. Such patterns may reflect distinct astrocyte phenotypes or degrees of activation that help shape the divergent clinical manifestations of MDD and AD. Moreover, these findings are consistent with existing literature that underscores the role of astrocytes in neuroinflammatory processes and highlights the contributions of disrupted signaling pathways to disease pathophysiology. DDR2 has been shown

to play a critical role in ECM remodeling, cell migration, and proliferation. Recent research has linked its dysregulation to several pathological conditions, including cancer metastasis, fibrosis, and neurodegenerative diseases [498-501]. TTBK1 has been found to directly phosphorylate tau at multiple AD-related sites, including Ser422, and its overexpression in transgenic mouse models accelerates tau accumulation, neuroinflammation, and neurodegeneration, suggesting a critical role in AD pathogenesis and potential involvement in astrocyte-mediated tau pathology [502-504]. BRSK2, primarily known for its role in neuronal polarization and axonogenesis, has been implicated in stress responses and synaptic function, with recent studies suggesting its involvement in autism spectrum disorder and potential links to broader neurodevelopmental and neurodegenerative processes [505, 506]. In summary, these differential kinase profiles underscore the complex interplay between astrocyte-mediated ECM remodeling and neuroinflammatory signaling in MDD and AD, reinforcing the potential for targeting these pathways in future therapeutic strategies.

To further explore potential therapeutic targets and mechanisms relevant to these conditions, we conducted a pharmacological profiling analysis using the LINCS database. This analysis revealed both shared and condition-specific drug signatures that complement our gene expression, TF, and kinase findings. Our LINCS-based analysis of concordant MOAs identified HDAC inhibitors as the most frequently represented pharmacological class across all disease groups, with strikingly higher representation in MDD conditions compared to fAD. This predominance of epigenetic modulators suggests that chromatin remodeling may play a central role in the pathophysiology of depression, especially in treatment-resistant phenotypes. The strong concordance of mTOR inhibitors in the MDD groups compared to fAD aligns with emerging evidence implicating altered mTOR signaling in mood disorders and antidepressant

response mechanisms. The identification of neurotransmitter-related MOAs, including potassium channel blockers, AChR agonists, and GluR antagonists, further highlights the potential involvement of synaptic dysregulation in these conditions.

Examination of specific concordant perturbagens revealed compounds with distinct disease-specific signatures. Geldanamycin (HSP inhibitor) and AZD-8055 (mTOR inhibitor) demonstrated particularly strong mimicry of the NR phenotype, whereas PG-9 CPD (acetylcholine receptor agonist) and plumbagin (apoptosis stimulant) showed preferential concordance with fAD signatures. These findings align with our pathway analyses showing distinct patterns of immune regulation and cell cycle modulation between MDD and fAD astrocytes, suggesting that targeted pharmacological intervention of these pathways might offer condition-specific therapeutic approaches.

Perhaps most intriguingly, our analysis of discordant signatures, those that potentially counteract disease-associated molecular changes, identified compounds with differential effects across the three conditions. Several tyrosine kinase inhibitors with complex MOAs, including sorafenib and amuvatinib (which inhibit FLT3, KIT, PDGFR, and other kinases), showed strong discordance with R astrocytes. In contrast, saracatinib (Src inhibitor) and LY294002 (with multiple MOAs, including mTOR and PI3K inhibition) demonstrated the greatest potential to reverse fAD-specific signatures. The strong discordance of saracatinib with fAD aligns with studies implicating Src kinases in tau hyperphosphorylation and neuroinflammation in AD, while the identification of LY294002 as a potential counteractive agent for fAD supports the emerging role of PI3K/mTOR signaling as a therapeutic target in neurodegenerative diseases. These pharmacological profiles complement our kinase analyses, particularly the identification of DDR2 as significantly activated in both NR and fAD astrocytes but suppressed in R, highlighting

potentially divergent therapeutic approaches for these conditions. For the MDD groups, the strong discordance of sorafenib and SB590885 (both with RAF inhibitor activity) with R signatures suggests a potential therapeutic avenue for SSRI-responsive depression, given the emerging evidence linking RAF/MAPK signaling to stress responses and antidepressant mechanisms.

Overall, our findings expand upon the existing literature by highlighting the astrocyte-specific regulation of key transcription factors and kinases that mediate neuroimmune signaling and ECM remodeling in MDD and AD. This integrated analysis not only underscores the heterogeneity of astrocyte responses in these disorders but also suggests that distinct regulatory networks may contribute to their pathogenesis. By providing a detailed molecular dissection of these pathways, our study lays the groundwork for future investigations aimed at developing astrocyte-targeted therapeutic interventions to modulate these complex signaling networks in both neuropsychiatric and neurodegenerative disorders.

Several limitations warrant consideration. First, as in any *in vitro* model, hiPSC-derived astrocytes might not fully capture the complexity of astrocyte behavior within the intact human brain, including influences from other cell types and the broader CNS microenvironment. Second, the sample size and specific genetic backgrounds of the donor lines could affect the generalizability of the findings, given that epigenetic memory and aberrations in hiPSCs can persist after reprogramming and influence differentiation potential [507-509]. Third, the functional consequences of these gene expression and regulatory changes remain to be fully elucidated. Future work could incorporate co-culture systems with neurons or microglia, as well as targeted perturbations of candidate pathways, to clarify the mechanistic impact of these transcriptional profiles on disease-relevant phenotypes.

Looking ahead, these findings highlight several avenues for further investigation. Comparative analyses between additional subtypes of depression and different AD variants might reveal overlapping astrocyte-driven pathways common to a broader range of neuropsychiatric and neurodegenerative disorders. Likewise, drug screening efforts that modulate specific TFs or kinases of interest could shed light on novel therapeutic approaches, potentially leading to interventions that more precisely target astrocyte-mediated processes. The identification of condition-specific pharmacological signatures through our LINCS analysis provides valuable candidates for such drug screening initiatives, particularly compounds like saracatinib and LY294002 for fAD and RAF inhibitors for SSRI-responsive depression. Validation of these predicted therapeutic agents through functional assays would be a critical next step to confirm their efficacy in modulating astrocyte-specific disease phenotypes. Moreover, elucidating how progressive changes in astrocyte function correlate with disease onset or progression may also provide new insights into the trajectory of MDD and AD. Together, these future directions underscore the promise of targeting astrocyte-mediated pathways to enhance our understanding and treatment of both MDD and AD.

Conclusions

In conclusion, our integrated transcriptomic, regulatory, and pharmacological analyses of hiPSC-derived astrocytes from MDD and fAD patients reveal both shared and distinct molecular signatures that underscore the central role of astrocyte-mediated neuroimmune signaling and ECM remodeling in these disorders. The LINCS-derived perturbagen analysis further strengthens these findings by identifying specific compounds and mechanisms that either mimic or potentially counteract disease-specific molecular signatures, offering promising candidates for

therapeutic development. These findings not only expand upon existing literature by linking astrocyte-specific transcriptional changes to causal molecular mechanisms but also highlight potential therapeutic targets for modulating astrocyte function in neuropsychiatric and neurodegenerative diseases. Future studies incorporating more complex cellular models, functional validation of predicted therapeutic agents, and larger patient cohorts will be essential to fully elucidate the mechanistic impact of these pathways on disease progression and treatment outcomes.

Chapter 5: Conclusions

Summary of key findings

Astrocytes, once regarded as mere support cells, are emerging as star regulators of neurobiological processes that critically influence brain homeostasis and the pathogenesis of neurological disorders. The studies herein systematically map astrocyte-specific molecular alterations in MDD and AD, conditions that collectively affect over 27 million Americans. Through an innovative integration of transcriptomic profiling, kinomic analysis, and computational pharmacology, this work elucidates convergent and divergent astrocytic mechanisms underlying these neuropsychiatric and neurodegenerative conditions. The findings reveal a complex interplay between neuroinflammatory signaling and ECM remodeling that modulates synaptic function and neuronal health, with significant implications for therapeutic intervention.

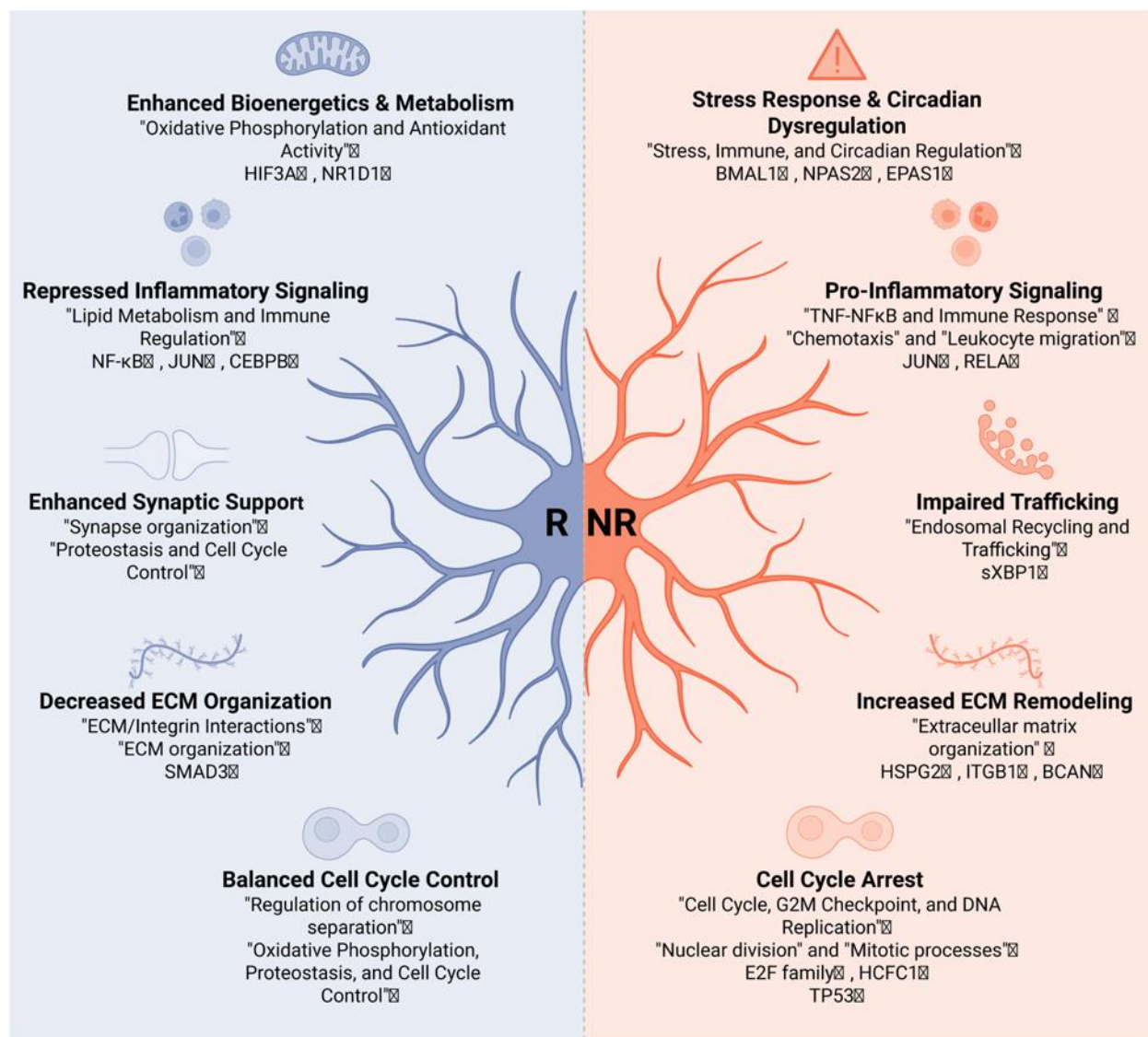


Figure 5.1 Distinct astrocyte states in SSRI-responders and non-responders. R and NR astrocytes exhibit distinct molecular profiles in depression. R astrocytes maintain homeostatic functions, including oxidative phosphorylation (HIF3A, NR1D1), synaptic support, and balanced cell cycle regulation. NR astrocytes show stress-primed signatures with circadian dysregulation (BMAL1, NPAS2), elevated inflammation (NF-κB, JUN, RELA), impaired trafficking, and ECM remodeling (HSPG2, ITGB1).

The first investigation profiled hiPSC-derived astrocytes from SSRI responders, non-responders, and healthy controls to uncover the cellular basis of treatment resistance. RNA sequencing identified distinct transcriptomic signatures in HC, R, and NR patient-derived astrocytes, with significant alterations in immunomodulatory, ECM-regulatory, and cell cycle-related gene expression (Figure 5.1). TF activity analysis revealed divergent regulatory networks between R and NR astrocytes, with NR cells exhibiting pronounced activation of stress-response pathways. Notably, coexpression network analysis demonstrated that R astrocytes upregulated modules associated with antioxidant activity and proteostasis while downregulating ECM and immune-related pathways. These contrasting molecular landscapes directly correlated with treatment outcomes. The mechanistic significance of these findings was further validated through isoform-specific analysis of XBP1, a stress-responsive transcription factor differentially modulated in NR astrocytes. LINCS-based pharmacological profiling yielded compelling evidence that FDA-approved antidepressants exhibit transcriptomic signatures opposing pathological gene expression, specifically in R astrocytes. This pharmacogenomic approach also identified novel therapeutic candidates for TRD, including compounds targeting kinase signaling and inflammatory pathways. These results reinforce astrocytes as active mediators of antidepressant efficacy through dynamic regulation of neuroinflammation and ECM remodeling.

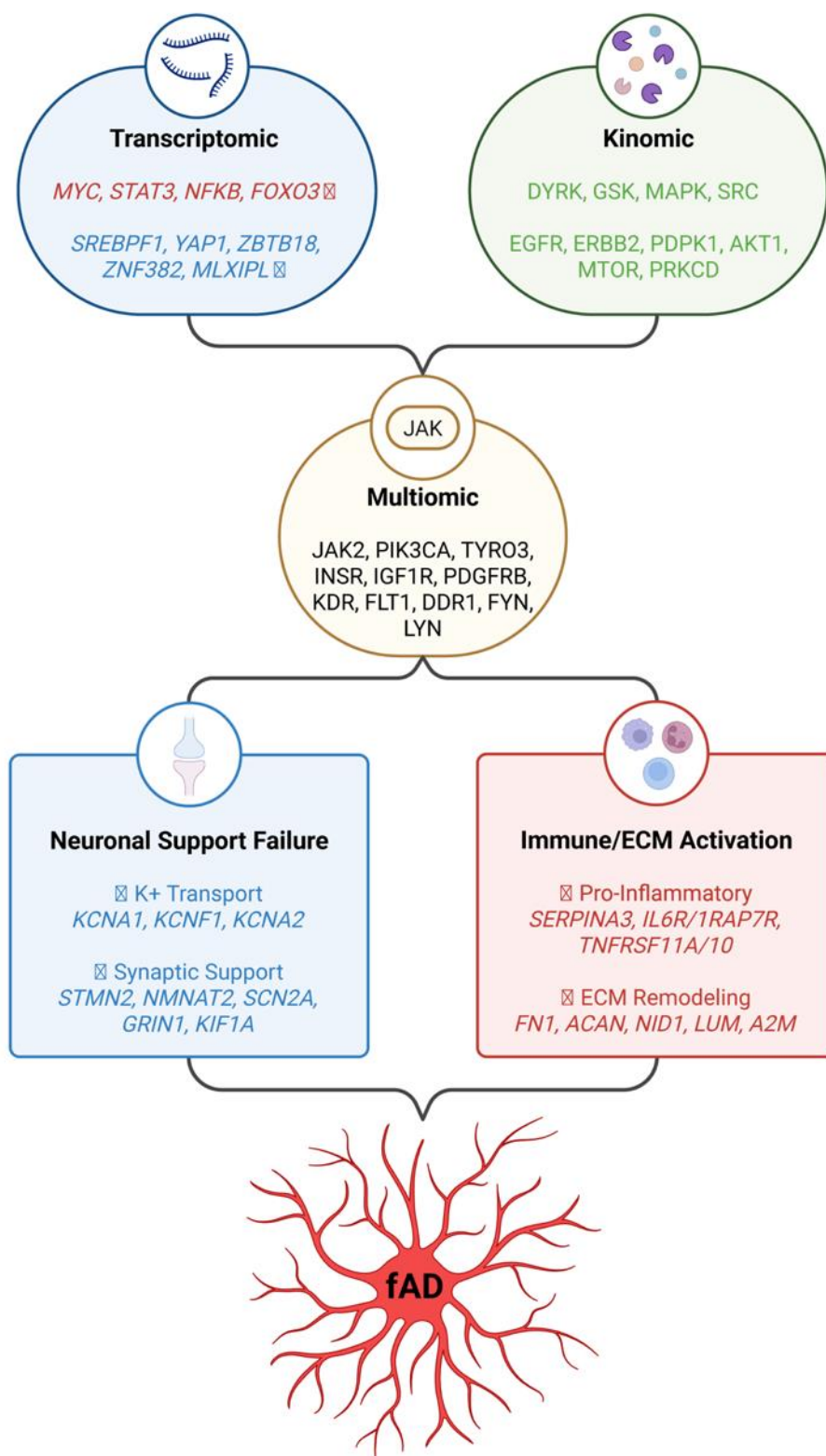


Figure 5.2 Transcriptomic and kinomic dysregulation in fAD astrocytes. Transcriptomic and kinomic profiling reveals dysregulated pathways in fAD astrocytes. Key molecular drivers include activated inflammatory transcription factors (MYC, STAT3, NF- κ B) alongside suppressed metabolic regulators (SREBF1, MLXIPL), with disrupted kinase signaling (DYRK, MAPK, GSK, SRC) and JAK2 as a central multiomic hub. A dual pathological phenotype emerges: (1) upregulated immune/ECM remodeling (SERPINA3, IL6R, FN1, ACAN) and (2) downregulated neuronal support genes (KCNA1, STMN2, GRIN1).

The second study employed an innovative multi-omic strategy to characterize molecular dysfunction in fAD astrocytes. The gene expression analysis of fAD astrocytes showed clearly different patterns compared to healthy control cells, particularly highlighting increased expression of inflammation-related genes alongside reduced expression of genes critical for supporting neuronal health and function (Figure 5.2). Integration with GWAS data validated the clinical relevance of key dysregulated genes, demonstrating that patient-derived astrocytes recapitulate the molecular signatures of patients with AD. Kinomic profiling revealed changed phosphorylation patterns, especially within the DYRK, GSK, and MAPK families, while network analysis identified STAT3, JAK2, and PI3K pathway components as key regulatory nodes driving astrocyte dysfunction in Alzheimer's disease. This multi-modal approach enabled the identification of therapeutic candidates, such as GSK-3 β inhibitors, PI3K/Akt/mTOR kinase inhibitors, and HDAC inhibitors, capable of reversing pathological astrocyte phenotypes. Together, these findings highlight how astrocyte dysfunction drives neurodegeneration through dysregulated inflammatory signaling and compromised neuronal support mechanisms.

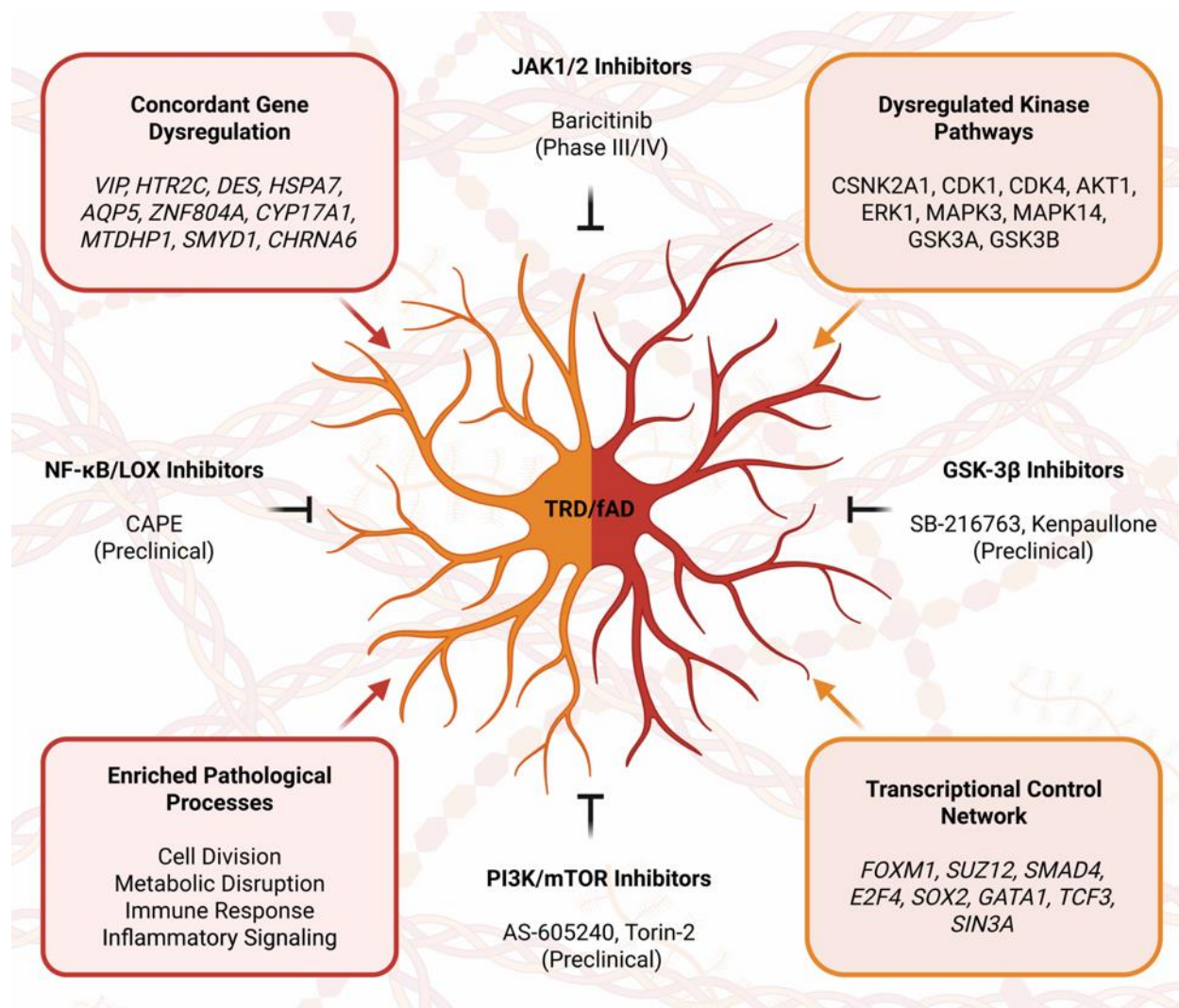


Figure 5.3 Shared Molecular Dysregulation in NR and fAD Astrocytes. Shared molecular dysregulation in NR and fAD astrocytes includes 115 concordantly altered genes, prominently VIP (most downregulated), alongside disrupted cell division, metabolism, and neuroinflammatory signaling. Key kinase pathways (GSK3B, MAPK14, AKT1) and master regulators (FOXM1, SUZ12) were identified. Therapeutic candidates include FDA-approved baricitinib (JAK1/2 inhibitor), preclinical GSK-3 β inhibitors (SB-216763, kenpaullone), CAPE (NF- κ B/LOX inhibitor), and PI3K/mTOR inhibitors (AS-605240, Torin-2).

The third study employed cross-condition comparative analyses to delineate shared and distinct astrocyte pathways in MDD and fAD. This systematic analysis identified distinct molecular signatures associated with each condition, with NR astrocytes showing pronounced alterations in chemotaxis-related pathways and fAD astrocytes exhibiting significant dysregulation of ECM components (Figure 5.3). Importantly, several gene clusters, particularly those involved in "external encapsulating structure organization" and "extracellular structure organization," showed consistent disruption across all conditions, establishing a molecular bridge between neuropsychiatric and neurodegenerative disorders. The study further validated previously reported overlapping MDD-AD risk genes, including HLA-DQB1 and ZNF804A, within the context of astrocyte biology. Computational pharmacology identified both concordant and discordant drug mechanisms across conditions. HDAC and mTOR inhibitors emerged as the primary pharmacological signatures in MDD models, whereas fAD signatures were associated with acetylcholine receptor modulation. This distinct pharmacological profiling highlighted potential therapeutic approaches that target shared biological vulnerabilities while addressing condition-specific molecular changes.

Collectively, these studies strengthen the evidence for astrocytes as critical immunomodulatory cells in both MDD and fAD pathogenesis. The observed upregulation of chemotaxis-related genes in MDD non-responders parallels the broader inflammatory profile in fAD astrocytes, while ECM dysregulation emerges as a shared pathology. The integration of transcriptomics, kinomics, and computational pharmacology provides a robust foundation for precision psychiatry approaches targeting astrocyte-specific molecular mechanisms. By highlighting the active immunoregulatory role of astrocytes in both MDD and AD, these findings

offer promising avenues for therapeutic improvements across both neuropsychiatric and neurodegenerative disorders.

Mechanistic insights into astrocyte dysfunction in MDD and AD

These studies reveal neuroinflammatory dysregulation as a fundamental mechanism connecting MDD and AD at the astrocyte level. Our transcriptomic analyses identified significant enrichment of immune signaling and chemotaxis-related pathways, particularly in SSRI-nonresponder astrocytes compared to healthy controls. Gene ontology analysis specifically highlighted terms such as "chemotaxis" (GO:0006935), "cell chemotaxis" (GO:0060326), and "leukocyte migration" (GO:0050900) in NR astrocytes, indicating their enhanced capacity for immune cell recruitment. Similarly, fAD astrocytes exhibited pronounced upregulation of inflammatory mediators, including SERPINA3, IL7R, IL6R, and TNFRSF11A, establishing a molecular basis for astrocyte-driven neuroinflammation in AD pathology. The identification of these shared inflammatory signatures across distinct neuropsychiatric and neurodegenerative conditions provides novel insight into their convergent pathophysiological mechanisms, suggesting potential for common therapeutic approaches targeting neuroinflammation.

Parallel to inflammation, ECM remodeling represents another critical shared pathway. Our findings demonstrate that ECM remodeling represents another critical astrocyte-mediated pathway disrupted in both disorders. Gene ontology enrichment analysis identified "extracellular matrix organization" (GO:0030198), "extracellular structure organization" (GO:0043062), and "external encapsulating structure organization" (GO:0045229) as significantly enriched terms across both conditions, though with differential expression patterns. In fAD astrocytes, we observed pronounced upregulation of ECM-related genes and pathways, while R astrocytes

showed downregulation of these same pathways compared to healthy controls. Notably, hierarchical cluster analysis revealed that a gene cluster linked to "extracellular matrix organization" was upregulated in NR vs. HC, with an even stronger increase observed in NR vs. R comparison. The silhouette-based clustering of genes mapped to these ECM-related GO terms identified two distinct clusters with divergent expression patterns between R, NR, and fAD lines, further supporting condition-specific ECM dysregulation despite shared pathway involvement.

Our transcription factor and kinase analyses revealed both convergent and divergent regulatory mechanisms across disorders. We identified SP1, TP53, and STAT3 as transcription factors showing complex activity patterns that differed between patient groups. For example, SP1 was significantly downregulated in R compared to HC but upregulated in NR and fAD patients relative to HC. Our analyses suggest the presence of condition-specific master regulators, including NRG1, which exhibited heightened activity in R compared to HC, TP53 in NR versus HC, and AR in fAD versus HC. These regulators may play pivotal roles in shaping the distinct transcriptional programs associated with each condition, though further investigation is needed to fully elucidate their contributions. Kinase profiling further supported condition-specific regulation, with DDR2 displaying positive associations in both NR and fAD astrocytes but a negative association in R astrocytes.

Despite shared mechanisms, our analyses identified notable disease-specific signatures. NR astrocytes exhibited enrichment in immune signaling pathways, whereas R astrocytes displayed upregulation of antioxidant activity and proteostasis-related modules. In contrast, fAD astrocytes uniquely upregulated genes associated with ECM organization and cell cycle-related processes. The identification of specific gene expression patterns, such as HLA-DQB1 and HLA-DQA1 alterations in MDD and PLCE1 and HNMT upregulation in AD, further illustrates how

astrocytes develop disease-specific molecular profiles despite sharing certain pathological mechanisms. Correlation analyses yielded the unexpected finding that SSRI-responder astrocytes show a positive correlation with fAD gene expression patterns, while non-responder astrocytes show a negative correlation with fAD patterns. This suggests that the transcriptional relationship between depression and Alzheimer's disease is more complex than previously understood and is significantly influenced by antidepressant responsiveness. These shared and distinct molecular signatures not only advance our understanding of astrocyte biology in brain disorders but also identify specific targets for therapeutic intervention tailored to different clinical scenarios.

Therapeutic implications and drug repurposing opportunities

The LINCS platform analysis revealed promising therapeutic candidates by identifying small molecules capable of reversing pathological astrocyte signatures in both depression and neurodegeneration. For AD, fluticasone propionate (a glucocorticoid with known anti-inflammatory properties), Akt inhibitors VIII and IV, and the PI3K γ inhibitor AS-605240 emerged as leading candidates with the potential to mitigate neuroinflammation and ECM disruption. For TRD, computational analyses identified monoamine oxidase inhibitors, including tranylcypromine and phenelzine, as compounds that specifically counteract pathological transcriptomic signatures in NR astrocytes. These findings suggest that broader-spectrum monoamine modulation may be necessary to ameliorate the distinct astrocyte-driven disturbances in TRD cases. MOA analysis identified HDAC inhibitors as the most prominent class of concordant perturbagens across disease groups, with a particularly strong representation in R and NR astrocytes. This suggests epigenetic mechanisms similar to those affected by HDAC inhibition may be involved in the underlying pathophysiology of depression, potentially

contributing to the transcriptomic alterations observed in these conditions. Additionally, mTOR inhibitors emerged as significant concordant mechanisms of action, highlighting the PI3K/Akt/mTOR signaling axis as a critical therapeutic target spanning both disorders.

These findings support a shift in psychiatric and neurodegenerative drug discovery, encouraging exploration beyond neuron-centric approaches to include strategies that incorporate astrocyte-targeted interventions. Traditional treatment paradigms have overlooked critical glial contributions to disease pathophysiology, potentially explaining the limited efficacy of many current therapies. By showing that patient-specific astrocyte models can recapitulate key disease phenotypes and respond to potential therapeutics in predictable ways, this work suggests astrocytes may be important targets for next-generation interventions. The hiPSC platform offers a particularly powerful avenue toward precision psychiatry by enabling patient-specific drug screening at the cellular level. This approach could significantly reduce the trial-and-error prescribing that characterizes current depression treatment, especially for TRD patients. Pharmacogenetic and phenotypic screenings using patient-derived astrocytes could be used to refine therapeutic selection, potentially improving treatment efficacy while reducing adverse effects and treatment delays.

The shared involvement of astrocyte-mediated neuroinflammatory processes in both MDD and AD highlights promising prospects for combinatorial therapeutic approaches. For treatment-resistant depression, pairing conventional antidepressants with immune-modulating agents could yield synergistic benefits, particularly for patients with elevated inflammatory biomarkers. Recent studies have shown that targeting specific chemokine pathways, including those involving CCL2 and CXCL10, may disrupt the self-perpetuating inflammatory cycles that contribute to both depression and neurodegeneration. For Alzheimer's disease, targeting CXCR3

signaling (the receptor for CXCL10) represents a promising approach, with recent research demonstrating that CXCR3 deficiency reduces A β plaques and rescues memory deficits in mouse models [510]. Similarly, interventions targeting the NLRP3 inflammasome pathway may address the neurotoxic astrocyte activation seen in both conditions.

The identification of specific molecular hubs within signaling networks offers particularly promising drug targets. The transcription factor STAT3 emerged as a central governor of astrocyte-driven inflammatory responses across both disorders. By interfering with STAT3-driven cytokine production, it may be possible to interrupt the inflammatory positive feedback loops in both depression and neurodegeneration. Similarly, disconnecting PI3K/Akt signaling and downstream effectors could mitigate multiple aspects of disease pathology. Kinomic profiling identified several kinase families, such as DYRK, GSK, and MAPK, as playing critical roles in neuroinflammatory and tau phosphorylation processes. These insights suggest that multi-target kinase inhibitors could address multiple disease mechanisms simultaneously. Particularly promising is the convergence of multiple lines of evidence on the PI3K/Akt/mTOR axis as a mediator of both neuroinflammation and ECM remodeling across disorders.

Comparative analysis with existing literature

The results of these studies align with established literature that positions astrocytes as active mediators rather than passive observers in the brain pathophysiology [191, 448, 511, 512]. The identification of astrocyte-driven chemotactic and inflammatory alterations corroborates previous observations on cytokine and chemokine signaling in both psychiatric and neurodegenerative contexts [197, 206, 394, 513, 514]. ECM-related changes observed in AD astrocytes similarly complement existing studies demonstrating how disrupted matrix dynamics

and glial remodeling contribute to synaptic dysfunction in neurodegeneration [515-518]. While building upon previous work, these studies introduce several distinctive advances. The LINCS-based computational drug repurposing approach represents a significant methodological innovation compared to earlier studies. Unlike conventional computational methods that broadly identify repurposable compounds, our signature-matching strategy specifically distinguishes between concordant signatures that mimic disease states and discordant signatures with therapeutic potential while also providing condition-specific resolution across responders, non-responders, and fAD patients. This differentiated approach enables more precise therapeutic targeting than previous work, which typically applied broader computational methods without distinguishing treatment response subtypes. For example, while prior literature has noted epigenetic and metabolic dysregulation in depression, our analysis uniquely quantifies the differential representation of HDAC and mTOR inhibitors between responder and non-responder phenotypes. Similarly, our identification of PG-9 CPD (an acetylcholine receptor agonist) as a highly concordant small molecule mimetic, specifically in fAD astrocytes, provides mechanistic specificity beyond previous reports of general acetylcholine involvement in AD pathology. Together, these advances refine our understanding of astrocytic disease mechanisms and highlight novel therapeutic opportunities.

Perhaps most significantly, this work moves beyond the common practice of broadly categorizing astrocyte dysfunction across various conditions. Instead, we highlight subtype-specific astrocyte responses associated with therapeutic outcomes in MDD, providing a detailed perspective that has been previously neglected. The discovery that TFs such as HIF3A and KLF17 are distinctly modulated in R vs. NR opens novel avenues for investigating the molecular mechanisms of antidepressant response. Our kinase profiling results add crucial specificity to

previous reports broadly implicating certain pathways in MDD and AD [519-527]. While prior literature has identified general kinase dysregulation in these disorders, this work uniquely delineates differential activity of individual kinases contingent upon clinical responsiveness. The finding that DDR2 displays opposing activity patterns between responders and non-responders exemplifies how kinase function can vary dramatically across clinical phenotypes, providing potential targets for precise therapeutic development. The comparative transcriptomic analysis across MDD and fAD astrocytes revealed shared dysregulations of specific immune-related genes (BMP8B, MYRIP, ZNF804A) that had not been previously examined in an astrocyte-specific context [528, 529]. This finding places astrocytes at the intersection of psychoneuroimmune interactions central to both disorders, a perspective that has been underexplored in prior research. By introducing these novel astrocyte-specific insights and therapeutic candidates while building upon established knowledge, these studies advance the conversation on precision psychiatry and neurology. It offers actionable insights grounded in rigorous comparative analyses that could transform our approach to treating both depression and neurodegeneration through targeted modulation of astrocyte function.

Limitations of the current research

While powerful, our hiPSC-derived astrocyte approach faces several important limitations that warrant acknowledgment. The simplified nature of these *in vitro* models enhances experimental control by reducing biological complexity, particularly through streamlined cellular interactions compared to those in the intact brain. *In vivo*, astrocytes dynamically interact with neurons, microglia, oligodendrocytes, and vascular cells. Consequently, this reduced cellular diversity may obscure pathological mechanisms that emerge

only within the complete neural ecosystem. Additionally, technical variables associated with differentiation protocols may influence our results. These protocols can generate astrocyte populations with varying degrees of heterogeneity and maturation, potentially influencing the expression of certain phenotypes. Prior studies indicate that distinct differentiation methods yield astrocytes with diverse transcriptional profiles and functional characteristics [457, 530, 531]. Moreover, epigenetic memory and aberrations in hiPSCs that persist after reprogramming may influence cellular phenotypes independently of the disease-related genetic factors under investigation.

Our sample sizes capture only a fraction of the genetic and phenotypic diversity present in clinical populations. This limited representation is particularly significant given the heterogeneous nature of both MDD and AD, which likely comprise multiple biological subtypes with distinct underlying mechanisms. Expanded cohorts incorporating greater demographic and genetic diversity would strengthen the generalizability of our findings. Furthermore, our cross-sectional experimental design provides only a static snapshot of astrocyte dysfunction, limiting our ability to track the progression of cellular pathology over time. This approach cannot fully capture the developmental trajectory of astrocyte dysfunction or the dynamic changes that occur during disease evolution and treatment response. Additionally, these models cannot adequately replicate the aging process, a significant limitation for AD research, where age-related factors such as cellular senescence and accumulated oxidative damage play critical roles in disease progression. Finally, the computational identification of therapeutic candidates through LINCS-based approaches requires extensive validation before clinical application. While our *in silico* analyses suggest promising compounds for repurposing, their efficacy, optimal dosing, and safety profiles remain unconfirmed without rigorous preclinical testing and carefully designed

clinical trials. The transition from cellular phenotypes to complex behavioral and cognitive outcomes involves numerous biological levels that our models cannot address in isolation. Overcoming these limitations will be crucial to fully harnessing the potential of hiPSC-derived astrocytes in enhancing our understanding of brain disorders and improving therapeutic strategies.

Future directions for astrocyte-centric research

These studies establish astrocytes as critical mediators in both MDD and AD pathophysiology, opening several promising avenues for future investigation and clinical translation. To overcome monoculture limitations, advanced co-culture platforms and three-dimensional organoid models incorporating neurons, astrocytes, and microglia could better replicate the neuroimmune signaling networks identified in our transcriptomic analyses. Additionally, longitudinal experimental designs with extended culture periods and induced aging protocols are essential for tracking astrocyte dysfunction evolution and understanding the progressive nature of treatment resistance in depression and neurodegeneration in AD.

The promising therapeutic candidates identified through our LINCS analyses, such as HDAC inhibitors and selective kinase inhibitors, require systematic *in vivo* validation. Animal models of depression and AD could test these compounds, with multi-modal assessments incorporating behavioral, electrophysiological, and molecular readouts. Combinatorial approaches, such as pairing conventional antidepressants with astrocyte-specific anti-inflammatory agents or combining amyloid-targeting therapies with compounds that restore astrocyte homeostatic functions, could yield synergistic benefits. By exploring these interconnected research avenues, the field can leverage this integrated understanding to deepen

our knowledge of astrocyte biology in brain disorders and drive the development of more effective therapies for depression and neurodegeneration.

Concluding remarks

These studies shift our understanding of astrocytes in brain disorders by positioning them as active participants rather than passive observers in the pathological processes underlying both MDD and AD. Through comprehensive molecular profiling of patient-derived astrocytes, we have identified evidence suggesting astrocyte-driven processes may link neuropsychiatric and neurodegenerative conditions. Dysregulated neuroimmune signaling, ECM remodeling, and stress-response pathways appear to converge across these disorders, highlighting astrocytes as potential contributors to common pathological mechanisms affecting millions of individuals. Our multi-omics approach has identified both shared and distinct astrocyte signatures across patient groups, highlighting common pathways such as chemokine signaling and ECM alterations, as well as distinct transcription factor networks and kinase activity patterns in SSRI responders, non-responders, and Alzheimer's patients. These findings offer valuable insights into condition-specific disease mechanisms and support the development of targeted therapeutics addressing astrocyte dysfunction. Our LINCS-based analyses identified promising therapeutic candidates: GSK-3 β inhibitors (kenpaullone, indirubin) for non-responder astrocytes, Akt inhibitors for familial Alzheimer's disease, and novel PI3K/Akt/mTOR kinase and HDAC inhibitors effective across all disease groups, supporting combinatorial approaches. These findings highlight the need for precision strategies targeting astrocyte-specific inflammatory and ECM remodeling pathways, tailored to each condition's molecular landscape. This work marks a significant shift from neuron-centric strategies to recognizing astrocytes as key players that warrant direct

therapeutic targeting. By developing patient-derived cellular platforms for drug discovery, functional validation, and mechanistic studies, we aim to bridge fundamental astrocyte biology with clinical applications. As the field progresses, the ability to target astrocyte-specific pathways opens new opportunities to create more effective, personalized treatments for depression and neurodegeneration.

References

1. Liu, J., et al., *Temporal and spatial trend analysis of all-cause depression burden based on Global Burden of Disease (GBD) 2019 study*. Scientific Reports, 2024. **14**(1): p. 12346.
2. Iancu, S.C., et al., *Long-term disability in major depressive disorder: a 6-year follow-up study*. Psychol Med, 2020. **50**(10): p. 1644-1652.
3. Reddy, M.S., *Depression: the disorder and the burden*. Indian J Psychol Med, 2010. **32**(1): p. 1-2.
4. Duivis, H.E., et al., *Differential association of somatic and cognitive symptoms of depression and anxiety with inflammation: Findings from the Netherlands Study of Depression and Anxiety (NESDA)*. Psychoneuroendocrinology, 2013. **38**(9): p. 1573-1585.
5. Christensen, M.C., C.M.J. Wong, and B.T. Baune, *Symptoms of Major Depressive Disorder and Their Impact on Psychosocial Functioning in the Different Phases of the Disease: Do the Perspectives of Patients and Healthcare Providers Differ?* Frontiers in Psychiatry, 2020. **11**.
6. Lopizzo, N., et al., *Gene-environment interaction in major depression: focus on experience-dependent biological systems*. Front Psychiatry, 2015. **6**: p. 68.
7. Zhao, M.Z., X.S. Song, and J.S. Ma, *Gene × environment interaction in major depressive disorder*. World J Clin Cases, 2021. **9**(31): p. 9368-9375.
8. Chiauzzi, E., et al., *Patient Perspective of Cognitive Symptoms in Major Depressive Disorder: Retrospective Database and Prospective Survey Analyses*. J Participat Med, 2019. **11**(2): p. e11167.
9. Baune, B.T. and M.C. Christensen, *Differences in Perceptions of Major Depressive Disorder Symptoms and Treatment Priorities Between Patients and Health Care Providers Across the Acute, Post-Acute, and Remission Phases of Depression*. Frontiers in Psychiatry, 2019. **10**.
10. Lohoff, F.W., *Overview of the genetics of major depressive disorder*. Curr Psychiatry Rep, 2010. **12**(6): p. 539-46.
11. Proudman, D., P. Greenberg, and D. Nellesen, *The Growing Burden of Major Depressive Disorders (MDD): Implications for Researchers and Policy Makers*. Pharmacoeconomics, 2021. **39**(6): p. 619-625.
12. Thomas, L., et al., *Prevalence of treatment-resistant depression in primary care: cross-sectional data*. Br J Gen Pract, 2013. **63**(617): p. e852-8.
13. McIntyre, R.S., et al., *Treatment-resistant depression: definition, prevalence, detection, management, and investigational interventions*. World Psychiatry, 2023. **22**(3): p. 394-412.
14. Kolasa, M. and A. Faron-Górecka, *Preclinical models of treatment-resistant depression: challenges and perspectives*. Pharmacol Rep, 2023. **75**(6): p. 1326-1340.
15. Voineskos, D., Z.J. Daskalakis, and D.M. Blumberger, *Management of Treatment-Resistant Depression: Challenges and Strategies*. Neuropsychiatr Dis Treat, 2020. **16**: p. 221-234.
16. Al-Harbi, K.S., *Treatment-resistant depression: therapeutic trends, challenges, and future directions*. Patient Prefer Adherence, 2012. **6**: p. 369-88.

17. Adekkanattu, P., et al., *Comorbidity and healthcare utilization in patients with treatment resistant depression: A large-scale retrospective cohort analysis using electronic health records*. J Affect Disord, 2023. **324**: p. 102-113.
18. Jaffe, D.H., B. Rive, and T.R. Deneer, *The humanistic and economic burden of treatment-resistant depression in Europe: a cross-sectional study*. BMC Psychiatry, 2019. **19**(1): p. 247.
19. Mrazek, D.A., et al., *A review of the clinical, economic, and societal burden of treatment-resistant depression: 1996-2013*. Psychiatr Serv, 2014. **65**(8): p. 977-87.
20. Corral, R., et al., *Suicidality and Quality of Life in Treatment-Resistant Depression Patients in Latin America: Secondary Interim Analysis of the TRAL Study*. Frontiers in Psychiatry, 2022. **13**.
21. Hannah, L.A., et al., *Economic evaluation of interventions for treatment-resistant depression: A systematic review*. Frontiers in Psychiatry, 2023. **14**.
22. Sussman, M., et al., *Economic Burden of Treatment-Resistant Depression on the U.S. Health Care System*. J Manag Care Spec Pharm, 2019. **25**(7): p. 823-835.
23. Zhou, X., et al., *Atypical Antipsychotic Augmentation for Treatment-Resistant Depression: A Systematic Review and Network Meta-Analysis*. Int J Neuropsychopharmacol, 2015. **18**(11): p. pyv060.
24. Parikh, S.V., et al., *Clinical outcomes in the biomarkers of ketamine (Bio-K) study of open-label IV ketamine for refractory depression*. Journal of Affective Disorders, 2024. **348**: p. 143-151.
25. Philip, N.S., et al., *Pharmacologic approaches to treatment resistant depression: a re-examination for the modern era*. Expert Opin Pharmacother, 2010. **11**(5): p. 709-22.
26. Tundo, A., R. de Filippis, and L. Proietti, *Pharmacologic approaches to treatment resistant depression: Evidences and personal experience*. World J Psychiatry, 2015. **5**(3): p. 330-41.
27. Rymaszewska, J., et al., *Various neuromodulation methods including Deep Brain Stimulation of the medial forebrain bundle combined with psychopharmacotherapy of treatment-resistant depression—Case report*. Frontiers in Psychiatry, 2023. **13**.
28. Deif, R. and M. Salama, *Depression From a Precision Mental Health Perspective: Utilizing Personalized Conceptualizations to Guide Personalized Treatments*. Front Psychiatry, 2021. **12**: p. 650318.
29. Jaber, M., et al., *Precision Medicine in Depression: The Role of Proteomics and Metabolomics in Personalized Treatment Approaches*. Adv Exp Med Biol, 2024. **1456**: p. 359-378.
30. Baune, B.T., et al., *An integrated precision medicine approach in major depressive disorder: a study protocol to create a new algorithm for the prediction of treatment response*. Front Psychiatry, 2023. **14**: p. 1279688.
31. *2024 Alzheimer's disease facts and figures*. Alzheimers Dement, 2024. **20**(5): p. 3708-3821.
32. *2023 Alzheimer's disease facts and figures*. Alzheimers Dement, 2023. **19**(4): p. 1598-1695.
33. Martinen, M., et al., *Molecular Mechanisms of Synaptotoxicity and Neuroinflammation in Alzheimer's Disease*. Frontiers in Neuroscience, 2018. **12**.
34. Bloom, G.S., *Amyloid- β and tau: the trigger and bullet in Alzheimer disease pathogenesis*. JAMA Neurol, 2014. **71**(4): p. 505-8.

35. Zhang, Y., et al., *Amyloid β -based therapy for Alzheimer's disease: challenges, successes and future*. Signal Transduction and Targeted Therapy, 2023. **8**(1): p. 248.
36. Lecca, D., et al., *Role of chronic neuroinflammation in neuroplasticity and cognitive function: A hypothesis*. Alzheimer's & Dementia, 2022. **18**(11): p. 2327-2340.
37. Guzmán-Vélez, E., et al., *Amyloid- β and tau pathologies relate to distinctive brain dysconnectomics in preclinical autosomal-dominant Alzheimer's disease*. Proceedings of the National Academy of Sciences, 2022. **119**(15): p. e2113641119.
38. Piaceri, I., B. Nacmias, and S. Sorbi, *Genetics of familial and sporadic Alzheimer's disease*. Front Biosci (Elite Ed), 2013. **5**(1): p. 167-77.
39. Ferreira, D., A. Nordberg, and E. Westman, *Biological subtypes of Alzheimer disease: A systematic review and meta-analysis*. Neurology, 2020. **94**(10): p. 436-448.
40. Levites, Y., et al., *Integrative proteomics identifies a conserved $A\beta$; amyloid responsive, novel plaque proteins, and pathology modifiers in Alzheimer's disease*. Cell Reports Medicine, 2024. **5**(8).
41. Avgerinos, K.I., L. Ferrucci, and D. Kapogiannis, *Effects of monoclonal antibodies against amyloid- β on clinical and biomarker outcomes and adverse event risks: A systematic review and meta-analysis of phase III RCTs in Alzheimer's disease*. Ageing Res Rev, 2021. **68**: p. 101339.
42. Li, J., et al., *The efficacy and safety of anti- $A\beta$ agents for delaying cognitive decline in Alzheimer's disease: a meta-analysis*. Frontiers in Aging Neuroscience, 2023. **15**.
43. Chhabra, A., et al., *A systematic review of the efficacy and safety of anti-amyloid beta monoclonal antibodies in treatment of Alzheimer's disease*. Expert Opin Biol Ther, 2024. **24**(11): p. 1261-1269.
44. Wong-Guerra, M., et al., *Revisiting the neuroinflammation hypothesis in Alzheimer's disease: a focus on the druggability of current targets*. Frontiers in Pharmacology, 2023. **14**.
45. Valenza, M., et al., *Alternative Targets to Fight Alzheimer's Disease: Focus on Astrocytes*. Biomolecules, 2021. **11**(4).
46. Sánchez-Sarasúa, S., et al., *Can We Treat Neuroinflammation in Alzheimer's Disease?* Int J Mol Sci, 2020. **21**(22).
47. Greene, A.N., M.B. Solomon, and L.M. Privette Vinnedge, *Novel molecular mechanisms in Alzheimer's disease: The potential role of DEK in disease pathogenesis*. Frontiers in Aging Neuroscience, 2022. **14**.
48. Liu, M., et al., *Early-onset Alzheimer's disease with depression as the first symptom: a case report with literature review*. Front Psychiatry, 2023. **14**: p. 1192562.
49. Sáiz-Vázquez, O., et al., *Depression as a Risk Factor for Alzheimer's Disease: A Systematic Review of Longitudinal Meta-Analyses*. J Clin Med, 2021. **10**(9).
50. Huang, Y.Y., et al., *Depression in Alzheimer's Disease: Epidemiology, Mechanisms, and Treatment*. Biol Psychiatry, 2024. **95**(11): p. 992-1005.
51. Gibson, J., et al., *Assessing the presence of shared genetic architecture between Alzheimer's disease and major depressive disorder using genome-wide association data*. Translational Psychiatry, 2017. **7**(4): p. e1094-e1094.
52. Ownby, R.L., et al., *Depression and Risk for Alzheimer Disease: Systematic Review, Meta-analysis, and Metaregression Analysis*. Archives of General Psychiatry, 2006. **63**(5): p. 530-538.

53. Green, R.C., et al., *Depression as a Risk Factor for Alzheimer Disease: The MIRAGE Study*. Archives of Neurology, 2003. **60**(5): p. 753-759.
54. Chi, S., et al., *Depression in Alzheimer's Disease: Epidemiology, Mechanisms, and Management*. Journal of Alzheimer's Disease, 2014. **42**(3): p. 739-755.
55. Wallensten, J., et al., *Stress, depression, and risk of dementia – a cohort study in the total population between 18 and 65 years old in Region Stockholm*. Alzheimer's Research & Therapy, 2023. **15**(1): p. 161.
56. Fernández, R.F., J.I. Martín, and M.A.M. Antón, *Depression as a Risk Factor for Dementia: A Meta-Analysis*. The Journal of Neuropsychiatry and Clinical Neurosciences, 2024. **36**(2): p. 101-109.
57. Dafsari, F.S. and F. Jessen, *Depression—an underrecognized target for prevention of dementia in Alzheimer's disease*. Translational Psychiatry, 2020. **10**(1): p. 160.
58. Geerlings, M.I., et al., *Depression and risk of cognitive decline and Alzheimer's disease. Results of two prospective community-based studies in The Netherlands*. Br J Psychiatry, 2000. **176**: p. 568-75.
59. Yan, Y., et al., *Effects of depression and cognitive impairment on increased risks of incident dementia: a prospective study from three elderly cohorts*. Translational Psychiatry, 2024. **14**(1): p. 427.
60. Hussain, M., et al., *Similarities Between Depression and Neurodegenerative Diseases: Pathophysiology, Challenges in Diagnosis and Treatment Options*. Cureus, 2020. **12**(11): p. e11613.
61. Diniz, B.S., et al., *Late-life depression and risk of vascular dementia and Alzheimer's disease: systematic review and meta-analysis of community-based cohort studies*. Br J Psychiatry, 2013. **202**(5): p. 329-35.
62. Kim, H., et al., *Association between depression and the risk of Alzheimer's disease using the Korean National Health Insurance Service-Elderly Cohort*. Scientific Reports, 2021. **11**(1): p. 22591.
63. Ly, M., et al., *Late-life depression and increased risk of dementia: a longitudinal cohort study*. Transl Psychiatry, 2021. **11**(1): p. 147.
64. Elser, H., et al., *Association of Early-, Middle-, and Late-Life Depression With Incident Dementia in a Danish Cohort*. JAMA Neurology, 2023. **80**(9): p. 949-958.
65. Szymkowicz, S.M., et al., *Biological factors influencing depression in later life: role of aging processes and treatment implications*. Translational Psychiatry, 2023. **13**(1): p. 160.
66. Crump, C., et al., *Risk of depression in persons with Alzheimer's disease: A national cohort study*. Alzheimers Dement (Amst), 2024. **16**(2): p. e12584.
67. Ma, L., *Depression, Anxiety, and Apathy in Mild Cognitive Impairment: Current Perspectives*. Frontiers in Aging Neuroscience, 2020. **12**.
68. Lyketsos, C.G., et al., *Treating Depression in Alzheimer Disease: Efficacy and Safety of Sertraline Therapy, and the Benefits of Depression Reduction: The DIADS*. Archives of General Psychiatry, 2003. **60**(7): p. 737-746.
69. Correia, A.S. and N. Vale, *Antidepressants in Alzheimer's Disease: A Focus on the Role of Mirtazapine*. Pharmaceuticals (Basel), 2021. **14**(9).
70. Mega, M.S., et al., *The Spectrum of Behavioral Responses to Cholinesterase Inhibitor Therapy in Alzheimer Disease*. Archives of Neurology, 1999. **56**(11): p. 1388-1393.
71. Pozuelo Moyano, B., et al., *Anti-Amyloid Drugs for Alzheimer's Disease: Considering the Role of Depression*. Neurodegenerative Diseases, 2024.

72. Reitz, C., *Toward precision medicine in Alzheimer's disease*. *Annals of Translational Medicine*, 2016. **4**(6): p. 107.
73. Lukiw, W.J., et al., *Biomarkers for Alzheimer's Disease (AD) and the Application of Precision Medicine*. *Journal of Personalized Medicine*, 2020. **10**(3): p. 138.
74. Bredesen, D.E., et al., *Precision Medicine Approach to Alzheimer's Disease: Rationale and Implications*. *J Alzheimers Dis*, 2023. **96**(2): p. 429-437.
75. Tang, L., et al., *Dissecting biological heterogeneity in major depressive disorder based on neuroimaging subtypes with multi-omics data*. *Translational Psychiatry*, 2025. **15**(1): p. 72.
76. Fuh, S.C., et al., *Multi-omic modeling of antidepressant response implicates dynamic immune and inflammatory changes in individuals who respond to treatment*. *PLoS One*, 2023. **18**(5): p. e0285123.
77. Hicks, E.M., et al., *Integrating genetics and transcriptomics to study major depressive disorder: a conceptual framework, bioinformatic approaches, and recent findings*. *Transl Psychiatry*, 2023. **13**(1): p. 129.
78. Johnson, E.C.B., et al., *Large-scale deep multi-layer analysis of Alzheimer's disease brain reveals strong proteomic disease-related changes not observed at the RNA level*. *Nat Neurosci*, 2022. **25**(2): p. 213-225.
79. Stolfi, F., et al., *Omics approaches open new horizons in major depressive disorder: from biomarkers to precision medicine*. *Frontiers in Psychiatry*, 2024. **15**.
80. Chen, S., et al., *Suicide risk stratification among major depressed patients based on a machine learning approach and whole-brain functional connectivity*. *J Affect Disord*, 2023. **322**: p. 173-179.
81. Kessler, R.C., et al., *Testing a machine-learning algorithm to predict the persistence and severity of major depressive disorder from baseline self-reports*. *Mol Psychiatry*, 2016. **21**(10): p. 1366-71.
82. Yang, L., et al., *Application of machine learning in depression risk prediction for connective tissue diseases*. *Scientific Reports*, 2025. **15**(1): p. 1706.
83. Waschkies, K.F., et al., *Machine learning-based classification of Alzheimer's disease and its at-risk states using personality traits, anxiety, and depression*. *International Journal of Geriatric Psychiatry*, 2023. **38**(10): p. e6007.
84. Drevets, W.C., et al., *Immune targets for therapeutic development in depression: towards precision medicine*. *Nature Reviews Drug Discovery*, 2022. **21**(3): p. 224-244.
85. Hampel, H., et al., *A Path Toward Precision Medicine for Neuroinflammatory Mechanisms in Alzheimer's Disease*. *Front Immunol*, 2020. **11**: p. 456.
86. Cerqueira, S.R., N.G. Ayad, and J.K. Lee, *Neuroinflammation Treatment via Targeted Delivery of Nanoparticles*. *Frontiers in Cellular Neuroscience*, 2020. **14**.
87. Correia, A.S., A. Cardoso, and N. Vale, *BDNF Unveiled: Exploring Its Role in Major Depression Disorder Serotonergic Imbalance and Associated Stress Conditions*. *Pharmaceutics*, 2023. **15**(8).
88. Chen, X.Q., M. Sawa, and W.C. Mobley, *Dysregulation of neurotrophin signaling in the pathogenesis of Alzheimer disease and of Alzheimer disease in Down syndrome*. *Free Radic Biol Med*, 2018. **114**: p. 52-61.
89. Triebelhorn, J., et al., *Induced neural progenitor cells and iPS-neurons from major depressive disorder patients show altered bioenergetics and electrophysiological properties*. *Molecular Psychiatry*, 2024. **29**(5): p. 1217-1227.

90. Villafranco, J., et al., *The use of induced pluripotent stem cells as a platform for the study of depression*. Front Psychiatry, 2024. **15**: p. 1470642.
91. Cerneckis, J., H. Cai, and Y. Shi, *Induced pluripotent stem cells (iPSCs): molecular mechanisms of induction and applications*. Signal Transduction and Targeted Therapy, 2024. **9**(1): p. 112.
92. Lee, D.H., et al., *Neuronal Cell Differentiation of iPSCs for the Clinical Treatment of Neurological Diseases*. Biomedicines, 2024. **12**(6).
93. Kumar, A., L. Stertz, and A.L. Teixeira, *Induce Pluripotent Stem Cells (iPSC) Technology in Depression*. Adv Exp Med Biol, 2024. **1456**: p. 85-91.
94. Vadodaria, K.C., et al., *Modeling Brain Disorders Using Induced Pluripotent Stem Cells*. Cold Spring Harb Perspect Biol, 2020. **12**(6).
95. Penney, J., W.T. Ralvenius, and L.H. Tsai, *Modeling Alzheimer's disease with iPSC-derived brain cells*. Mol Psychiatry, 2020. **25**(1): p. 148-167.
96. Stöberl, N., et al., *Human iPSC-derived glia models for the study of neuroinflammation*. J Neuroinflammation, 2023. **20**(1): p. 231.
97. Bassil, R., et al., *Improved modeling of human AD with an automated culturing platform for iPSC neurons, astrocytes and microglia*. Nature Communications, 2021. **12**(1): p. 5220.
98. Soliman, M.A., et al., *Pluripotent stem cells in neuropsychiatric disorders*. Molecular Psychiatry, 2017. **22**(9): p. 1241-1249.
99. Lewis, D.A., *The Human Brain Revisited: Opportunities and Challenges in Postmortem Studies of Psychiatric Disorders*. Neuropsychopharmacology, 2002. **26**(2): p. 143-154.
100. McCullumsmith, R.E., et al., *Postmortem Brain: An Underutilized Substrate for Studying Severe Mental Illness*. Neuropsychopharmacology, 2014. **39**(1): p. 65-87.
101. Vornholt, E., et al., *Postmortem brain tissue as an underutilized resource to study the molecular pathology of neuropsychiatric disorders across different ethnic populations*. Neurosci Biobehav Rev, 2019. **102**: p. 195-207.
102. Mekkes, N.J., et al., *Identification of clinical disease trajectories in neurodegenerative disorders with natural language processing*. Nature Medicine, 2024. **30**(4): p. 1143-1153.
103. Li, L., J. Chao, and Y. Shi, *Modeling neurological diseases using iPSC-derived neural cells : iPSC modeling of neurological diseases*. Cell Tissue Res, 2018. **371**(1): p. 143-151.
104. Dong, Y., et al., *Plasticity of Synaptic Transmission in Human Stem Cell-Derived Neural Networks*. iScience, 2020. **23**(2): p. 100829.
105. Gouder, L., et al., *Altered spinogenesis in iPSC-derived cortical neurons from patients with autism carrying de novo SHANK3 mutations*. Scientific Reports, 2019. **9**(1): p. 94.
106. Li, B.-Z., et al., *Current Best Practices for Analysis of Dendritic Spine Morphology and Number in Neurodevelopmental Disorder Research*. ACS Chemical Neuroscience, 2023. **14**(9): p. 1561-1572.
107. Yu, H. and Z.-y. Chen, *The role of BDNF in depression on the basis of its location in the neural circuitry*. Acta Pharmacologica Sinica, 2011. **32**(1): p. 3-11.
108. Yang, T., et al., *The Role of BDNF on Neural Plasticity in Depression*. Frontiers in Cellular Neuroscience, 2020. **14**.
109. Ochalek, A., et al., *Neurons derived from sporadic Alzheimer's disease iPSCs reveal elevated TAU hyperphosphorylation, increased amyloid levels, and GSK3B activation*. Alzheimers Res Ther, 2017. **9**(1): p. 90.

110. Oakley, D.H., et al., *β -Amyloid species production and tau phosphorylation in iPSC-neurons with reference to neuropathologically characterized matched donor brains*. Journal of Neuropathology & Experimental Neurology, 2024. **83**(9): p. 772-782.
111. Flannagan, K., et al., *Cell type and sex specific mitochondrial phenotypes in iPSC derived models of Alzheimer's disease*. Frontiers in Molecular Neuroscience, 2023. **16**.
112. Israel, M.A., et al., *Probing sporadic and familial Alzheimer's disease using induced pluripotent stem cells*. Nature, 2012. **482**(7384): p. 216-20.
113. Kaltschmidt, B., et al., *Transcription factor NF- κ B is activated in primary neurons by amyloid β peptides and in neurons surrounding early plaques from patients with Alzheimer disease*. Proceedings of the National Academy of Sciences, 1997. **94**(6): p. 2642-2647.
114. MERAZ RIOS, M.A., et al., *Inflammatory process in Alzheimer's Disease*. Frontiers in Integrative Neuroscience, 2013. **7**.
115. Guo, P., et al., *A Systematic Analysis on the Genes and Their Interaction Underlying the Comorbidity of Alzheimer's Disease and Major Depressive Disorder*. Frontiers in Aging Neuroscience, 2022. **13**.
116. Cheng, Y., et al., *Identification of Hub Genes Related to Alzheimer's Disease and Major Depressive Disorder*. Am J Alzheimers Dis Other Demen, 2021. **36**: p. 15333175211046123.
117. Miyata, S., et al., *Involvement of inflammatory responses in the brain to the onset of major depressive disorder due to stress exposure*. Frontiers in Aging Neuroscience, 2022. **14**.
118. Yuan, M., et al., *Epigenetic regulation in major depression and other stress-related disorders: molecular mechanisms, clinical relevance and therapeutic potential*. Signal Transduction and Targeted Therapy, 2023. **8**(1): p. 309.
119. Abdolmaleky, H.M., J.R. Zhou, and S. Thiagalingam, *Cataloging recent advances in epigenetic alterations in major mental disorders and autism*. Epigenomics, 2021. **13**(15): p. 1231-1245.
120. Rahman, M.F. and P.O. McGowan, *Cell-type-specific epigenetic effects of early life stress on the brain*. Translational Psychiatry, 2022. **12**(1): p. 326.
121. Lemche, E., *Early Life Stress and Epigenetics in Late-onset Alzheimer's Dementia: A Systematic Review*. Curr Genomics, 2018. **19**(7): p. 522-602.
122. He, F. and Y.E. Sun, *Glial cells more than support cells?* The International Journal of Biochemistry & Cell Biology, 2007. **39**(4): p. 661-665.
123. Theparambil, S.M., et al., *Astrocytes regulate brain extracellular pH via a neuronal activity-dependent bicarbonate shuttle*. Nature Communications, 2020. **11**(1): p. 5073.
124. Liu, X., et al., *Astrocytes in Neural Circuits: Key Factors in Synaptic Regulation and Potential Targets for Neurodevelopmental Disorders*. Frontiers in Molecular Neuroscience, 2021. **14**.
125. Goubard, V., E. Fino, and L. Venance, *Contribution of astrocytic glutamate and GABA uptake to corticostriatal information processing*. J Physiol, 2011. **589**(Pt 9): p. 2301-19.
126. Purushotham, S.S. and Y. Buskila, *Astrocytic modulation of neuronal signalling*. Frontiers in Network Physiology, 2023. **3**.
127. Ota, Y., A.T. Zanetti, and R.M. Hallock, *The role of astrocytes in the regulation of synaptic plasticity and memory formation*. Neural Plast, 2013. **2013**: p. 185463.

128. Petr, G.T., et al., *Conditional Deletion of the Glutamate Transporter GLT-1 Reveals That Astrocytic GLT-1 Protects against Fatal Epilepsy While Neuronal GLT-1 Contributes Significantly to Glutamate Uptake into Synaptosomes*. The Journal of Neuroscience, 2015. **35**(13): p. 5187-5201.
129. Romanos, J., et al., *Differences in glutamate uptake between cortical regions impact neuronal NMDA receptor activation*. Communications Biology, 2019. **2**(1): p. 127.
130. Todd, A.C. and G.E. Hardingham, *The Regulation of Astrocytic Glutamate Transporters in Health and Neurodegenerative Diseases*. International Journal of Molecular Sciences, 2020. **21**(24): p. 9607.
131. Rose, C.R., et al., *Astroglial Glutamate Signaling and Uptake in the Hippocampus*. Frontiers in Molecular Neuroscience, 2018. **10**.
132. Covelo, A. and A. Araque, *Neuronal activity determines distinct gliotransmitter release from a single astrocyte*. Elife, 2018. **7**.
133. Goenaga, J., et al., *Calcium signaling in astrocytes and gliotransmitter release*. Frontiers in Synaptic Neuroscience, 2023. **15**.
134. Lam, D., et al., *Tissue-specific extracellular matrix accelerates the formation of neural networks and communities in a neuron-glia co-culture on a multi-electrode array*. Scientific Reports, 2019. **9**(1): p. 4159.
135. Dityatev, A., M. Schachner, and P. Sonderegger, *The dual role of the extracellular matrix in synaptic plasticity and homeostasis*. Nature Reviews Neuroscience, 2010. **11**(11): p. 735-746.
136. Mubuchi, A., et al., *Assembly of neuron- and radial glial-cell-derived extracellular matrix molecules promotes radial migration of developing cortical neurons*. eLife, 2024. **12**: p. RP92342.
137. Dankovich, T.M. and S.O. Rizzoli, *The Synaptic Extracellular Matrix: Long-Lived, Stable, and Still Remarkably Dynamic*. Frontiers in Synaptic Neuroscience, 2022. **14**.
138. Suryadevara, R., et al., *Regulation of tissue inhibitor of metalloproteinase-1 by astrocytes: links to HIV-1 dementia*. Glia, 2003. **44**(1): p. 47-56.
139. Moore, C.S., et al., *Astrocytic Tissue Inhibitor of Metalloproteinase-1 (TIMP-1) Promotes Oligodendrocyte Differentiation and Enhances CNS Myelination*. The Journal of Neuroscience, 2011. **31**(16): p. 6247-6254.
140. Sutter, P.A., et al., *Astrocytic TIMP-1 regulates production of Anastellin, an inhibitor of oligodendrocyte differentiation and FTY720 responses*. Proceedings of the National Academy of Sciences, 2024. **121**(5): p. e2306816121.
141. Cabral-Pacheco, G.A., et al., *The Roles of Matrix Metalloproteinases and Their Inhibitors in Human Diseases*. Int J Mol Sci, 2020. **21**(24).
142. Ardaya, M., et al., *Gliogenesis from the subventricular zone modulates the extracellular matrix at the glial scar after brain ischemia*. 2025, eLife Sciences Publications, Ltd.
143. Wiese, S., M. Karus, and A. Faissner, *Astrocytes as a source for extracellular matrix molecules and cytokines*. Front Pharmacol, 2012. **3**: p. 120.
144. Vargová, L. and E. Syková, *Astrocytes and extracellular matrix in extrasynaptic volume transmission*. Philos Trans R Soc Lond B Biol Sci, 2014. **369**(1654): p. 20130608.
145. Woo, A.M. and H. Sontheimer, *Interactions between astrocytes and extracellular matrix structures contribute to neuroinflammation-associated epilepsy pathology*. Frontiers in Molecular Medicine, 2023. **3**.

146. Choi, S.S., et al., *Human astrocytes: secretome profiles of cytokines and chemokines*. PLoS One, 2014. **9**(4): p. e92325.
147. Hyvärinen, T., et al., *Co-stimulation with IL-1 β and TNF- α induces an inflammatory reactive astrocyte phenotype with neurosupportive characteristics in a human pluripotent stem cell model system*. Scientific Reports, 2019. **9**(1): p. 16944.
148. Liu, Z. and M. Chopp, *Astrocytes, therapeutic targets for neuroprotection and neurorestoration in ischemic stroke*. Prog Neurobiol, 2016. **144**: p. 103-20.
149. Lee, M., C. Schwab, and P.L. McGeer, *Astrocytes are GABAergic cells that modulate microglial activity*. Glia, 2011. **59**(1): p. 152-65.
150. Valles, S.L., et al., *Functions of Astrocytes under Normal Conditions and after a Brain Disease*. Int J Mol Sci, 2023. **24**(9).
151. Bylicky, M.A., G.P. Mueller, and R.M. Day, *Mechanisms of Endogenous Neuroprotective Effects of Astrocytes in Brain Injury*. Oxid Med Cell Longev, 2018. **2018**: p. 6501031.
152. Liu, L.-r., et al., *Interaction of Microglia and Astrocytes in the Neurovascular Unit*. Frontiers in Immunology, 2020. **11**.
153. Martin, J.B., *The Integration of Neurology, Psychiatry, and Neuroscience in the 21st Century*. American Journal of Psychiatry, 2002. **159**(5): p. 695-704.
154. Staudt, M.D., et al., *Evolution in the Treatment of Psychiatric Disorders: From Psychosurgery to Psychopharmacology to Neuromodulation*. Frontiers in Neuroscience, 2019. **13**.
155. Lovinger, D.M., *Neurotransmitter roles in synaptic modulation, plasticity and learning in the dorsal striatum*. Neuropharmacology, 2010. **58**(7): p. 951-61.
156. Appelbaum, L.G., et al., *Synaptic plasticity and mental health: methods, challenges and opportunities*. Neuropsychopharmacology, 2023. **48**(1): p. 113-120.
157. Kumar, J., et al., *Innovative Approaches and Therapies to Enhance Neuroplasticity and Promote Recovery in Patients With Neurological Disorders: A Narrative Review*. Cureus, 2023. **15**(7): p. e41914.
158. Dupuy, J.M., et al., *A critical review of pharmacotherapy for major depressive disorder*. International Journal of Neuropsychopharmacology, 2011. **14**(10): p. 1417-1431.
159. Zhang, X., et al., *Role of Astrocytes in Major Neuropsychiatric Disorders*. Neurochem Res, 2021. **46**(10): p. 2715-2730.
160. Verkhatsky, A., et al., *Astrocytes in human central nervous system diseases: a frontier for new therapies*. Signal Transduction and Targeted Therapy, 2023. **8**(1): p. 396.
161. Stevenson, R., et al., *Neuromodulation of Glial Function During Neurodegeneration*. Frontiers in Cellular Neuroscience, 2020. **14**.
162. Papouin, T., et al., *Astrocytic control of synaptic function*. Philosophical Transactions of the Royal Society B: Biological Sciences, 2017. **372**(1715): p. 20160154.
163. Sanmarco, L.M., et al., *Functional immune cell-astrocyte interactions*. J Exp Med, 2021. **218**(9).
164. Hu, Y., et al., *Matrix stiffness changes affect astrocyte phenotype in an in vitro injury model*. NPG Asia Materials, 2021. **13**(1): p. 35.
165. Fisher, T.M. and S.A. Liddelow, *Emerging roles of astrocytes as immune effectors in the central nervous system*. Trends Immunol, 2024. **45**(10): p. 824-836.
166. Sanz-Gálvez, R., et al., *The role of astrocytes from synaptic to non-synaptic plasticity*. Frontiers in Cellular Neuroscience, 2024. **18**.

167. Cabezas, R., et al., *Astrocytic modulation of blood brain barrier: perspectives on Parkinson's disease*. Front Cell Neurosci, 2014. **8**: p. 211.
168. Toth, A.E., et al., *SorLA in astrocytes regulates blood-brain barrier integrity*. Frontiers in Drug Delivery, 2023. **2**.
169. Lawal, O., F.P. Ulloa Severino, and C. Eroglu, *The role of astrocyte structural plasticity in regulating neural circuit function and behavior*. Glia, 2022. **70**(8): p. 1467-1483.
170. Han, R.T., et al., *Astrocyte-immune cell interactions in physiology and pathology*. Immunity, 2021. **54**(2): p. 211-224.
171. Puentes-Orozco, M., S.L. Albarracin, and M.M. Velásquez, *Neuroinflammation and major depressive disorder: astrocytes at the crossroads*. Front Cell Neurosci, 2024. **18**: p. 1504555.
172. Dolotov, O.V., et al., *Stress-Induced Depression and Alzheimer's Disease: Focus on Astrocytes*. International Journal of Molecular Sciences, 2022. **23**(9): p. 4999.
173. Wang, Q., et al., *The link between neuroinflammation and the neurovascular unit in synucleinopathies*. Science Advances, 2023. **9**(7): p. eabq1141.
174. Rajkowska, G. and C.A. Stockmeier, *Astrocyte pathology in major depressive disorder: insights from human postmortem brain tissue*. Curr Drug Targets, 2013. **14**(11): p. 1225-36.
175. Tsai, S.-F., et al., *High-fat diet induces depression-like phenotype via astrocyte-mediated hyperactivation of ventral hippocampal glutamatergic afferents to the nucleus accumbens*. Molecular Psychiatry, 2022. **27**(11): p. 4372-4384.
176. Liu, J., et al., *Astrocyte dysfunction drives abnormal resting-state functional connectivity in depression*. Science Advances, 2022. **8**(46): p. eabo2098.
177. Sun, Y., et al., *Role of the Extracellular Matrix in Alzheimer's Disease*. Frontiers in Aging Neuroscience, 2021. **13**.
178. Frost, G.R. and Y.-M. Li, *The role of astrocytes in amyloid production and Alzheimer's disease*. Open Biology, 2017. **7**(12): p. 170228.
179. Perez-Nievas, B.G. and A. Serrano-Pozo, *Deciphering the Astrocyte Reaction in Alzheimer's Disease*. Frontiers in Aging Neuroscience, 2018. **10**.
180. Yin, K.J., et al., *Matrix metalloproteinases expressed by astrocytes mediate extracellular amyloid-beta peptide catabolism*. J Neurosci, 2006. **26**(43): p. 10939-48.
181. Wang, X.-X., et al., *Matrix Metalloproteinases and Their Multiple Roles in Alzheimer's Disease*. BioMed Research International, 2014. **2014**(1): p. 908636.
182. Sweeney, M.D., A.P. Sagare, and B.V. Zlokovic, *Blood-brain barrier breakdown in Alzheimer disease and other neurodegenerative disorders*. Nature Reviews Neurology, 2018. **14**(3): p. 133-150.
183. Sousa, J.A., et al., *Reconsidering the role of blood-brain barrier in Alzheimer's disease: From delivery to target*. Frontiers in Aging Neuroscience, 2023. **15**.
184. Kim, J., et al., *Pathological phenotypes of astrocytes in Alzheimer's disease*. Experimental & Molecular Medicine, 2024. **56**(1): p. 95-99.
185. Lawrence, J.M., et al., *Roles of neuropathology-associated reactive astrocytes: a systematic review*. Acta Neuropathol Commun, 2023. **11**(1): p. 42.
186. Lopez-Rodriguez, A.B., et al., *Acute systemic inflammation exacerbates neuroinflammation in Alzheimer's disease: IL-1 β drives amplified responses in primed astrocytes and neuronal network dysfunction*. Alzheimer's & Dementia, 2021. **17**(10): p. 1735-1755.

187. Zhao, Y., et al., *Astrocyte-Mediated Neuroinflammation in Neurological Conditions*. *Biomolecules*, 2024. **14**(10).
188. Frost, G.R. and Y.M. Li, *The role of astrocytes in amyloid production and Alzheimer's disease*. *Open Biol*, 2017. **7**(12).
189. Monterey, M.D., et al., *The Many Faces of Astrocytes in Alzheimer's Disease*. *Frontiers in Neurology*, 2021. **12**.
190. Gao, M., et al., *TNF- α /TNFR1 activated astrocytes exacerbate depression-like behavior in CUMS mice*. *Cell Death Discovery*, 2024. **10**(1): p. 220.
191. Nakano-Kobayashi, A., et al., *Astrocyte-targeting therapy rescues cognitive impairment caused by neuroinflammation via the Nrf2 pathway*. *Proceedings of the National Academy of Sciences*, 2023. **120**(33): p. e2303809120.
192. Bellaver, B., et al., *Astrocyte reactivity influences amyloid- β effects on tau pathology in preclinical Alzheimer's disease*. *Nature Medicine*, 2023. **29**(7): p. 1775-1781.
193. Shah, D., et al., *Astrocyte calcium dysfunction causes early network hyperactivity in Alzheimer's disease*. *Cell Rep*, 2022. **40**(8): p. 111280.
194. Ageeva, T., A. Rizvanov, and Y. Mukhamedshina, *NF- κ B and JAK/STAT Signaling Pathways as Crucial Regulators of Neuroinflammation and Astrocyte Modulation in Spinal Cord Injury*. *Cells*, 2024. **13**(7).
195. Chou, T.-W., et al., *Fibrillar α -synuclein induces neurotoxic astrocyte activation via RIP kinase signaling and NF- κ B*. *Cell Death & Disease*, 2021. **12**(8): p. 756.
196. Passamonti, L., et al., *Neuroinflammation and Functional Connectivity in Alzheimer's Disease: Interactive Influences on Cognitive Performance*. *The Journal of Neuroscience*, 2019. **39**(36): p. 7218-7226.
197. Giovannoni, F. and F.J. Quintana, *The Role of Astrocytes in CNS Inflammation*. *Trends Immunol*, 2020. **41**(9): p. 805-819.
198. Zhou, X., et al., *Astrocyte, a Promising Target for Mood Disorder Interventions*. *Frontiers in Molecular Neuroscience*, 2019. **12**.
199. Kim, C.K., et al., *Alzheimer's Disease: Key Insights from Two Decades of Clinical Trial Failures*. *J Alzheimers Dis*, 2022. **87**(1): p. 83-100.
200. Hampel, H., et al., *The Amyloid- β Pathway in Alzheimer's Disease*. *Molecular Psychiatry*, 2021. **26**(10): p. 5481-5503.
201. Sidoryk-Wegrzynowicz, M., et al., *Role of astrocytes in brain function and disease*. *Toxicol Pathol*, 2011. **39**(1): p. 115-23.
202. Novakovic, M.M., et al., *Astrocyte reactivity and inflammation-induced depression-like behaviors are regulated by Orai1 calcium channels*. *Nat Commun*, 2023. **14**(1): p. 5500.
203. Becerra-Calixto, A. and G.P. Cardona-Gómez, *The Role of Astrocytes in Neuroprotection after Brain Stroke: Potential in Cell Therapy*. *Frontiers in Molecular Neuroscience*, 2017. **10**.
204. Bi, W., et al., *Potential of astrocytes in targeting therapy for Alzheimer's disease*. *Int Immunopharmacol*, 2022. **113**(Pt A): p. 109368.
205. Grazyna, R. and A.S. Craig, *Astrocyte Pathology in Major Depressive Disorder: Insights from Human Postmortem Brain Tissue*. *Current Drug Targets*, 2013. **14**(11): p. 1225-1236.
206. Garland, E.F., I.J. Hartnell, and D. Boche, *Microglia and Astrocyte Function and Communication: What Do We Know in Humans?* *Frontiers in Neuroscience*, 2022. **16**.

207. Li, J., et al., *Conservation and divergence of vulnerability and responses to stressors between human and mouse astrocytes*. Nature Communications, 2021. **12**(1): p. 3958.
208. Spanos, F. and S.A. Liddelow, *An Overview of Astrocyte Responses in Genetically Induced Alzheimer's Disease Mouse Models*. Cells, 2020. **9**(11).
209. Guttenplan, K.A. and S.A. Liddelow, *Astrocytes and microglia: Models and tools*. Journal of Experimental Medicine, 2018. **216**(1): p. 71-83.
210. Heard, K.J., et al., *Chronic cortisol differentially impacts stem cell-derived astrocytes from major depressive disorder patients*. Translational Psychiatry, 2021. **11**(1): p. 608.
211. di Domenico, A., et al., *Patient-Specific iPSC-Derived Astrocytes Contribute to Non-Cell-Autonomous Neurodegeneration in Parkinson's Disease*. Stem Cell Reports, 2019. **12**(2): p. 213-229.
212. Szabo, A., et al., *A human iPSC-astroglia neurodevelopmental model reveals divergent transcriptomic patterns in schizophrenia*. Translational Psychiatry, 2021. **11**(1): p. 554.
213. Jones, V.C., et al., *Aberrant iPSC-derived human astrocytes in Alzheimer's disease*. Cell Death & Disease, 2017. **8**(3): p. e2696-e2696.
214. Perriot, S., et al., *Human Induced Pluripotent Stem Cell-Derived Astrocytes Are Differentially Activated by Multiple Sclerosis-Associated Cytokines*. Stem Cell Reports, 2018. **11**(5): p. 1199-1210.
215. Lanciotti, A., et al., *Human iPSC-Derived Astrocytes: A Powerful Tool to Study Primary Astrocyte Dysfunction in the Pathogenesis of Rare Leukodystrophies*. Int J Mol Sci, 2021. **23**(1).
216. Clayton, B.L.L., et al., *A phenotypic screening platform for identifying chemical modulators of astrocyte reactivity*. Nature Neuroscience, 2024. **27**(4): p. 656-665.
217. Cutler, A.J., et al., *Annual costs among patients with major depressive disorder and the impact of key clinical events*. J Manag Care Spec Pharm, 2022. **28**(12): p. 1335-1343.
218. Greenberg, P.E., et al., *The Economic Burden of Adults with Major Depressive Disorder in the United States (2010 and 2018)*. Pharmacoeconomics, 2021. **39**(6): p. 653-665.
219. Greenberg, P., et al., *The Economic Burden of Adults with Major Depressive Disorder in the United States (2019)*. Adv Ther, 2023. **40**(10): p. 4460-4479.
220. Vilhauer, J.S., et al., *Improving Quality of Life for Patients with Major Depressive Disorder by Increasing Hope and Positive Expectations with Future Directed Therapy (FDT)*. Innov Clin Neurosci, 2013. **10**(3): p. 12-22.
221. Iliou, K., et al., *Exploring the Effects of Major Depressive Disorder on Daily Occupations and the Impact of Psychotherapy: A Literature Review*. Cureus, 2024. **16**(3): p. e55831.
222. Kapfhammer, H.P., *Somatic symptoms in depression*. Dialogues Clin Neurosci, 2006. **8**(2): p. 227-39.
223. Kennedy, S.H., *Beyond Response: Aiming for Quality Remission in Depression*. Adv Ther, 2022. **39**(Suppl 1): p. 20-28.
224. Simon, G.E., N. Moise, and D.C. Mohr, *Management of Depression in Adults: A Review*. JAMA, 2024. **332**(2): p. 141-152.
225. Karrouri, R., et al., *Major depressive disorder: Validated treatments and future challenges*. World J Clin Cases, 2021. **9**(31): p. 9350-9367.
226. Toups, M., *Inflammation and Depression: the Neuroimmune Connection*. Curr Treat Options Psychiatry, 2018. **5**(4): p. 452-458.

227. Sforzini, L., et al., *A Delphi-method-based consensus guideline for definition of treatment-resistant depression for clinical trials*. *Molecular Psychiatry*, 2022. **27**(3): p. 1286-1299.
228. Zhdanova, M., et al., *Economic Burden of Treatment-Resistant Depression in Privately Insured U.S. Patients with Physical Conditions*. *Journal of Managed Care & Specialty Pharmacy*, 2020. **26**(8): p. 996-1007.
229. van Bronswijk, S.C., et al., *Precision medicine for long-term depression outcomes using the Personalized Advantage Index approach: cognitive therapy or interpersonal psychotherapy?* *Psychological Medicine*, 2021. **51**(2): p. 279-289.
230. Maslej, M.M., et al., *Individual Differences in Response to Antidepressants: A Meta-analysis of Placebo-Controlled Randomized Clinical Trials*. *JAMA Psychiatry*, 2021. **78**(5): p. 490-497.
231. *Variability in antidepressant response lower for SSRIs and in recent studies*. *The Brown University Psychopharmacology Update*, 2020. **31**(6): p. 1-6.
232. Haddad, P.M., et al., *Managing inadequate antidepressant response in depressive illness*. *British Medical Bulletin*, 2015. **115**(1): p. 183-201.
233. Corey-Lisle, P.K., et al., *Response, Partial Response, and Nonresponse in Primary Care Treatment of Depression*. *Archives of Internal Medicine*, 2004. **164**(11): p. 1197-1204.
234. *Tackling partial response to depression treatment*. *Prim Care Companion J Clin Psychiatry*, 2009. **11**(4): p. 155-62.
235. Jakubovski, E., et al., *Systematic Review and Meta-Analysis: Dose-Response Relationship of Selective Serotonin Reuptake Inhibitors in Major Depressive Disorder*. *Am J Psychiatry*, 2016. **173**(2): p. 174-83.
236. *Common genetic variation and antidepressant efficacy in major depressive disorder: a meta-analysis of three genome-wide pharmacogenetic studies*. *Am J Psychiatry*, 2013. **170**(2): p. 207-17.
237. Xu, Z., et al., *Targeted exome sequencing identifies five novel loci at genome-wide significance for modulating antidepressant response in patients with major depressive disorder*. *Translational Psychiatry*, 2020. **10**(1): p. 30.
238. Tansey, K.E., et al., *Contribution of Common Genetic Variants to Antidepressant Response*. *Biological Psychiatry*, 2013. **73**(7): p. 679-682.
239. Duman, R.S., et al., *Signaling pathways underlying the rapid antidepressant actions of ketamine*. *Neuropharmacology*, 2012. **62**(1): p. 35-41.
240. Targum, S.D., et al., *A novel peripheral biomarker for depression and antidepressant response*. *Molecular Psychiatry*, 2022. **27**(3): p. 1640-1646.
241. Chang, B., et al., *ARNet: Antidepressant Response Prediction Network for Major Depressive Disorder*. *Genes*, 2019. **10**(11): p. 907.
242. Ju, C., et al., *Integrated genome-wide methylation and expression analyses reveal functional predictors of response to antidepressants*. *Translational Psychiatry*, 2019. **9**(1): p. 254.
243. Taliáz, D., et al., *Optimizing prediction of response to antidepressant medications using machine learning and integrated genetic, clinical, and demographic data*. *Translational Psychiatry*, 2021. **11**(1): p. 381.
244. Hudock, A., et al., *Exploring mood disorders and treatment options using human stem cells*. *Genet Mol Biol*, 2024. **47Suppl 1**(Suppl 1): p. e20230305.

245. Avior, Y., et al., *Depression patient-derived cortical neurons reveal potential biomarkers for antidepressant response*. *Transl Psychiatry*, 2021. **11**(1): p. 201.
246. Vaz, A., et al., *Patient-derived induced pluripotent stem cells: Tools to advance the understanding and drug discovery in Major Depressive Disorder*. *Psychiatry Research*, 2024. **339**: p. 116033.
247. Cardon, I., et al., *Serotonin effects on human iPSC-derived neural cell functions: from mitochondria to depression*. *Molecular Psychiatry*, 2024. **29**(9): p. 2689-2700.
248. Vadodaria, K.C., et al., *Altered serotonergic circuitry in SSRI-resistant major depressive disorder patient-derived neurons*. *Mol Psychiatry*, 2019. **24**(6): p. 808-818.
249. Villafranco, J., et al., *The use of induced pluripotent stem cells as a platform for the study of depression*. *Frontiers in Psychiatry*, 2024. **15**.
250. Marcatili, M., et al., *Human induced pluripotent stem cells technology in treatment resistant depression: novel strategies and opportunities to unravel ketamine's fast-acting antidepressant mechanisms*. *Ther Adv Psychopharmacol*, 2020. **10**: p. 2045125320968331.
251. Zivko, C., et al., *iPSC-derived hindbrain organoids to evaluate escitalopram oxalate treatment responses targeting neuropsychiatric symptoms in Alzheimer's disease*. *Molecular Psychiatry*, 2024. **29**(11): p. 3644-3652.
252. Heard, K.J., et al., *Chronic cortisol differentially impacts stem cell-derived astrocytes from major depressive disorder patients*. *Transl Psychiatry*, 2021. **11**(1): p. 608.
253. Yao, J., et al., *A Review of Research on the Association between Neuron-Astrocyte Signaling Processes and Depressive Symptoms*. *Int J Mol Sci*, 2023. **24**(8).
254. Zhang, Y.M., et al., *Astrocyte metabolism and signaling pathways in the CNS*. *Front Neurosci*, 2023. **17**: p. 1217451.
255. Barcia, C., et al., *Imaging the microanatomy of astrocyte-T-cell interactions in immune-mediated inflammation*. *Frontiers in Cellular Neuroscience*, 2013. **7**.
256. Mrazek, D.A., et al., *Treatment Outcomes of Depression: The Pharmacogenomic Research Network Antidepressant Medication Pharmacogenomic Study*. *Journal of Clinical Psychopharmacology*, 2014. **34**(3): p. 313-317.
257. Rush, A.J., et al., *An evaluation of the quick inventory of depressive symptomatology and the hamilton rating scale for depression: a sequenced treatment alternatives to relieve depression trial report*. *Biol Psychiatry*, 2006. **59**(6): p. 493-501.
258. Vadodaria, K.C., et al., *Serotonin-induced hyperactivity in SSRI-resistant major depressive disorder patient-derived neurons*. *Molecular Psychiatry*, 2019. **24**(6): p. 795-807.
259. Canals, I., et al., *Rapid and efficient induction of functional astrocytes from human pluripotent stem cells*. *Nat Methods*, 2018. **15**(9): p. 693-696.
260. Wen, Z., et al., *Synaptic dysregulation in a human iPSC model of mental disorders*. *Nature*, 2014. **515**(7527): p. 414-418.
261. Bolger, A.M., M. Lohse, and B. Usadel, *Trimmomatic: a flexible trimmer for Illumina sequence data*. *Bioinformatics*, 2014. **30**(15): p. 2114-20.
262. Harrison, P.W., et al., *Ensembl 2024*. *Nucleic Acids Research*, 2023. **52**(D1): p. D891-D899.
263. Patro, R., et al., *Salmon provides fast and bias-aware quantification of transcript expression*. *Nat Methods*, 2017. **14**(4): p. 417-419.

264. Love, M.I., et al., *Tximeta: Reference sequence checksums for provenance identification in RNA-seq*. PLOS Computational Biology, 2020. **16**(2): p. e1007664.
265. Love, M.I., W. Huber, and S. Anders, *Moderated estimation of fold change and dispersion for RNA-seq data with DESeq2*. Genome Biol, 2014. **15**(12): p. 550.
266. Wickham, H., *ggplot2: Elegant Graphics for Data Analysis*. 2016, Springer-Verlag New York.
267. Yu, G., et al., *clusterProfiler: an R Package for Comparing Biological Themes Among Gene Clusters*. OMICS: A Journal of Integrative Biology, 2012. **16**(5): p. 284-287.
268. Wu, T., et al., *clusterProfiler 4.0: A universal enrichment tool for interpreting omics data*. The Innovation, 2021. **2**(3).
269. Xu, S., et al., *Using clusterProfiler to characterize multiomics data*. Nature Protocols, 2024. **19**(11): p. 3292-3320.
270. Yu, G., *Thirteen years of clusterProfiler*. The Innovation, 2024. **5**(6).
271. Bengtsson, H., *matrixStats: Functions that Apply to Rows and Columns of Matrices (and to Vectors)*. 2009.
272. Langfelder, P. and S. Horvath, *WGCNA: an R package for weighted correlation network analysis*. BMC Bioinformatics, 2008. **9**(1): p. 559.
273. Langfelder, P. and S. Horvath, *Fast R Functions for Robust Correlations and Hierarchical Clustering*. J Stat Softw, 2012. **46**(11).
274. Mootha, V.K., et al., *PGC-1 α -responsive genes involved in oxidative phosphorylation are coordinately downregulated in human diabetes*. Nature Genetics, 2003. **34**(3): p. 267-273.
275. Subramanian, A., et al., *Gene set enrichment analysis: A knowledge-based approach for interpreting genome-wide expression profiles*. Proceedings of the National Academy of Sciences, 2005. **102**(43): p. 15545-15550.
276. Yoon, S.B., et al., *Real-time PCR quantification of spliced X-box binding protein 1 (XBPI) using a universal primer method*. PLoS One, 2019. **14**(7): p. e0219978.
277. Livak, K.J. and T.D. Schmittgen, *Analysis of relative gene expression data using real-time quantitative PCR and the 2^{-Delta Delta C(T)} Method*. Methods, 2001. **25**(4): p. 402-8.
278. Kassambara, A., *ggpubr: 'ggplot2' Based Publication Ready Plots*. 2023.
279. Liska, O., et al., *TFLink: an integrated gateway to access transcription factor–target gene interactions for multiple species*. Database, 2022. **2022**.
280. Kolde, R., *pheatmap: Pretty Heatmaps*. 2018.
281. R Core Team, *R: A Language and Environment for Statistical Computing*. 2013, R Foundation for Statistical Computing.
282. Maechler, M., et al., *cluster: Cluster Analysis Basics and Extensions*. 2024.
283. Zohdy, Y.M., et al., *Complement inhibition targets a rich-club within the neuroinflammatory network after stroke to improve radiographic and functional outcomes*. J Neuroinflammation, 2025. **22**(1): p. 1.
284. Wickham, H., et al., *dplyr: A Grammar of Data Manipulation*. 2023.
285. Wickham, H., D. Vaughan, and M. Girlich, *tidyr: Tidy Messy Data*. 2024.
286. Wickham, H. and J. Bryan, *readxl: Read Excel Files*. 2023.
287. Rosen, D.A., et al., *Modulation of the sigma-1 receptor-IRE1 pathway is beneficial in preclinical models of inflammation and sepsis*. Sci Transl Med, 2019. **11**(478).

288. Alam, S., et al., *Sigmar1 regulates endoplasmic reticulum stress-induced C/EBP-homologous protein expression in cardiomyocytes*. Biosci Rep, 2017. **37**(4).
289. Wang, F.M., Y.J. Chen, and H.J. Ouyang, *Regulation of unfolded protein response modulator XBP1s by acetylation and deacetylation*. Biochem J, 2011. **433**(1): p. 245-52.
290. Prischi, F., et al., *Phosphoregulation of Ire1 RNase splicing activity*. Nature Communications, 2014. **5**(1): p. 3554.
291. Park, S.M., T.I. Kang, and J.S. So, *Roles of XBP1s in Transcriptional Regulation of Target Genes*. Biomedicines, 2021. **9**(7).
292. Ishikawa, T., et al., *Unfolded protein response transducer IRE1-mediated signaling independent of XBP1 mRNA splicing is not required for growth and development of medaka fish*. eLife, 2017. **6**: p. e26845.
293. Lee, K., et al., *IRE1-mediated unconventional mRNA splicing and S2P-mediated ATF6 cleavage merge to regulate XBP1 in signaling the unfolded protein response*. Genes Dev, 2002. **16**(4): p. 452-66.
294. Hayashi, T. and T.-P. Su, *Sigma-1 Receptor Chaperones at the ER- Mitochondrion Interface Regulate Ca²⁺ Signaling and Cell Survival*. Cell, 2007. **131**(3): p. 596-610.
295. Calton, M., et al., *IRE1 couples endoplasmic reticulum load to secretory capacity by processing the XBP-1 mRNA*. Nature, 2002. **415**(6867): p. 92-96.
296. Ajoolabady, A., et al., *ER stress and UPR in Alzheimer's disease: mechanisms, pathogenesis, treatments*. Cell Death & Disease, 2022. **13**(8): p. 706.
297. Smith, H.L., et al., *Astrocyte Unfolded Protein Response Induces a Specific Reactivity State that Causes Non-Cell-Autonomous Neuronal Degeneration*. Neuron, 2020. **105**(5): p. 855-866.e5.
298. Sims, S.G., et al., *The role of endoplasmic reticulum stress in astrocytes*. Glia, 2022. **70**(1): p. 5-19.
299. Maes, M., et al., *Depression and sickness behavior are Janus-faced responses to shared inflammatory pathways*. BMC Medicine, 2012. **10**(1): p. 66.
300. Min, X., et al., *Association between inflammatory cytokines and symptoms of major depressive disorder in adults*. Front Immunol, 2023. **14**: p. 1110775.
301. Haroon, E., C.L. Raison, and A.H. Miller, *Psychoneuroimmunology Meets Neuropsychopharmacology: Translational Implications of the Impact of Inflammation on Behavior*. Neuropsychopharmacology, 2012. **37**(1): p. 137-162.
302. Dantzer, R., et al., *From inflammation to sickness and depression: when the immune system subjugates the brain*. Nat Rev Neurosci, 2008. **9**(1): p. 46-56.
303. Liao, Y., et al., *Astrocytes in depression and Alzheimer's disease*. Front Med, 2021. **15**(6): p. 829-841.
304. Rodgers, K.R., et al., *Innate Immune Functions of Astrocytes are Dependent Upon Tumor Necrosis Factor-Alpha*. Scientific Reports, 2020. **10**(1): p. 7047.
305. Aten, S., et al., *Chronic Stress Impairs the Structure and Function of Astrocyte Networks in an Animal Model of Depression*. Neurochem Res, 2023. **48**(4): p. 1191-1210.
306. Novakovic, M.M., et al., *Astrocyte reactivity and inflammation-induced depression-like behaviors are regulated by Orai1 calcium channels*. Nature Communications, 2023. **14**(1): p. 5500.
307. Irwin, M., *Psychoneuroimmunology of depression: clinical implications*. Brain Behav Immun, 2002. **16**(1): p. 1-16.

308. Roman, M. and M.R. Irwin, *Novel neuroimmunologic therapeutics in depression: A clinical perspective on what we know so far*. *Brain Behav Immun*, 2020. **83**: p. 7-21.
309. Richardson, B., A. MacPherson, and F. Bambico, *Neuroinflammation and neuroprogression in depression: Effects of alternative drug treatments*. *Brain Behav Immun Health*, 2022. **26**: p. 100554.
310. Beckett, C.W. and M.V. Niklison-Chirou, *The role of immunomodulators in treatment-resistant depression: case studies*. *Cell Death Discovery*, 2022. **8**(1): p. 367.
311. Chan, V.K.Y., et al., *Treatment-resistant depression and risk of autoimmune diseases: evidence from a population-based cohort and nested case-control study*. *Translational Psychiatry*, 2023. **13**(1): p. 76.
312. Mancuso, E., et al., *Biological correlates of treatment resistant depression: a review of peripheral biomarkers*. *Frontiers in Psychiatry*, 2023. **14**.
313. Strawbridge, R., et al., *Inflammatory profiles of severe treatment-resistant depression*. *J Affect Disord*, 2019. **246**: p. 42-51.
314. Koo, J.W., et al., *Nuclear factor-kappaB is a critical mediator of stress-impaired neurogenesis and depressive behavior*. *Proc Natl Acad Sci U S A*, 2010. **107**(6): p. 2669-74.
315. Kimelberg, H.K. and D.M. Katz, *High-affinity uptake of serotonin into immunocytochemically identified astrocytes*. *Science*, 1985. **228**(4701): p. 889-91.
316. Anderson, E.J., D. McFarland, and H.K. Kimelberg, *Serotonin uptake by astrocytes in situ*. *Glia*, 1992. **6**(2): p. 154-8.
317. Blanco, I. and K. Conant, *Extracellular matrix remodeling with stress and depression: Studies in human, rodent and zebrafish models*. *Eur J Neurosci*, 2021. **53**(12): p. 3879-3888.
318. Cathomas, F., et al., *Circulating myeloid-derived MMP8 in stress susceptibility and depression*. *Nature*, 2024. **626**(8001): p. 1108-1115.
319. Soles, A., et al., *Extracellular Matrix Regulation in Physiology and in Brain Disease*. *Int J Mol Sci*, 2023. **24**(8).
320. Wheeler, M.A., et al., *Environmental Control of Astrocyte Pathogenic Activities in CNS Inflammation*. *Cell*, 2019. **176**(3): p. 581-596.e18.
321. Chen, L., et al., *Mesencephalic Astrocyte-Derived Neurotrophic Factor Is Involved in Inflammation by Negatively Regulating the NF- κ B Pathway*. *Scientific Reports*, 2015. **5**(1): p. 8133.
322. Van den Eynde, V., et al., *The prescriber's guide to classic MAO inhibitors (phenelzine, tranylcypromine, isocarboxazid) for treatment-resistant depression*. *CNS Spectr*, 2023. **28**(4): p. 427-440.
323. Köhler, O., et al., *Effect of Anti-inflammatory Treatment on Depression, Depressive Symptoms, and Adverse Effects: A Systematic Review and Meta-analysis of Randomized Clinical Trials*. *JAMA Psychiatry*, 2014. **71**(12): p. 1381-1391.
324. Covington, H.E., 3rd, et al., *Antidepressant actions of histone deacetylase inhibitors*. *J Neurosci*, 2009. **29**(37): p. 11451-60.
325. Hou, L. and E. Klann, *Activation of the Phosphoinositide 3-Kinase-Akt-Mammalian Target of Rapamycin Signaling Pathway Is Required for Metabotropic Glutamate Receptor-Dependent Long-Term Depression*. *The Journal of Neuroscience*, 2004. **24**(28): p. 6352-6361.

326. Nagayama, H., J.N. Hingtgen, and M.H. Aprison, *Postsynaptic action by four antidepressive drugs in an animal model of depression*. *Pharmacol Biochem Behav*, 1981. **15**(1): p. 125-30.
327. Valic, M., et al., *Intermittent hypercapnia-induced phrenic long-term depression is revealed after serotonin receptor blockade with methysergide in anaesthetized rats*. *Exp Physiol*, 2016. **101**(2): p. 319-31.
328. Arciniegas Ruiz, S.M. and H. Eldar-Finkelman, *Glycogen Synthase Kinase-3 Inhibitors: Preclinical and Clinical Focus on CNS-A Decade Onward*. *Frontiers in Molecular Neuroscience*, 2022. **14**.
329. Parekh, A., et al., *The Role of Lipid Biomarkers in Major Depression*. *Healthcare (Basel)*, 2017. **5**(1).
330. Głombik, K., et al., *Changes in regulators of lipid metabolism in the brain: a study of animal models of depression and hypothyroidism*. *Pharmacol Rep*, 2022. **74**(5): p. 859-870.
331. Duda, P., et al., *GSK3 β : A Master Player in Depressive Disorder Pathogenesis and Treatment Responsiveness*. *Cells*, 2020. **9**(3).
332. Jope, R.S., *Glycogen Synthase Kinase-3 in the Etiology and Treatment of Mood Disorders*. *Frontiers in Molecular Neuroscience*, 2011. **4**.
333. Yeo, M., et al., *Repurposing cancer drugs identifies kenpaullone which ameliorates pathologic pain in preclinical models via normalization of inhibitory neurotransmission*. *Nature Communications*, 2021. **12**(1): p. 6208.
334. *2024 Alzheimer's disease facts and figures*. *Alzheimer's & Dementia*, 2024. **20**(5): p. 3708-3821.
335. Beshir, S.A., et al., *Aducanumab Therapy to Treat Alzheimer's Disease: A Narrative Review*. *Int J Alzheimers Dis*, 2022. **2022**: p. 9343514.
336. van Dyck, C.H., et al., *Lecanemab in Early Alzheimer's Disease*. *N Engl J Med*, 2023. **388**(1): p. 9-21.
337. Sevigny, J., et al., *The antibody aducanumab reduces A β plaques in Alzheimer's disease*. *Nature*, 2016. **537**(7618): p. 50-56.
338. Sims, J.R., et al., *Donanemab in Early Symptomatic Alzheimer Disease: The TRAILBLAZER-ALZ 2 Randomized Clinical Trial*. *JAMA*, 2023. **330**(6): p. 512-527.
339. *A Placebo-Controlled, Double-Blind, Parallel-Group, 18-Month Study With an Open-Label Extension Phase to Confirm Safety and Efficacy of BAN2401 in Subjects With Early Alzheimer's Disease*, Biogen, Editor. 2019.
340. *Assessment of Safety, Tolerability, and Efficacy of Donanemab in Early Symptomatic Alzheimer's Disease*. 2020.
341. Carter, S.F., et al., *Astrocyte Biomarkers in Alzheimer's Disease*. *Trends in Molecular Medicine*, 2019. **25**(2): p. 77-95.
342. Rodríguez-Giraldo, M., et al., *Astrocytes as a Therapeutic Target in Alzheimer's Disease-Comprehensive Review and Recent Developments*. *Int J Mol Sci*, 2022. **23**(21).
343. Verkhratsky, A., et al., *Astrocytes in Alzheimer's Disease*. *Neurotherapeutics*, 2010. **7**(4): p. 399-412.
344. Takahashi, K., et al., *Restored glial glutamate transporter EAAT2 function as a potential therapeutic approach for Alzheimer's disease*. *J Exp Med*, 2015. **212**(3): p. 319-32.
345. Gorshkov, K., et al., *Astrocytes as targets for drug discovery*. *Drug Discov Today*, 2018. **23**(3): p. 673-680.

346. Katafuchi, T. and M. Noda, *Dysfunction of Glial Cells in Neurological and Psychological Disorders: From Bench to Bedside*. Advances in Neuroimmune Biology, 2016. **6**: p. 59-60.
347. Rempe, D.A. and M. Nedergaard, *Targeting Glia for Treatment of Neurological Disease*. Neurotherapeutics, 2010. **7**(4): p. 335-337.
348. Toral-Rios, D., et al., *Activation of STAT3 Regulates Reactive Astroglialosis and Neuronal Death Induced by A β O Neurotoxicity*. Int J Mol Sci, 2020. **21**(20).
349. Reichenbach, N., et al., *Inhibition of Stat3-mediated astroglialosis ameliorates pathology in an Alzheimer's disease model*. EMBO Mol Med, 2019. **11**(2).
350. Ceyzériat, K., et al., *Modulation of astrocyte reactivity improves functional deficits in mouse models of Alzheimer's disease*. Acta Neuropathol Commun, 2018. **6**(1): p. 104.
351. Yu, W., et al., *Disease-Associated Neurotoxic Astrocyte Markers in Alzheimer Disease Based on Integrative Single-Nucleus RNA Sequencing*. Cellular and Molecular Neurobiology, 2024. **44**(1): p. 20.
352. Galea, E., et al., *Multi-transcriptomic analysis points to early organelle dysfunction in human astrocytes in Alzheimer's disease*. Neurobiol Dis, 2022. **166**: p. 105655.
353. Serrano-Pozo, A., et al., *A brain atlas of astrocyte transcriptomics unveils complex states and responses to Alzheimer's disease neuropathology*. Alzheimer's & Dementia, 2022. **18**(S4): p. e060866.
354. Xia, Q., et al., *Phosphoproteomic Analysis of Human Brain by Calcium Phosphate Precipitation and Mass Spectrometry*. Journal of Proteome Research, 2008. **7**(7): p. 2845-2851.
355. Ping, L., et al., *Global quantitative analysis of the human brain proteome and phosphoproteome in Alzheimer's disease*. Scientific Data, 2020. **7**(1): p. 315.
356. Dammer, E.B., et al., *Quantitative phosphoproteomics of Alzheimer's disease reveals cross-talk between kinases and small heat shock proteins*. Proteomics, 2015. **15**(2-3): p. 508-519.
357. Herskowitz, J.H., et al., *Phosphoproteomic Analysis Reveals Site-Specific Changes in GFAP and NDRG2 Phosphorylation in Frontotemporal Lobar Degeneration*. Journal of Proteome Research, 2010. **9**(12): p. 6368-6379.
358. D'Argenio, V. and D. Sarnataro, *New Insights into the Molecular Bases of Familial Alzheimer's Disease*. J Pers Med, 2020. **10**(2).
359. Kuehner, J.N., et al., *5-hydroxymethylcytosine is dynamically regulated during forebrain organoid development and aberrantly altered in Alzheimer's disease*. Cell Reports, 2021. **35**(4).
360. Bray, N.L., et al., *Near-optimal probabilistic RNA-seq quantification*. Nature Biotechnology, 2016. **34**(5): p. 525-527.
361. Soneson, C., M. Love, and M. Robinson, *Differential analyses for RNA-seq: transcript-level estimates improve gene-level inferences [version 1; peer review: 2 approved]*. F1000Research, 2015. **4**(1521).
362. Robinson, M.D., D.J. McCarthy, and G.K. Smyth, *edgeR: a Bioconductor package for differential expression analysis of digital gene expression data*. Bioinformatics, 2010. **26**(1): p. 139-40.
363. Rangaraju, S., et al., *Identification and therapeutic modulation of a pro-inflammatory subset of disease-associated-microglia in Alzheimer's disease*. Molecular Neurodegeneration, 2018. **13**(1): p. 24.

364. Ryan, W., *willgryan/3PodR_bookdown: Pre-release for Zenodo DOI*. 2023.
365. Ryan, V.W., et al., *Interpreting and visualizing pathway analyses using embedding representations with PAVER*. *Bioinformatics*, 2024. **20**(7): p. 700-704.
366. Consortium, T.G.O., et al., *The Gene Ontology knowledgebase in 2023*. *Genetics*, 2023. **224**(1).
367. Ashburner, M., et al., *Gene Ontology: tool for the unification of biology*. *Nature Genetics*, 2000. **25**(1): p. 25-29.
368. Szklarczyk, D., et al., *The STRING database in 2023: protein-protein association networks and functional enrichment analyses for any sequenced genome of interest*. *Nucleic Acids Res*, 2023. **51**(D1): p. D638-d646.
369. Csárdi, G. and T. Nepusz. *The igraph software package for complex network research*. 2006.
370. Badia-i-Mompel, P., et al., *decoupleR: ensemble of computational methods to infer biological activities from omics data*. *Bioinformatics Advances*, 2022. **2**(1).
371. Müller-Dott, S., et al., *Expanding the coverage of regulons from high-confidence prior knowledge for accurate estimation of transcription factor activities*. *Nucleic Acids Research*, 2023. **51**(20): p. 10934-10949.
372. Subramanian, A., et al., *A Next Generation Connectivity Map: L1000 Platform and the First 1,000,000 Profiles*. *Cell*, 2017. **171**(6): p. 1437-1452.e17.
373. Lamb, J., et al., *The Connectivity Map: using gene-expression signatures to connect small molecules, genes, and disease*. *Science*, 2006. **313**(5795): p. 1929-35.
374. Goshi, N., et al., *Direct effects of prolonged TNF- α and IL-6 exposure on neural activity in human iPSC-derived neuron-astrocyte co-cultures*. *Frontiers in Cellular Neuroscience*, 2025. **19**.
375. Han, X., et al., *Serpina3N Regulates the Secretory Phenotype of Mouse Senescent Astrocytes Contributing to Neurodegeneration*. *The Journals of Gerontology: Series A*, 2024. **79**(4).
376. Liu, C., et al., *Astrocyte-derived SerpinA3N promotes neuroinflammation and epileptic seizures by activating the NF- κ B signaling pathway in mice with temporal lobe epilepsy*. *J Neuroinflammation*, 2023. **20**(1): p. 161.
377. Vanni, S., et al., *Differential overexpression of SERPINA3 in human prion diseases*. *Scientific Reports*, 2017. **7**(1): p. 15637.
378. Fissolo, N., et al., *CSF SERPINA3 Levels Are Elevated in Patients With Progressive MS*. *Neurology Neuroimmunology & Neuroinflammation*, 2021. **8**(2): p. e941.
379. Zattoni, M., et al., *Serpin Signatures in Prion and Alzheimer's Diseases*. *Molecular Neurobiology*, 2022. **59**(6): p. 3778-3799.
380. Haddick, P.C., et al., *A Common Variant of IL-6R is Associated with Elevated IL-6 Pathway Activity in Alzheimer's Disease Brains*. *J Alzheimers Dis*, 2017. **56**(3): p. 1037-1054.
381. Quillen, D., et al., *Levels of Soluble Interleukin 6 Receptor and Asp358Ala Are Associated With Cognitive Performance and Alzheimer Disease Biomarkers*. *Neurology Neuroimmunology & Neuroinflammation*, 2023. **10**(3): p. e200095.
382. Zettergren, A., et al., *Association of IL1RAP-related genetic variation with cerebrospinal fluid concentration of Alzheimer-associated tau protein*. *Sci Rep*, 2019. **9**(1): p. 2460.

383. Ramanan, V.K., et al., *GWAS of longitudinal amyloid accumulation on 18F-florbetapir PET in Alzheimer's disease implicates microglial activation gene IL1RAP*. *Brain*, 2015. **138**(Pt 10): p. 3076-88.
384. Jin, S., et al., *Inhibition of GPR17 with cangrelor improves cognitive impairment and synaptic deficits induced by A β (1-42) through Nrf2/HO-1 and NF- κ B signaling pathway in mice*. *Int Immunopharmacol*, 2021. **101**(Pt B): p. 108335.
385. Liang, Y., et al., *Knockdown and inhibition of hippocampal GPR17 attenuates lipopolysaccharide-induced cognitive impairment in mice*. *J Neuroinflammation*, 2023. **20**(1): p. 271.
386. Tansey, K.E., D. Cameron, and M.J. Hill, *Genetic risk for Alzheimer's disease is concentrated in specific macrophage and microglial transcriptional networks*. *Genome Med*, 2018. **10**(1): p. 14.
387. Salih, D.A., et al., *Genetic variability in response to amyloid beta deposition influences Alzheimer's disease risk*. *Brain Commun*, 2019. **1**(1): p. fcz022.
388. Miyashita, A., et al., *SORL1 is genetically associated with late-onset Alzheimer's disease in Japanese, Koreans and Caucasians*. *PLoS One*, 2013. **8**(4): p. e58618.
389. Krus, K.L., et al., *Reduced STMN2 and pathogenic TDP-43, two hallmarks of ALS, synergize to accelerate motor decline in mice*. *bioRxiv*, 2024.
390. Cheng, X.S., et al., *Nmnat2 attenuates Tau phosphorylation through activation of PP2A*. *J Alzheimers Dis*, 2013. **36**(1): p. 185-95.
391. Cheng, X.S., et al., *Nmnat2 attenuates amyloidogenesis and up-regulates ADAM10 in AMPK activity-dependent manner*. *Aging (Albany NY)*, 2021. **13**(20): p. 23620-23636.
392. Liddelow, S.A., et al., *Neurotoxic reactive astrocytes are induced by activated microglia*. *Nature*, 2017. **541**(7638): p. 481-487.
393. Akiyama, H., et al., *Inflammation and Alzheimer's disease*. *Neurobiol Aging*, 2000. **21**(3): p. 383-421.
394. Kim, H., et al., *Reactive astrocytes transduce inflammation in a blood-brain barrier model through a TNF-STAT3 signaling axis and secretion of alpha 1-antichymotrypsin*. *Nature Communications*, 2022. **13**(1): p. 6581.
395. Choi, M., et al., *Inhibition of STAT3 phosphorylation attenuates impairments in learning and memory in 5XFAD mice, an animal model of Alzheimer's disease*. *Journal of Pharmacological Sciences*, 2020. **143**(4): p. 290-299.
396. Ben Haim, L., et al., *The JAK/STAT3 Pathway Is a Common Inducer of Astrocyte Reactivity in Alzheimer's and Huntington's Diseases*. *The Journal of Neuroscience*, 2015. **35**(6): p. 2817-2829.
397. Ceyzériat, K., et al., *Modulation of astrocyte reactivity improves functional deficits in mouse models of Alzheimer's disease*. *Acta Neuropathologica Communications*, 2018. **6**(1): p. 104.
398. Zhou, Q. and L. Xu, *The regulation of BAI1 in astrocytes through the STAT3/EZH2 axis relieves neuronal apoptosis in rats with Alzheimer's disease*. *Brain Research*, 2024. **1839**: p. 149007.
399. Mehla, J., et al., *STAT3 inhibitor mitigates cerebral amyloid angiopathy and parenchymal amyloid plaques while improving cognitive functions and brain networks*. *Acta Neuropathologica Communications*, 2021. **9**(1): p. 193.
400. Morabito, S., et al., *Single-nucleus chromatin accessibility and transcriptomic characterization of Alzheimer's disease*. *Nat Genet*, 2021. **53**(8): p. 1143-1155.

401. Mohamed, A., et al., *A β inhibits SREBP-2 activation through Akt inhibition*. J Lipid Res, 2018. **59**(1): p. 1-13.
402. Xu, X., et al., *YAP prevents premature senescence of astrocytes and cognitive decline of Alzheimer's disease through regulating CDK6 signaling*. Aging Cell, 2021. **20**(9): p. e13465.
403. Xu, J., et al., *Multimodal single-cell/nucleus RNA sequencing data analysis uncovers molecular networks between disease-associated microglia and astrocytes with implications for drug repurposing in Alzheimer's disease*. Genome Res, 2021. **31**(10): p. 1900-1912.
404. Lehrer, S. and P.H. Rheinstein, *Alzheimer's Disease and Intranasal Fluticasone Propionate in the FDA MedWatch Adverse Events Database*. Journal of Alzheimer's Disease Reports, 2018. **2**: p. 111-115.
405. Zang, C., et al., *High-throughput target trial emulation for Alzheimer's disease drug repurposing with real-world data*. Nature Communications, 2023. **14**(1): p. 8180.
406. Yang, C.-C., et al., *Lipopolysaccharide-Induced Matrix Metalloproteinase-9 Expression Associated with Cell Migration in Rat Brain Astrocytes*. International Journal of Molecular Sciences, 2020. **21**(1): p. 259.
407. WOODS, Y.L., et al., *The kinase DYRK phosphorylates protein-synthesis initiation factor eIF2B ϵ at Ser539 and the microtubule-associated protein tau at Thr212: potential role for DYRK as a glycogen synthase kinase 3-priming kinase*. Biochemical Journal, 2001. **355**(3): p. 609-615.
408. Sayas, C.L. and J. Ávila, *GSK-3 and Tau: A Key Duet in Alzheimer's Disease*. Cells, 2021. **10**(4): p. 721.
409. Saha, P., S. Guha, and S.C. Biswas, *P38K and JNK pathways are induced by amyloid- β in astrocyte: Implication of MAPK pathways in astrogliosis in Alzheimer's disease*. Molecular and Cellular Neuroscience, 2020. **108**: p. 103551.
410. Webster, B., et al., *Astroglial Activation of Extracellular-Regulated Kinase in Early Stages of Alzheimer Disease*. Journal of Neuropathology & Experimental Neurology, 2006. **65**(2): p. 142-151.
411. Heneka, M.T., et al., *Neuroinflammation in Alzheimer's disease*. Lancet Neurol, 2015. **14**(4): p. 388-405.
412. Calsolaro, V. and P. Edison, *Neuroinflammation in Alzheimer's disease: Current evidence and future directions*. Alzheimers Dement, 2016. **12**(6): p. 719-32.
413. National Institute of Mental Health. *Major Depression*. 2023 February 5, 2025]; Available from: <https://www.nimh.nih.gov/health/statistics/major-depression>.
414. World Health Organization. *Depression Fact Sheet*. 2023 February 5, 2025]; Available from: <https://www.who.int/news-room/fact-sheets/detail/depression>.
415. *Global prevalence and burden of depressive and anxiety disorders in 204 countries and territories in 2020 due to the COVID-19 pandemic*. Lancet, 2021. **398**(10312): p. 1700-1712.
416. Hasin, D.S., et al., *Epidemiology of Adult DSM-5 Major Depressive Disorder and Its Specifiers in the United States*. JAMA Psychiatry, 2018. **75**(4): p. 336-346.
417. Gutiérrez-Rojas, L., et al., *Prevalence and correlates of major depressive disorder: a systematic review*. Braz J Psychiatry, 2020. **42**(6): p. 657-672.
418. Kessler, R.C., et al., *The Epidemiology of Major Depressive Disorder Results From the National Comorbidity Survey Replication (NCS-R)*. JAMA, 2003. **289**(23): p. 3095-3105.

419. Lim, G.Y., et al., *Prevalence of Depression in the Community from 30 Countries between 1994 and 2014*. Scientific Reports, 2018. **8**(1): p. 2861.
420. Tahami Monfared, A.A., et al., *Alzheimer's Disease: Epidemiology and Clinical Progression*. Neurol Ther, 2022. **11**(2): p. 553-569.
421. Mega, M.S., et al., *The spectrum of behavioral changes in Alzheimer's disease*. Neurology, 1996. **46**(1): p. 130-135.
422. Özge, A., et al., *Predictive factors for Alzheimer's disease progression: a comprehensive retrospective analysis of 3,553 cases with 211 months follow-up*. Frontiers in Neurology, 2023. **14**.
423. Selkoe, D.J. and J. Hardy, *The amyloid hypothesis of Alzheimer's disease at 25 years*. EMBO Mol Med, 2016. **8**(6): p. 595-608.
424. Skaria, A.P., *The economic and societal burden of Alzheimer disease: managed care considerations*. Am J Manag Care, 2022. **28**(10 Suppl): p. S188-s196.
425. Lanctôt, K.L., et al., *Burden of Illness in People with Alzheimer's Disease: A Systematic Review of Epidemiology, Comorbidities and Mortality*. J Prev Alzheimers Dis, 2024. **11**(1): p. 97-107.
426. Nandi, A., et al., *Cost of care for Alzheimer's disease and related dementias in the United States: 2016 to 2060*. NPJ Aging, 2024. **10**(1): p. 13.
427. Frederiksen, K.S., et al., *A Literature Review on the Burden of Alzheimer's Disease on Care Partners*. Journal of Alzheimer's Disease, 2023. **96**(3): p. 947-966.
428. Avitan, I., et al., *Towards a Consensus on Alzheimer's Disease Comorbidity?* J Clin Med, 2021. **10**(19).
429. Muliya, K.P. and M. Varghese, *The complex relationship between depression and dementia*. Ann Indian Acad Neurol, 2010. **13**(Suppl 2): p. S69-73.
430. Yin, J., A. John, and D. Cadar, *Bidirectional Associations of Depressive Symptoms and Cognitive Function Over Time*. JAMA Network Open, 2024. **7**(6): p. e2416305-e2416305.
431. Padovani, A., et al., *Exploring depression in Alzheimer's disease: an Italian Delphi Consensus on phenomenology, diagnosis, and management*. Neurol Sci, 2023. **44**(12): p. 4323-4332.
432. Li, X., W. Su, and L. Cai, *A bibliometric analysis of research on dementia comorbid with depression from 2005 to 2024*. Frontiers in Neuroscience, 2025. **19**.
433. Asmer, M.S., et al., *Meta-Analysis of the Prevalence of Major Depressive Disorder Among Older Adults With Dementia*. J Clin Psychiatry, 2018. **79**(5).
434. Watt, J.A., et al., *Comparative efficacy of interventions for reducing symptoms of depression in people with dementia: systematic review and network meta-analysis*. BMJ, 2021. **372**: p. n532.
435. Cantón-Habas, V., et al., *Depression as a Risk Factor for Dementia and Alzheimer's Disease*. Biomedicines, 2020. **8**(11).
436. Brenowitz, W.D., et al., *Depressive Symptoms Imputed Across the Life Course Are Associated with Cognitive Impairment and Cognitive Decline*. J Alzheimers Dis, 2021. **83**(3): p. 1379-1389.
437. Burke, A.D., et al., *Diagnosing and Treating Depression in Patients with Alzheimer's Disease*. Neurol Ther, 2019. **8**(2): p. 325-350.
438. Cassano, T., et al., *Pharmacological Treatment of Depression in Alzheimer's Disease: A Challenging Task*. Front Pharmacol, 2019. **10**: p. 1067.

439. Holmquist, S., A. Nordström, and P. Nordström, *The association of depression with subsequent dementia diagnosis: A Swedish nationwide cohort study from 1964 to 2016*. PLOS Medicine, 2020. **17**(1): p. e1003016.
440. Johansson, L., et al., *Associations between Depression, Depressive Symptoms, and Incidence of Dementia in Latin America: A 10/66 Dementia Research Group Study*. J Alzheimers Dis, 2019. **69**(2): p. 433-441.
441. Kitching, D., *Depression in dementia*. Aust Prescr, 2015. **38**(6): p. 209-2011.
442. Yu, O.-C., et al., *Association between dementia and depression: a retrospective study using the Korean National Health Insurance Service-National Sample Cohort database*. BMJ Open, 2020. **10**(10): p. e034924.
443. Hakim, A., *Perspectives on the complex links between depression and dementia*. Frontiers in Aging Neuroscience, 2022. **14**.
444. Rapp, M.A., et al., *Cognitive decline in patients with dementia as a function of depression*. Am J Geriatr Psychiatry, 2011. **19**(4): p. 357-63.
445. Singh-Manoux, A., et al., *Trajectories of Depressive Symptoms Before Diagnosis of Dementia: A 28-Year Follow-up Study*. JAMA Psychiatry, 2017. **74**(7): p. 712-718.
446. Mirza, S.S., et al., *10-year trajectories of depressive symptoms and risk of dementia: a population-based study*. The Lancet Psychiatry, 2016. **3**(7): p. 628-635.
447. Barnes, D.E., et al., *Midlife vs Late-Life Depressive Symptoms and Risk of Dementia: Differential Effects for Alzheimer Disease and Vascular Dementia*. Archives of General Psychiatry, 2012. **69**(5): p. 493-498.
448. Zhao, Y., et al., *Astrocyte-Mediated Neuroinflammation in Neurological Conditions*. Biomolecules, 2024. **14**(10): p. 1204.
449. Rueda-Carrasco, J., et al., *SFRP1 modulates astrocyte-to-microglia crosstalk in acute and chronic neuroinflammation*. EMBO reports, 2021. **22**(11): p. e51696.
450. Priego, N. and M. Valiente, *The Potential of Astrocytes as Immune Modulators in Brain Tumors*. Frontiers in Immunology, 2019. **10**.
451. Santiago-Balmaseda, A., et al., *Neurodegenerative Diseases: Unraveling the Heterogeneity of Astrocytes*. Cells, 2024. **13**(11): p. 921.
452. Lee, H.G., M.A. Wheeler, and F.J. Quintana, *Function and therapeutic value of astrocytes in neurological diseases*. Nat Rev Drug Discov, 2022. **21**(5): p. 339-358.
453. Pathak, D. and K. Sriram, *Neuron-astrocyte omnidirectional signaling in neurological health and disease*. Frontiers in Molecular Neuroscience, 2023. **16**.
454. Fernandez Tde, S., C. de Souza Fernandez, and A.L. Mencalha, *Human induced pluripotent stem cells from basic research to potential clinical applications in cancer*. Biomed Res Int, 2013. **2013**: p. 430290.
455. Chamberlain, S.J., *Disease modelling using human iPSCs*. Human Molecular Genetics, 2016. **25**(R2): p. R173-R181.
456. Liu, C., et al., *Modeling human diseases with induced pluripotent stem cells: from 2D to 3D and beyond*. Development, 2018. **145**(5).
457. Chandrasekaran, A., et al., *Astrocyte Differentiation of Human Pluripotent Stem Cells: New Tools for Neurological Disorder Research*. Frontiers in Cellular Neuroscience, 2016. **10**.
458. Deng, B., *Mouse models and induced pluripotent stem cells in researching psychiatric disorders*. Stem Cell Investig, 2017. **4**: p. 62.

459. Kim, S.H. and M.Y. Chang, *Application of Human Brain Organoids-Opportunities and Challenges in Modeling Human Brain Development and Neurodevelopmental Diseases*. Int J Mol Sci, 2023. **24**(15).
460. Lee, C.-T., et al., *3D brain Organoids derived from pluripotent stem cells: promising experimental models for brain development and neurodegenerative disorders*. Journal of Biomedical Science, 2017. **24**(1): p. 59.
461. Luciani, M., A. Gritti, and V. Meneghini, *Human iPSC-Based Models for the Development of Therapeutics Targeting Neurodegenerative Lysosomal Storage Diseases*. Frontiers in Molecular Biosciences, 2020. **7**.
462. Rouhani, F., et al., *Genetic Background Drives Transcriptional Variation in Human Induced Pluripotent Stem Cells*. PLOS Genetics, 2014. **10**(6): p. e1004432.
463. Kim, K., et al., *Epigenetic memory in induced pluripotent stem cells*. Nature, 2010. **467**(7313): p. 285-90.
464. Cardon, I., et al., *Serotonin effects on human iPSC-derived neural cell functions: from mitochondria to depression*. Mol Psychiatry, 2024. **29**(9): p. 2689-2700.
465. Supakul, S., et al., *Mutual interaction of neurons and astrocytes derived from iPSCs with APP V717L mutation developed the astrocytic phenotypes of Alzheimer's disease*. Inflamm Regen, 2024. **44**(1): p. 8.
466. Brezovakova, V., E. Sykova, and S. Jadhav, *Astrocytes Derived from Familial and Sporadic Alzheimer's Disease iPSCs Show Altered Calcium Signaling and Respond Differently to Misfolded Protein Tau*. Cells, 2022. **11**(9).
467. Ritchie, M.E., et al., *limma powers differential expression analyses for RNA-sequencing and microarray studies*. Nucleic Acids Research, 2015. **43**(7): p. e47-e47.
468. Law, C.W., et al., *voom: precision weights unlock linear model analysis tools for RNA-seq read counts*. Genome Biology, 2014. **15**(2): p. R29.
469. Alboukadel Kassambara, F.M., *factoextra: Extract and Visualize the Results of Multivariate Data Analyses*. 2020.
470. Conway, J.R., A. Lex, and N. Gehlenborg, *UpSetR: an R package for the visualization of intersecting sets and their properties*. Bioinformatics, 2017. **33**(18): p. 2938-2940.
471. Chen, H. and P.C. Boutros, *VennDiagram: a package for the generation of highly-customizable Venn and Euler diagrams in R*. BMC Bioinformatics, 2011. **12**(1): p. 35.
472. Lachmann, A. and A. Ma'ayan, *KEA: kinase enrichment analysis*. Bioinformatics, 2009. **25**(5): p. 684-6.
473. Keenan, A.B., et al., *The Library of Integrated Network-Based Cellular Signatures NIH Program: System-Level Cataloging of Human Cells Response to Perturbations*. Cell Syst, 2018. **6**(1): p. 13-24.
474. Tewari, B.P., et al., *A glial perspective on the extracellular matrix and perineuronal net remodeling in the central nervous system*. Frontiers in Cellular Neuroscience, 2022. **16**.
475. Chiareli, R.A., et al., *The Role of Astrocytes in the Neurorepair Process*. Front Cell Dev Biol, 2021. **9**: p. 665795.
476. Jones, E.V. and D.S. Bouvier, *Astrocyte-secreted matricellular proteins in CNS remodelling during development and disease*. Neural Plast, 2014. **2014**: p. 321209.
477. Li, M., et al., *Microvascular and cellular dysfunctions in Alzheimer's disease: an integrative analysis perspective*. Scientific Reports, 2024. **14**(1): p. 20944.

478. Jacobson, K.R. and H. Song, *Changes in the Extracellular Matrix with Aging: A Larger Role in Alzheimer's Disease*. The Journal of Neuroscience, 2024. **44**(22): p. e0081242024.
479. Sun, Y., et al., *Role of the Extracellular Matrix in Alzheimer's Disease*. Front Aging Neurosci, 2021. **13**: p. 707466.
480. Kim, S., et al., *Upregulation of extracellular proteins in a mouse model of Alzheimer's disease*. Scientific Reports, 2023. **13**(1): p. 6998.
481. Anwar, M.M., E. Özkan, and Y. Gürsoy-Özdemir, *The role of extracellular matrix alterations in mediating astrocyte damage and pericyte dysfunction in Alzheimer's disease: A comprehensive review*. Eur J Neurosci, 2022. **56**(9): p. 5453-5475.
482. Yang, L., et al., *Affective Immunology: The Crosstalk Between Microglia and Astrocytes Plays Key Role?* Frontiers in Immunology, 2020. **11**.
483. Morales, I., et al., *Neuroinflammation in the pathogenesis of Alzheimer's disease. A rational framework for the search of novel therapeutic approaches*. Frontiers in Cellular Neuroscience, 2014. **8**.
484. Wingo, T.S., et al., *Shared mechanisms across the major psychiatric and neurodegenerative diseases*. Nature Communications, 2022. **13**(1): p. 4314.
485. Zhong, S., et al., *BMP8B Activates Both SMAD2/3 and NF- κ B Signals to Inhibit the Differentiation of 3T3-L1 Preadipocytes into Mature Adipocytes*. Nutrients, 2023. **16**(1).
486. Mabie, P.C., et al., *Bone Morphogenetic Proteins Induce Astroglial Differentiation of Oligodendroglial–Astroglial Progenitor Cells*. The Journal of Neuroscience, 1997. **17**(11): p. 4112-4120.
487. Araya, R., et al., *BMP signaling through BMPRIA in astrocytes is essential for proper cerebral angiogenesis and formation of the blood-brain-barrier*. Mol Cell Neurosci, 2008. **38**(3): p. 417-30.
488. Megiorni, F. and A. Pizzuti, *HLA-DQA1 and HLA-DQB1 in Celiac disease predisposition: practical implications of the HLA molecular typing*. J Biomed Sci, 2012. **19**(1): p. 88.
489. Jia, Y., et al., *HLA-DQA1, -DQB1, and -DRB1 Alleles Associated with Acute Tubulointerstitial Nephritis in a Chinese Population: A Single-Center Cohort Study*. The Journal of Immunology, 2018. **201**(2): p. 423-431.
490. Hill, M.A. and S.C. Gammie, *Alzheimer's disease large-scale gene expression portrait identifies exercise as the top theoretical treatment*. Sci Rep, 2022. **12**(1): p. 17189.
491. Flores-Clemente, C., et al., *Inhibition of Astrocytic Histamine N-Methyltransferase as a Possible Target for the Treatment of Alzheimer's Disease*. Biomolecules, 2021. **11**(10).
492. Hung, C.Y., et al., *Sp1 in Astrocyte Is Important for Neurite Outgrowth and Synaptogenesis*. Mol Neurobiol, 2020. **57**(1): p. 261-277.
493. Dąbrowska, K. and M. Zielińska, *Silencing of Transcription Factor Sp1 Promotes SN1 Transporter Regulation by Ammonia in Mouse Cortical Astrocytes*. International Journal of Molecular Sciences, 2019. **20**(2): p. 234.
494. Jebelli, J.D., et al., *Emerging roles of p53 in glial cell function in health and disease*. Glia, 2012. **60**(4): p. 515-25.
495. Chang, J.R., et al., *Role of p53 in neurodegenerative diseases*. Neurodegener Dis, 2012. **9**(2): p. 68-80.

496. Wolfrum, P., et al., *The function of p53 and its role in Alzheimer's and Parkinson's disease compared to age-related macular degeneration*. *Frontiers in Neuroscience*, 2022. **16**.
497. Reichenbach, N., et al., *Inhibition of Stat3-mediated astrogliosis ameliorates pathology in an Alzheimer's disease model*. *EMBO Molecular Medicine*, 2019. **11**(2): p. e9665.
498. Vessella, T., et al., *Investigation of Cell Mechanics and Migration on DDR2-Expressing Neuroblastoma Cell Line*. *Life (Basel)*, 2024. **14**(10).
499. Chen, L., et al., *Recent Advances in the Role of Discoidin Domain Receptor Tyrosine Kinase 1 and Discoidin Domain Receptor Tyrosine Kinase 2 in Breast and Ovarian Cancer*. *Frontiers in Cell and Developmental Biology*, 2021. **9**.
500. Min, Y., et al., *Cross species systems biology discovers glial DDR2, STOM, and KANK2 as therapeutic targets in progressive supranuclear palsy*. *Nat Commun*, 2023. **14**(1): p. 6801.
501. Pal, R., et al., *Advancement of DDR1 and DDR2 Inhibitors: Therapeutic Potential of Bioactive Compounds, Designing Strategies, and Structure-Activity Relationship (SAR)*. *ChemistrySelect*, 2024. **9**(30): p. e202401216.
502. Lund, H., et al., *Tau-tubulin kinase 1 expression, phosphorylation and co-localization with phospho-Ser422 tau in the Alzheimer's disease brain*. *Brain Pathol*, 2013. **23**(4): p. 378-89.
503. Ikezu, S. and T. Ikezu, *Tau-tubulin kinase*. *Frontiers in Molecular Neuroscience*, 2014. **7**.
504. Bashore, F.M., et al., *Modulation of tau tubulin kinases (TTBK1 and TTBK2) impacts ciliogenesis*. *Scientific Reports*, 2023. **13**(1): p. 6118.
505. Tamir, T.Y., et al., *Gain-of-function genetic screen of the kinome reveals BRSK2 as an inhibitor of the NRF2 transcription factor*. *J Cell Sci*, 2020. **133**(14).
506. Deng, J., et al., *Deleterious Variation in BR Serine/Threonine Kinase 2 Classified a Subtype of Autism*. *Frontiers in Molecular Neuroscience*, 2022. **15**.
507. Nashun, B., P.W. Hill, and P. Hajkova, *Reprogramming of cell fate: epigenetic memory and the erasure of memories past*. *The EMBO Journal*, 2015. **34**(10): p. 1296-1308.
508. Ruiz, S., et al., *Identification of a specific reprogramming-associated epigenetic signature in human induced pluripotent stem cells*. *Proceedings of the National Academy of Sciences*, 2012. **109**(40): p. 16196-16201.
509. Buckberry, S., et al., *Transient naive reprogramming corrects hiPS cells functionally and epigenetically*. *Nature*, 2023. **620**(7975): p. 863-872.
510. Krauthausen, M., et al., *CXCR3 promotes plaque formation and behavioral deficits in an Alzheimer's disease model*. *The Journal of Clinical Investigation*, 2015. **125**(1): p. 365-378.
511. Farhy-Tselnicker, I., et al., *Activity-dependent modulation of synapse-regulating genes in astrocytes*. *eLife*, 2021. **10**: p. e70514.
512. Le, A.D., et al., *Astrocyte modulation of synaptic plasticity mediated by activity-dependent Sonic hedgehog signaling*. *The Journal of Neuroscience*, 2025: p. e1336242025.
513. Ramesh, G., A.G. MacLean, and M.T. Philipp, *Cytokines and chemokines at the crossroads of neuroinflammation, neurodegeneration, and neuropathic pain*. *Mediators Inflamm*, 2013. **2013**: p. 480739.

514. Vida, H., et al., *Chemokines in neurodegenerative diseases*. Immunology & Cell Biology, 2025. **103**(3): p. 275-292.
515. Leipp, F., et al., *Glial fibrillary acidic protein in Alzheimer's disease: a narrative review*. Brain Communications, 2024. **6**(6).
516. Al-Ghraiyybah, N.F., et al., *Glial Cell-Mediated Neuroinflammation in Alzheimer's Disease*. International Journal of Molecular Sciences, 2022. **23**(18): p. 10572.
517. Zhou, L.T., et al., *Tau pathology epigenetically remodels the neuron-glia cross-talk in Alzheimer's disease*. Sci Adv, 2023. **9**(16): p. eabq7105.
518. Companys-Alemany, J., et al., *Glial cell reactivity and oxidative stress prevention in Alzheimer's disease mice model by an optimized NMDA receptor antagonist*. Scientific Reports, 2022. **12**(1): p. 17908.
519. Fowler, A.J., et al., *Discoidin Domain Receptor 1 is a therapeutic target for neurodegenerative diseases*. Hum Mol Genet, 2020. **29**(17): p. 2882-2898.
520. Arnés, M., et al., *PI3K activation prevents A β 42-induced synapse loss and favors insoluble amyloid deposit formation*. Molecular Biology of the Cell, 2020. **31**(4): p. 244-260.
521. Cuesto, G., et al., *Phosphoinositide-3-kinase activation controls synaptogenesis and spinogenesis in hippocampal neurons*. J Neurosci, 2011. **31**(8): p. 2721-33.
522. Sánchez-Alegría, K., et al., *PI3K Signaling in Neurons: A Central Node for the Control of Multiple Functions*. Int J Mol Sci, 2018. **19**(12).
523. Yuan, L.L., E. Wauson, and V. Duric, *Kinase-mediated signaling cascades in mood disorders and antidepressant treatment*. J Neurogenet, 2016. **30**(3-4): p. 178-184.
524. Pandey, G.N., et al., *Dysregulation of Protein Kinase C in Adult Depression and Suicide: Evidence From Postmortem Brain Studies*. International Journal of Neuropsychopharmacology, 2021. **24**(5): p. 400-408.
525. Chottekalapanda, R.U., et al., *AP-1 controls the p11-dependent antidepressant response*. Molecular Psychiatry, 2020. **25**(7): p. 1364-1381.
526. Biernacka, J.M., et al., *The International SSRI Pharmacogenomics Consortium (ISPC): a genome-wide association study of antidepressant treatment response*. Translational Psychiatry, 2015. **5**(4): p. e553-e553.
527. Llorens-Marín, M., et al., *GSK-3 β , a pivotal kinase in Alzheimer disease*. Frontiers in Molecular Neuroscience, 2014. **7**.
528. Chang, H., X. Xiao, and M. Li, *The schizophrenia risk gene ZNF804A: clinical associations, biological mechanisms and neuronal functions*. Mol Psychiatry, 2017. **22**(7): p. 944-953.
529. de Castro-Catala, M., et al., *The genome-wide associated candidate gene ZNF804A and psychosis-proneness: Evidence of sex-modulated association*. PLoS One, 2017. **12**(9): p. e0185072.
530. Szeky, B., et al., *Efficient derivation of functional astrocytes from human induced pluripotent stem cells (hiPSCs)*. PLOS ONE, 2024. **19**(12): p. e0313514.
531. Smith, M.D., et al., *Reactive Astrocytes Derived From Human Induced Pluripotent Stem Cells Suppress Oligodendrocyte Precursor Cell Differentiation*. Frontiers in Molecular Neuroscience, 2022. **15**.